NBSIR 80-2120

Fire Development in Residential Basement Rooms

J. B. Fang and J. N. Breese

Center for Fire Research
National Engineering Laboratory
National Bureau of Standards
U.S. Department of Commerce
Washington, DC 20234

Interim Report

October 1980

Prepared for:

Division of Energy, Building Technology and Standards
Office of Policy Development and Research
U.S. Department of Housing and Urban Development
Washington, DC 20410

NBSIR 80-2120

FIRE DEVELOPMENT IN RESIDENTIAL BASEMENT ROOMS

J. B. Fang and J. N. Breese

Center for Fire Research
National Engineering Laboratory
National Bureau of Standards
U.S. Department of Commerce
Washington, DC 20234

Interim Report

October 1980

Prepared for:
Division of Energy, Building Technology and Standards
Office of Policy Development and Research
U.S. Department of Housing and Urban Development
Washington, DC 20410

U.S. DEPARTMENT OF COMMERCE, Philip M. Klutznick, *Secretary*

Luther H. Hodges, Jr., *Deputy Secretary*
Jordan J. Baruch, *Assistant Secretary for Productivity, Technology, and Innovation*

NATIONAL BUREAU OF STANDARDS, Ernest Ambler, *Director*

TABLE OF CONTENTS

LIST OF TABLES

LIST OF FIGURES

LIST OF FIGURES (continued)

FIRE DEVELOPMENT IN RESIDENTIAL BASEMENT ROOMS

J. B. Fang and J. N. Breese

Abstract

A multi-phase study program has been established to develop a rational test procedure for evaluating the fire resistance of residential floor assemblies. The first phase of this research program was aimed at characterizing the severity of fires originating in residential rooms and developing a specified set of fire exposure conditions applicable for fire resistance testing of floor constructions.

A total of 16 burnout tests were conducted to investigate the fire behavior in typical residential recreation rooms of single family houses. These fire tests were usually run for one hour and were performed in two instrumented test rooms, 3.3 x 3.3 x 2.4 m and 3.3 x 4.9 x 2.4 m in width, length, and height respectively, furnished with household furniture and lined with interior finish materials typical of actual occupancies. Measurements were made of the temperature, heat flux, static pressure, smoke density, gas velocity, species concentration, and oxygen consumption. The effects of such parameters as the ventilation, fire load density, initial item ignited, room size, and thermal and flammable properties of the wall and ceiling materials on the fire severity were evaluated quantitatively. A fire exposure temperature-time curve which is different from the ASTM E 119 curve, has been developed for testing the fire resistance of such building structures.

Key Words: Building fires; fire resistance; fire tests; flow measurement; gas temperatures; heat release rate; interior finishes; residential buildings; room fires.

1. INTRODUCTION

The fire performance of construction materials and assemblies is conventionally determined by subjecting the building components and structural elements to a standardized exposure in a laboratory fire endurance test. Due to extensive research on compartment fires and increased information available on fire behavior, some doubts have been raised about the validity of the test environments relative to actual fires.

The ASTM Standard E 119 time-temperature curve has been used widely in the U.S. for over 60 years. The curve was developed in 1917 based on experience derived from all the known temperatures measured or inferred from building fires and from fire tests made at various institutions such as the New York Building Code Authority and Columbia University, and no major change has taken place in the curve since then. The design of residential buildings has changed considerably from that six decades ago, with the use of lightweight construction instead of heavy masonry, and large windows versus small ones. Also, many new products including synthetic fabrics, finishes, laminates and composites, have been introduced as the primary components for the furnishings and lining materials of residential rooms. These materials tend to burn more rapidly and may lose their integrity earlier and at lower temperatures than woodbase materials. The real temperature development can be expected to be quite different from the temperature history described by the standard curve.

To establish the fire resistance required for a structure or a partition to withstand the action of the fully-developed fire without losing its structural integrity, insulating function or its load carrying capacity, it is necessary to estimate the severity and duration of the expected fire. Several years ago, an international cooperative research program [1][1] was carried out under the auspices of the Conseil International du Batiment (CIB) to investigate the effects of various factors on the behavior of fully-developed fires in single compartments. Numerous experiments were performed by burning standardized wood cribs in small-scale compartments under a wide range of conditions resulting from different combinations of such variables as compartment size and shape, ventilation conditions, the amount and distribution of fuel and type of wall materials. The results of this intensive experimental study indicated that there was a substantial difference between fires in compartments of different shapes, the influence of the compartment size was small, and the effect of the thermal properties of the wall and ceiling materials was minor. However, in real room fires the combustible contents such as the furnishings

[1] Numbers in brackets refer to the literature references listed at the end of this report.

in the form of fabrics, sheets, and foam padding may contain a certain amount of highly combustible plastic materials, and it is not clear if the data derived from using wood cribs are applicable.

In 1939, a total of five full-scale burnout tests involving typical furnishings in a simulated three room residential occupancy building were conducted at NBS to investigate the effect of different combustible loads on the intensity and duration of room fires. The fire load density studied ranged from 25.4 to 58.6 kg/m^2 (5.2 to 12 lb/ft^2) of floor area. It was found that average spatial temperatures of individual rooms were generally lower than the ASTM standard curve, except for fire load density greater than 41.5 kg/m^2 where the average temperature exceeded the standard curve for periods up to 22 minutes.

The severity of developing room fires depends upon the fire load, the surface area and the thermal properties of the room boundaries, and the ventilation conditions. A knowledge of the effect of these various parameters on the development of fires in residential rooms is needed as a basis for developing a rational procedure for evaluating the fire resistance of construction materials and assemblies.

The overall objectives of the current fire endurance study sponsored by the Office of Policy Development and Research within the U.S. Department of Housing and Urban Development (HUD) at NBS are to develop a meaningful test procedure for more realistically evaluating the fire resistance of floor/ceiling assemblies in residential occupancies, and to suggest improved performance criteria for the fire-safe use of load-bearing structural components. The first phase of this research program was specifically aimed at characterizing the behavior of fires originating in typically furnished basement recreation rooms, providing technical data needed for the development of a mathematical model of fire growth and developing a rational set of fire exposure conditions applicable to the fire resistance testing of residential floor constructions.

This report presents the experimental results of a series of sixteen full-scale room burnout tests. The test series was conducted to determine the fire behavior over a range of typical fire load densities, room sizes, ventilation conditions, and interior finish materials. The data include a description of the fire growth process in the fire room; the time to room flashover, the time when flames emerged from the doorway, the time histories of the upper gas temperature, the rate of heat released within the room; the developed static pressure and heat flux levels at selected locations; and the fire induced air flow at the door opening.

2. EXPERIMENTAL DETAILS

2.1 Test Compartments

Two burn rooms, one 3.3 x 3.3 m (10.7 x 10.7 ft) and the other 3.3 x 4.9 m (10.7 x 16 ft) both with 2.4 m (8 ft) ceiling height were constructed consecutively to investigate the effects of room geometry on the fire behavior. Both rooms had a 0.76 m (30 in) wide by 2.03 m (80 in) high finished doorway opening located centrally in one of the 3.3 x 2.4 m (10.7 x 8 ft) walls to serve as the single source of natural ventilation for the rooms. Figures 1 to 3 show the construction details of the test rooms. The rooms also had a heat-resistant glass window, 0.41 m (16 in) wide by 0.2 m (8 in) high situated symmetrically in one of the side walls and at a height of 1.4 m (56 in) above the floor for observation purposes. The basic structure of the burn rooms was 0.2 m (8 in) thick standard lightweight aggregate-concrete block walls. The floor was concrete protected by a layer of 16 mm, Type X gypsum wallboard. The ceiling was 13 mm (1/2 in) mineral board covered by a layer of 16 mm (5/8 in) Type X gypsum wallboard attached to W6 x 12 steel I-beams resting on the top of the block walls through a layer of ceramic fiber. The burn rooms were built within a large building to minimize the exterior weather effects and the indoor air was controlled to provide an air temperature of 21 $\pm$ 4°C and a relative humidity of 42 $\pm$ 8 percent. The combustion products from the burn room were exhausted through a collection hood to an afterburner for smoke abatement.

2.2 Fire Load Density

In order to select a typical range of loading density, material type and geometric arrangement of the combustible contents for the present series of full-scale room burnout tests, field data on fire loads in basement rooms for residential occupancies were collected and analyzed. Figure 4 shows the frequency distribution of the fire load density for the occupied recreation rooms based on 70 surveyed homes situated in the Washington, D.C. metropolitan area. These 70 homes were those for which information was available at the time and represented a portion of the sample from an ongoing project to survey fire and live loads in single family and mobile homes [2]. In figure 4, the fire load density is expressed in terms of the total weight of combustible materials per unit floor area. The numerical values shown at the top and those at the bottom of each column represent the mean values of the total and the movable fire loads, respectively, lying within a given interval. The movable fire load included all of the combustible materials in the furnishings and other items brought in for the service of the occupants after

the house was built. The total fire load consisted of the combustible structural elements including the interior finish materials as well as the movable fire load. The total weights of the combustible items were obtained by comparing their dimensions measured during the survey with the manufacturers' data for items of similar size, materials and construction [2]. The three levels of the total fire load density selected were 21, 28 and 42 kg/m^2 (4.3, 5.8 and 8.5 lb/ft^2) representing low, average and high ranges of the combustible loads, which corresponded to the 28%, 50% and 83% fractiles based on the normal distribution for approximating the total fire load observations. From figure 4, the low, average and high levels of the movable fire loads corresponding to these total fire loads chosen for basement fire studies were respectively 15, 23 and 37 kg/m^2 (3.1, 4.7 and 7.6 lb/ft^2) which were equivalent to the 26%, 50% and 88% fractiles on the basis of considering the spread of combustible contents to be normally distributed. The frequency distributions of the total fire load data for utility rooms and other rooms such as basements or unfinished storage rooms are given in figures 5 and 6. In general, the fire load density for utility rooms was slightly lower than that for recreation rooms and its frequency seemed to follow a skew distribution, whereas the frequency for other rooms decreased continuously with an increase in the total fire load. The normal value of the movable fire load density for an occupied basement utility room and that for other rooms in the basement were found to be approximately 13.7 kg/m^2 (2.8 lb/ft^2) and 15.6 kg/m^2 (3.2 lb/ft^2) of floor space, respectively. A summary of the type of interior finish materials employed for the basement rooms of those 70 surveyed homes located in the Washington, D.C. metropolitan area is given in table 1. As illustrated in the table, most of the recreation rooms had gypsum wallboard or plaster materials as the ceiling and plywood panels as the wall linings. The majority of the utility and other rooms had exposed wood joists overhead and concrete block or gypsum board finished walls.

The frequency distribution of the movable fire load in basement recreation rooms based on 200 homes is shown in figure 7. These 200 homes are the total number of single family detached homes included in the fire load survey [2]. The average value of the movable fire load density was 24 kg/m^2 (4.9 lb/ft^2). The 23 kg/m^2 (4.7 lb/ft^2) movable fire load density used in these tests was based on a smaller sample of 70 homes which was available at the initiation of this project. The floor area over which the combustible loads were distributed in the 200 single family detached homes surveyed ranged from 4.5 m^2 (49 ft^2) to over 46 m^2 (500 ft^2) with a mean value of 32 m^2 (344 ft^2), which was approximately twice that of the larger burn room used for the fire tests in this series.

The composition of the movable fire load employed in a typical test run was estimated based on the information supplied by the furniture manufacturers. As given in table 2, these were found to be 11.1 kg/m^2 of wood, 7.4 kg/m^2 of paper, 0.92 kg/m^2 of fabric, 1.02 kg/m^2 of plastic materials and 2.5 kg/m^2 of others for a 3.3 x 3.3 m recreation room furnished with 23 kg/m^2 of combustible contents. These material types and weights are comparable with those found in the typical basement family rooms of single family detached homes in the Washington, D.C. metropolitan area [2], where the average movable contents consisted of 8.3 kg/m^2 of wood, 9.4 kg/m^2 of paper, 2.3 kg/m^2 of plastics, 1.2 kg/m^2 of fabric and 0.2 kg/m^2 of others.

2.3 Furnishings

In order to minimize the possible effects due to the variations in material type, weights and constructions of the movable combustibles on fire behavior, and to duplicate the room contents for a number of fire tests, identical pieces of household furniture were purchased in large lots directly from either furniture manufacturers or large retail stores. For most of the fire tests, the furnishings consisted of a sofa, an upholstered chair and ottoman, an end table, a bookcase and a coffee table. For the tests involving the large burn room, a loveseat, an end table and another bookcase were used in addition to these furniture items. A description of the dimensions, materials and weights of the combustible portions is given in table 2. These varied slightly in size for the upholstered chair and the coffee and end tables since the original styles used in the early stage of the test series were subsequently discontinued. Figure 8(a) shows the floor plan of a furnished room illustrating the layout of the furniture and wall finish materials for a typical test run. The large recreation room was furnished similarly and is shown in figure 8(b). Included among the furnishings were old record file papers (22 x 28 cm), which were used to reach the required fire load density. A total of 4.54 kg of the papers were placed on the coffee table and 1.81 kg each were placed on the tops of the ottoman and the end table, with the remainder in the bookcase(s).

The floor was covered with wall-to-wall carpeting except for two areas directly beneath the platforms of the weighing cells, where two identical-sized pieces of the carpet were placed atop the platforms. For all of the fire tests, an olefin carpet with rubber foam cushion backing was used to cover the concrete floor through a layer of 16 mm thick fire rated gypsum wallboard.

2.4 Interior Finish Materials

A summary of the test conditions and the interior finish materials used in this study is presented in table 3. For each test, the interior walls of the test room were finished with one of the following three types of wall covering materials:

Gypsum wallboard. The wall framing consisted of nominal 25 x 76 mm (1 x 3 in) wood furring strips spaced 0.40 m (16 in) on center and attached to the concrete block walls with masonry nails. A single plate was used both at the top and at the bottom of the furring strips. The 13 mm (1/2 in) thick gypsum wallboard was applied with its long dimension parallel to the frame with dry wall screws. All joints were taped and covered with joint compound. The floor and ceiling seams were finished with wood trim. The walls were painted with two coats of white interior flat latex paint.

Plywood paneling. The wall framing was constructed in a manner similar to that of the gypsum wallboard. The 4 mm (5/32 in) thick prefinished and printed 3-ply lauan plywood panels were nailed parallel to the framing with interior hardened 25.4 mm (1 in) long paneling nails, 0.20 m (8 in) on center. Prefinished wood shoe moulding (15.9 x 9.5 mm) was used to trim the edges of the paneling walls.

Painted concrete block. The concrete block walls of the burn room were painted with two coats of common masonry paint (calcium oxide 64%, silicon oxide 22%, aluminum oxide, etc., 14%) to represent a typical finish for basement rooms.

The following four types of ceiling materials were used:

Suspended ceiling. The installation included lay-in wood fiber base ceiling tiles in a suspension grid. This system consisted of painted light metal, wall angles 19 x 19 x 0.56 mm (3/4 x 3/4 in x 25 ga), 38 x 25 x 1.12 mm (1-1/2 x 1 in x double layer of 25 ga) main tee runners and 25 x 25 x 0.56 mm (1 x 1 in x 25 ga) cross tees. The wall angles were nailed firmly to the wood furring strips fastened to the block walls. The main tee runners were installed at right angles to the steel studs, and the cross tees were hung from the suspension wires fastened to the studs. The 0.61 m x 1.22 m x 12.7 mm (2 ft x 4 ft x 1/2 in) thick, wood fiber base ceiling tiles (acoustical, lay-in panel with washable finish, flame spread index class 200) were dropped approximately 90 mm (3.5 in) below the steel studs to provide a ceiling height of 2.26 m (89 in) measured above the carpet flooring.

Gypsum board. The ceiling framing members used were light gage, galvanized C shape 92 x 33 x 0.56 mm (3-5/8 x 1-5/16 in x 25 ga) thick steel stud, and spaced 0.4 m (16 in) apart. The 16 mm (5/8 in) thick, type X, gypsum board sheet was applied with its long edges at right angles to the steel stud, and fastened to its bottom flange with screws. All joints between the adjoining pieces of gypsum board and screw heads were filled and taped with joint compound. The gypsum wallboard surfaces were painted with two coats of white color flat latex paint. The height of the finished gypsum board ceiling above the olefin carpet floor was 2.33 m (92 in).

Exposed wood joists. The construction contained nominal 50.8 x 203.2 mm (2 x 8 in) wood joists spaced 0.41 m (16 in) on center, and a single layer of 15.9 mm (5/8 in) thick underlayment grade plywood subfloor. The joists were resting on the upper sides of two nominal 51 x 203 mm (2 x 8 in) wood beams supported by two nominal 51 x 203 mm wood posts. All of the wood beams and posts were boxed within a double layer of fire rated 16 mm (5/8 in) thick gypsum wallboard for eliminating fire penetration and fastened by nailing into the block walls with masonry nails. Except for the joist spacing near the center of the ceiling where heat flux meters were located, solid bridging was installed at the midspan between the joists. Subflooring was laid perpendicular to the joists and fastened to each joist with nails. The ceiling height measured from the top of the carpet floor to the bottom of the wood joists was 2.14 m (84.2 in). In order to protect the mineral board sub-ceiling from the intense fire, a layer of 19 mm to 25 mm thick plaster spray mixture was applied to a metal lath hung approximately 13 mm (0.5 in) below the sub-ceiling.

Exposed steel joists. The framing used for the ceiling structure was 45 x 184 mm deep x 1.27 mm (1-3/4 x 7-1/4 in x 18 gage) thick, channel shaped steel joists spaced at 0.61 m (24 in) on center. The joists were fastened to nominal 51 x 203 mm (2 x 8 in) wood rim joists. Each rim joist was attached to the top side of an identical size of wood beam supported by two pieces of nominal 51 x 203 mm wood posts. Wood rim joists, beams and posts were fastened to the concrete block walls and protected from the fire by two layers of 16 mm (5/8 in) thick, type X gypsum wallboard. No bridging was installed. A single layer of 16 mm (5/8 in) thick underlayment grade plywood subfloor was installed at right angles to the joists and secured to the steel framing with screws. The height of the bottom flanges of the joists above the carpet flooring was found to be 2.21 m.

2.5 Forced Ventilation

In three tests, air was supplied to the room to simulate operation of a forced air central heating or cooling system.

For the fire tests involving forced draft, a constant rate of 170 m^3/h (100 CFM) air flow supplied by a blower was introduced into the test room via a light gauge metal duct of 152 mm (6 in) in outside diameter and a 105 x 305 mm (6 x 12 in) multi-louver register located at 1.83 m above the concrete floor and 0.41 m from one of the room corners opposite of the doorway.

A 0.76 m wide by 1.99 m high metal door with one 0.20 m square, heat resistant glass window for observation purposes, was employed for the two tests with the door closed. The door in closed position provided a small opening, 0.76 m wide x 0.04 m high, between its bottom edge and the concrete floor for venting the hot gases out of the fire room. Since the fire performance of the door was not a research objective, the door was protected on the fire side with 13 mm (1/2 in) thick noncombustible mineral board.

2.6 Test Parameters

The experimental conditions of the sixteen full-scale room burnout tests conducted for determining the effects of various parameters on the behavior of compartment fires are given in table 3. Several tests in the series were designed to provide data related to specific materials and situations and they would also be useful for development of mathematical models of fire growth. Tests 1, 2 and 6 were intended to examine the influences of the thermal and flammability properties of the wall materials on the fire buildup process. The data from tests 1, 4, and 5 were expected to show the relationship between the heat release rate in the room and the fire load density. An additional experiment (test 9) was performed to repeat test 1, which had to be terminated early due to an unexpected fire involvement of the surrounding structures. Also, test 10 was a repeat of test 3 since much of the temperature data was lost in the earlier test. Data from tests 3, 7, 9 and 11 were intended to establish the effects of open and closed doors and forced ventilation. Test 9 was performed with a basic room configuration and average level of combustible load to provide base line data. Data from tests 6 and 13 along with tests 8 and 14 were planned to compare the severity characteristics of room fires as a function of room size. In test 11A, the combustible loads employed were those remaining from test 11, where no room flashover and flame extinction were observed. In test 11A, the upholstered chair instead of the sofa was used as the first ignition item to supply information

for establishing the effect of the ignition source on fire development. The change in fire severity with gypsum board replacing plywood panel as wall linings was determined in tests 12 and 13 for the larger burn room, and in tests 6 and 9 for the smaller room. Tests 12 and 14 showed the influence of the flammability properties of the ceiling finishes on the overall room fire development. The data from tests 13, 15 and 16 provided the basis for comparing the fire growth in rooms with unprotected floor joists with those having finished ceilings.

The initial weights of the combustible materials used for all of the fire tests are summarized in table 4. The wall finishes include the combustibles employed as the covering material, and the framing and moulding strips for trimming the edges of the room walls. The estimate of total available heat from the burning of the combustible materials for each run, also tabulated in table 4, was made using these weight data for interior finishes and furnishings along with the information on weight percentages of the constituent materials employed for constructing various furniture items as given in table 2. The calorific values used for these calculations were 18.6 MJ/kg (8000 Btu/lb) for wood, 46.5 MJ/kg (19900 Btu/lb) for olefin fabric, 16.7 MJ/kg (7200 Btu/lb) for paper, and 26.5 MJ/kg (11400 Btu/lb) for polyurethane foam, respectively. The estimated total available heat from the combustible loads for all of the tests are also tabulated in table 4 and found to range from approximately 5400 to 14000 MJ (5.12×10^6 to 13.3×10^6 Btu).

3. TEST MEASUREMENTS

3.1 Temperature

The temperatures within the room and on the exposed surfaces of the walls and ceiling at selected locations were measured by bare beaded chromel-alumel thermocouples constructed from 0.51 mm (No. 24 B. and S. gage) diameter wire with a spherical junction of approximately 1.5 mm in diameter. After test 7, the thermocouples were formed from the wires of two different cables in order to prevent leakage of electric current between wires when it was found that there was a reduction in the readings due to the charring of the cable insulation for gas temperatures above 800°C. Gas temperature measurements were made at 10 stations including nine locations within the test room and one in the doorway opening. A total of 42 thermocouples were distributed vertically along nine thermocouple "trees" inside the room, located as shown in figures 8(a) and (b), and 12 thermocouples were positioned at various heights along the vertical centerline of the doorway as shown in figure 9. Indications of the upper room gas temperatures were also determined with three commercial

metallic-sheathed mineral insulated fast response thermocouples and with three ASTM E 119 standard protected furnace thermocouples. These sheathed thermocouples provided direct comparison with the ASTM E 119 curve and would be used to control the gas temperature in the fire endurance furnace because they required less frequent replacement than the bare beaded thermocouples due to their greater mechanical strength. These thermocouples were placed centrally 0.58 m below the ceiling at the mid-point and the sixth point of the lengthwise span. The fast response thermocouples were made from chromel-alumel wires with diameter of 1.02 mm (0.04 in) and their hot junctions enclosed in the sealed stainless steel sheaths, 6.4 mm (0.25 in) in outside diameter and 0.9 mm (0.036 in) in wall thickness, and insulated with magnesium oxide. The ASTM furnace thermocouples were of 1.02 mm (0.04 in) chromel and alumel wires with their hot junctions surrounded completely within sealed black wrought iron pipes, nominal 13 mm (0.5 in) in outside diameter and electrically insulated with porcelain tubes.

The wall and ceiling surface temperatures were measured at 20 stations by thermocouple beads mounted on the exposed and unexposed surfaces at the selected locations. Five stations were located at the ceiling as shown in figures 8(a) and (b); one was at the front wall inside the test room for monitoring full involvement of the combustible linings, shown in figure 9; eight stations were distributed over the back wall near the ignition point on the sofa as illustrated in figure 10, and three each were placed at the left and the right walls of the test rooms as shown in figures 11(a) to 12(b).

3.2 Heat Flux

A total of nine water-cooled, Gardon type gauges were used for incident total heat flux measurements. Three of these heat flux gauges were located along the centerline of the ceiling, flush with its exposed surface: one flush with the bottom face of the mineral board sub-ceiling, two in the exposed surface of the back wall, one each in the left wall and at the center of the carpet floor viewing the ceiling as shown in figures 8, 10 and 11; and one on a stand located outside the front of the room with its vertically oriented sensing element positioned 3.05 m from the doorway opening and 1.02 m above the concrete floor. One Gardon type, wide angle, water-cooled, radiometer with an air-purged sapphire window attachment was mounted at the center of the ceiling to measure the radiation from the hot gas layer and the heated surrounding walls.

3.3 Air Velocity at Doorway

The vertical distribution of the gas velocity in the doorway was monitored with six bidirectional flow probes [3] connected to variable reluctance differential pressure transducers and carrier demodulators. These probes were located along the vertical centerline of the opening and positioned at 0.13, 0.48, 0.84, 1.19, 1.55 and 1.91 m from the top of the doorway as shown in figure 9.

3.4 Static Pressure

Static pressure measurements of the gases in the fire room were made with 64 mm (0.25 in) steel pipes installed horizontally through the left wall (south wall) with their open ends flush with the inner surfaces of the wall lining panels. Five of these pressure probes were located along a vertical line 0.3 m from the front block wall at distances of 0.1, 0.3, 0.76, 1.32 and 2.13 m below the ceiling. Another probe was placed 0.3 m from the rear block wall at 0.1 m below the ceiling. The probes were connected by copper and tygon tubing to variable reluctance pressure transducers which in turn were connected to carrier demodulators for continuous monitoring of the static pressures in the room.

3.5 Optical Density of the Smoke

Optical density measurements of the smoke were made horizontally at five heights, 0.08, 0.30, 0.53, 0.97 and 1.50 m from the top of the doorway, over a 0.76 m long path along the doorway width as shown in figure 9, and over a 207 m path across the width of the exhaust hood, utilizing automobile spot lights as the light sources and phototube detectors (PIN3DP) as the receivers. Another measurement, with a path length of 2.07 m was made with a laser beam collimated vertically along the doorway height. The receiver was a phototube (1P39) located in a water-cooled, air purged insulated enclosure situated 0.30 m above the top of the doorway. The laser beam passed through a small hole in the floor at the front of the doorway.

3.6 Gas Concentrations

The gas concentrations were monitored continuously at four locations. Three sampling ports were situated in the doorway opening at heights of 0.08, 0.38 and 0.76 m down from the doorway top, and one was located in the smoke stack, which was connected to the exhaust hood installed above the opening. For the tests with the door closed, the open ends of three gas sampling probes

in the doorway opening were extended horizontally 0.31 m into the test room. After passing through a series of cold traps and glass wool filters, the gas samples from the top and the middle ports were analyzed for O_2, CO_2 and CO, and those from the bottom port were analyzed for O_2 and CO. Samples withdrawn from combustion products flowing in the smoke stack were analyzed for O_2, CO_2 and CO. The oxygen concentrations were measured with electrochemical type oxygen cells. The CO_2 and the CO were measured with non-dispersive infrared analyzers.

3.7 Weight Loss

Continuous measurements were made of the weights of the sofa and the upholstered chair during the tests. Each was located on a steel-frame platform suspended from a 227 kg capacity strain gage load cell. In order to resist the intense heat from long duration fires, the platform was a monocoque structure fabricated by bolting together two pieces of 3.6 mm (10 gage) thick steel plate as the facings and two layers of 19 mm (3/4 in) noncombustible mineral board as the core material. The entire platform was suspended by a steel rod attached to the load cell transducer mounted on the I-beams resting on the top of the concrete block walls.

3.8 Flashover Indicators

Two indicator specimens of crumpled ordinary newsprint and 0.78 mm thick horizontally-oriented filter paper, each placed on the ring of a tripod located at the center of the floor, were used to provide a direct indication of the involvement of typical combustibles in room fires.

3.9 Data Acquisition

During the test, the data were collected with a digital data acquisition system. The output signals from the thermocouples and the various transducers were logged every 8 seconds on magnetic tape. The data were processed, tabulated and plotted using a computer.

4. TEST PROCEDURE

Since the test series aimed to quantify the severity characteristics of basement room fires, which generally involved various stages of physical processes from flaming fire spread to full room involvement and complete burnout of combustible contents, a simulated newspaper ignition of the sofa was employed. A section of the daily newspaper weighing 400 g was placed

along the backrest and the seat cushions in the middle of the sofa and supported by a steel frame holder in order to provide a reproducible ignition source. The paper was conditioned to equilibrium at an ambient temperature of 23 $\pm$ 3°C and a relative humidity of 50 $\pm$ 5 percent prior to the fire test. The test was started by remotely igniting the newspaper with an electrically heated book of paper matches. During the course of the test, visual observations were made of the progress of the room fire and recorded with an audio tape cassette. Video tape and 35 mm slide coverage was provided on each test. On some tests 16 mm motion picture film coverage was also provided. The fire was allowed to burn completely for at least one hour, except for two tests (tests 1 and 2) where the tests were shortened to avoid serious damage to the surroundings and to the ceiling structures. A manually controlled, fine spray sprinkler located near the center of the ceiling and manually operated water sprays from hoses were used to extinguish the glowing ember fires remaining after one hour.

5. RESULTS

The photographic records of the fire development in test 12 involving a 3.3 x 4.9 m recreation room lined with lauan plywood panels on the walls and a gypsum board ceiling, and furnished with combustible contents of 23 kg/m^2 of the floor space, are shown in photos 1 to 3. The majority of the test fires had a similar history of development. A log of both visual observations and records deduced from the video tape made through the doorway of the fire room in a typical test (test 14) is given in table 5.

Selected results from this series of full-scale basement room burnout tests are summarized in tables 6 and 7. Table 6 includes: time to appearance of visible flames on the newspaper utilized as the ignition source; room flashover times derived on the basis of spontaneous ignition of two indicator specimens, on attainment of a level of 20 kW/m^2 for the incident heat flux at the center of the floor; times for flames to emerge from the doorway; times for spontaneous ignition of the olefin carpet flooring; the maximum rates of heat released within the fire room calculated by two methods and the maximum upper room gas temperature. The data show that the time required to obtain sustained flaming of the newspaper ignition source varied from approximately 0.1 to 1.4 min with an average of 0.5 min after start of the test.

The times taken from the appearance of sustained flaming of the newspaper to the spontaneous ignition of the flashover indicators and of the carpet flooring, and to flame emergence from the doorway were obtained from visual observations. As illustrated in table 6, no room flashover was observed

for fire tests with the door closed (tests 7 and 11). Excluding the supplementary test, where the fire starting from an upholstered chair took slightly longer to reach flashover, the elapsed times ranged from 1.8 to 2.55 min with an average of 2.03 min for the ignition of the newsprint; and 1.8 to 2.72 min , with a mean of 2.13 min for the ignition of the filter paper. The time at which the incident heat flux measured at the center of the floor reached a level of 20 kW/m^2 varied from 1.67 to 2.97 min with an average value of 2.03 min. This was in good agreement with the times required for onset of ignition of the indicators. The times taken for the flames to issue out of the doorway and for the ignition of the carpet on the floor ranged from 1.68 to 4.32 min (average 2.14 min) and 1.87 to 3.50 min , (average 2.35 min), respectively.

The mean temperature of the hot gas within the upper part of the fire room for tests 1 to 7 was obtained by averaging the readings of thermocouples placed at 27 stations; nine evenly-spaced locations each at 0.025, 0.584 and 1.17 m below the ceiling. It was found later that charring of the silicone impregnation of the thermocouple wire insulation due to the fire, caused the indicated temperatures above 800°C to be too low. This type thermocouple with its insulation left on was also checked against an NBS standard type S thermocouple in an electric furnace controlled at two selected temperature levels. The accuracy of the thermocouple used was found to be 2 degrees high at 500°C and ranged from 48 to 122 degrees low at 1000°C level maintained for a period of one hour. This error was reduced by using a double-cable thermocouple in which two cables ran in parallel and the bare measuring junction was formed by welding the positive wire (chromel) from one cable together with the negative wire (alumel) from the other one. For tests 8 to 16, the results from the average of the temperature measurements by the fast response thermocouples at three locations were used to represent the room gas temperature since small thermocouple wires were easily broken and involved frequent replacement. These metallic sheathed thermocouples will also be used for monitoring and controlling the gas temperature of a gas-fired test furnace in the latter part of this research project. As shown in table 6, the peak temperature of the upper room gas varied from approximately 190°C to 410°C for the tests with closed door and 950°C to about 1080°C for the tests with the open door.

Data on the rate of heat release in the fire room can provide useful information for verification of the mathematical models of room fire growth. The heat release rate can be computed using the oxygen consumption technique since a great number of organic fuels under the presence of sufficient oxygen burn completely and produce nearly the same amount of heat per unit mole, mass or volume of oxygen consumed, which is almost independent of fuel type [4].

Recently, Parker [5] employed this principle to calculate the total rate of heat production for a wide range of building materials tested in the ASTM E 84 tunnel. Christian and Waterman [6] conducted full-scale fire tests to characterize the fire hazard of various occupancies and used the data on oxygen depletion and air flow rate measurements to estimate the heat release rate for various fires. Huggett [7] has recently reviewed the oxygen consumption technique for the measurement of heat release and found that incomplete combustion and variation in the type of fuel have only a minor effect on the result.

With the assumption that the combustion gas, which consists of the combustion products and the depleted air, behaves as an ideal gas, the rate of heat release from the complete combustion of the combustibles within the fire room to carbon dioxide and water vapor can be derived based on the conservation of mass and oxygen species as below

$$\dot{Q} = K \left(X_{O_2 a} - X_{O_2 g} \right) \Big/ \left[1 + (\alpha \Delta \nu^{*} + 1) X_{O_2 a} \nu^{*}_{O_2} \right] \left(298.15/T_g \right) U_g A \qquad (1)$$

where $\dot{Q}$ is the rate of heat release, in kW; K is heat of combustion of combustible materials, expressed as the heat produced per unit volume of oxygen consumed at the standard state of 25°C and 1 atm, in kJ/m^3; $X_{O_2 a}$ and $X_{O_2 g}$ are the concentrations of oxygen in the incoming air and in the combustion gas stream, respectively, in mole fractions; $\Delta \nu^{*} = \Delta \nu / \nu_f$, the change in the mole numbers per mole of combustible material or the fuel reacted; $\Delta \nu = \nu_{H_2O} + \nu_{CO_2} + \nu_{CO} - \nu_{O_2} - \nu_f$, in which ν_j is the stoichiometric coefficient of gas species j; $\nu^{*}_{O_2} = \nu_{O_2} / \nu_f$, the ratio of stoichiometric coefficient of oxygen to that of the fuel; α is the fraction of the fuel reacted, $\alpha = 1.0$ for the fires under fuel controlled burning regime and $0 \leq \alpha < 1.0$ for ventilation limited fires; T_g is the absolute temperature of the combustion gas, in °K; U_g is the component of the velocity of the combustion gas normal to the plane of the doorway in m/s, and A is the cross-sectional area through which it is exhausted, in m^2. The detailed derivations of the equations utilized for the heat release rate calculations are given in appendix A.

The total heat release rate in the fire room was computed based on the data from the oxygen depletion, gas velocity and temperature measurements of the combustion gas in the doorway, using equation 1 along with a constant K value of 17010 KJ/m^3 [7] and assuming that the molecular weight of the unburned fuel is equal to that of nitrogen gas during ventilation limited burning. Since the major components of room combustibles were cellulosic materials, wood with a chemical formula of $CH_{1.46}O_{0.65} \cdot 0.1H_2O$, in which

the attached 0.1 molecules of water account for 7 percent of moisture content [8], was used to represent typical fire loads. The assumption that the velocity, temperature and oxygen concentration can be approximated by a finite number of linear segments was employed for the energy production calculation.

In order to check the reliability of heat release rates derived based on the oxygen consumption method, one gas burner fire experiment was made with the 3.3 x 4.9 m burn room having concrete block on the walls and gypsum board ceiling. Two gas burners, each 0.31 m square in size, were placed side by side, 0.71 m away from the back wall and 1.3 m from the side walls with a height of 0.31 m above the floor. These gas burners were used to serve as the fire source where propane gas was introduced into them at three known flow rates ranging from 0.472 to 0.944 m^3/min. The heat release rates computed from the data on the oxygen concentration and gas flow rate measurements at the doorway opening were compared with the rates of heat output by the gas burners calculated based on gas supply rate and found to agree within $\pm$ 12 percent.

The computed maximum heat release rate of an individual room fire during its peak burning period is presented in table 6. As shown, the maximum rate of heat produced inside the fire room based on the various measurements at the doorway was found to range from 3530 to 6240 kW with an average of 5250 kW for the fires involving natural ventilation through an open door. Significant quantities of gaseous fuel or excess pyrolyzates were observed to burn outside of the fire room because of insufficient oxygen available for combustion within the room. With the supply of air at a rate equal to that of normal operating condition of the HVAC system in residential rooms, the calculated heat output rate of the compartment fire increased significantly as illustrated in table 6.

The rates of heat transfer to the selected locations on the room ceiling, walls and floor, and in front of the doorway outside of the room are presented in table 7. The peak level of heat flux incident at the ceiling varied from approximately 90 to 180 kW/m^2 with a mean of about 130 kW/m^2 for the rooms with an open door, and between 30 and 40 kW/m^2 for the rooms with the door closed. The data also show that with the fiberboard ceiling tile, higher levels of surface heat flux were obtained due to the contribution from the ceiling flames in addition to radiant and convective heating from hot gas layer and the upper walls. The exposed surfaces of room walls were subject to more intense heat flux than those at the ceiling, and the peak wall surface flux produced from the fires in the well-ventilated room varied from about 120 to 230 kW/m^2.

The maximum heat flux incident at the center of the floor during the fire test in the room with the open doorway, excluding test 2, which was stopped early, ranged from approximately 110 to 160 kW/m^2 with an average of 130 kW/m^2. Also shown in the table, the peak rates of heat transfer, mainly by means of radiative transport, to a point outside the room, 3.05 m from the opening, were of the order of 33 kW/m^2. This heat flux level was capable of causing ignition of nearby combustible materials. An estimate of the magnitude of radiative heat flux impinging on the vertically-oriented sensing element of the heat flux gauge located outside of the room, due to the emerging flames and the room fire was made. The assumptions employed in the calculations are that (1) the flames emerge above the neutral plane located at the lower one-third of the doorway height, (2) the flame axis has a constant angle of inclination of 45 degrees from the vertical plane; and (3) both the flames and the room fire via the doorway opening can be considered as plane emitters at a constant temperature equal to that of the room gas. The estimated radiant flux from the doorway alone was found to vary from 1.5 to 2.6 kW/m^2 with a mean of 2.1 kW/m^2, for the six tests included in table 7. The intensity of the thermal radiation emitted by the turbulent buoyant flames issuing out from the room above the doorway was estimated to range from 26 to 46 kW/m^2 with an average of 35 kW/m^2, using an absorption coefficient of 1.1 m^{-1} for the flame gas. It is obvious that the radiation emitted by the emerging flames constituted the major portion of the total energy received by the heat flux gauge. Some difficulties were encountered with the radiometer used for the direct measurement of the radiant flux inside the burning compartment due to the deposition of soot and condensable matter on the window; this caused a significant reduction in the total transmissivity throughout the test.

Table 8 summarizes the experimentally-determined flow rates of the inflowing air and outflowing gas through the doorway opening; the static pressure developed within the room; the neutral plane height above the floor level at the peak of the fire; the maximum smoke densities of the exhausting gases along the doorway width and across the length of the exhaust hood; and the peak concentrations of CO and CO_2 measured at the doorway and in the smoke stack. The data show that the maximum rate of air inflow induced by the room fire ranged from approximately 1.0 to 1.8 kg/s and the hot gas outflow varied from about 2.2 to 3.4 kg/s. These variations in flow rates may be attributed to differences in the characteristics of the room fires such as the temperatures of room gases.

The peak levels of the static pressure measured at 0.1 m below the ceiling for all test fires were found to be relatively constant with an

average value of approximately 14 Pa for the rooms with an open door. The pressure increased to 31 Pa for the tightly-closed compartment. The lowest height of the neutral plane in the doorway ranged from 0.57 to 0.71 m for all tests except for test 1 which was extinguished after only 7.5 minutes.

The optical density of the smoke and the concentrations of CO and CO_2 measured in the doorway of the ventilated room for most of the tests were of the order of 3.5 OD/m, 9 percent and 20 percent, respectively.

The time variation of the spatially-averaged temperature of the hot gas in the upper part of the room due to fires involving typical furniture and interior finish materials for all of the tests is shown in figures 13(a) to (e). These gas temperature versus time curves characterize the intensity and duration of fires likely to arise in residential rooms under the specific conditions of this test series and cover all stages of the fire development including growth, flashover, active burning and decay. The gas temperature data shown in the figures were obtained by bare bead, 0.5 mm wire diameter thermocouples for tests 1 to 7, where the temperatures above 800°C were not reliable, and the fast response furnace thermocouples were used for the remaining tests. No radiation correction was made. As shown in the figures, the rate of gas temperature rise and decay varies appreciably between the tests, depending upon the air supply rate, the fire load density, the thermal and combustible properties of the wall and ceiling materials, and the dimensions of the room involved.

5.1 Effect of Induced and Forced Ventilation

The change with time of the measured average gas temperature and the computed rate of heat release within the fire room as a function of room ventilation are shown in figures 14 and 15, respectively. For the tests with the open door, the fires were frequently controlled at different stages by both regimes of combustion including fuel bed and ventilation control. During the increase in gas temperature covering the period from ignition to flashover, the rate of burning was determined by the exposed surface area of the burning fuels and the rate of energy feedback from the overhead flames, hot gas layer and the surrounding walls. During the ventilation controlled active burning period which immediately followed room flashover, the increase in gas temperature followed the slowly rising temperature of the walls and ceiling enhanced by an increase in the burning rate due to the increased rate of fire-induced air flow through the doorway opening. During the decay period of the fire, the gas temperature continuously fell because of the decline in the burning rate, which was controlled by the diminishing fuel surface area.

The time histories of the computed heat release rate for the two closed door tests (7 and 11) illustrated in figure 15 were derived based on the calorific value multiplied by the measured weight loss rate of the burning sofa involved. As shown in figure 15, the heat release rate increased with an increase in the rate of air supply to the room either by mechanical means or by natural ventilation (tests 9 and 10). However, with the door open over the range studied, forced ventilation had little influence on the rise in the gas temperature since the heat gain arising from the increased rate of heat released in the room was compensated by the increased rate of sensible heat carried out by the hot gases. For the room with the door closed, no room flashover occurred and extinction of the fire was observed, in spite of the presence of a small ventilating opening located between the bottom of the door and the room floor because the oxygen concentration in the room depleted to levels approximately 9 to 11 percent, no longer supporting flaming combustion. The lower heat release rates for the closed room with forced ventilation (test 11) compared to the room with the door closed and no forced ventilation (test 7) as illustrated in figure 15, was attributed to test variability.

5.2 Effect of Fire Load Density

A typical plot of the time variation of the average room gas temperature as a function of the fire load density for fires developed in the 3.3 x 4.9 m residential room with an open door as the single source of induced ventilation is shown in figure 16. There was shift in the time of the peak in the gas temperature versus time curves and the duration of the vigorous burning stage of the fire varied from approximately 25 to 55 minutes depending on fire load density, which ranged from 30 to 45 kg/m^2. This time shift was probably due in part to an additional sensible heat loss and gas dilution resulting from the greater volatile generation rate during the early part of the test for the higher fire load density thereby lowering the gas temperature in the ventilation limited burning regime. The different thermal inertias of the bounding surfaces in these tests also influenced the time of the peak temperature. In general, the time duration increased with an increase in fire load density because of more combustible materials available for the fire to burn. If the duration of the active burning stage of a fire is defined as the time interval between the rise in the heat release rate immediately following room flashover and the start of the decrease in the heat release rate from fuel combustion, this duration can be approximated by

$$t = K \frac{LA_f(\Delta H_c)}{\dot{Q}} \qquad (2)$$

where L is the fire load density, A_f is floor area of the room, ΔH_c is calorific value of the combustibles, K is a proportionality constant and $\dot{Q}$ is the heat release rate during the active burning period. Equation 2 assumes that a linear relationship exists between the total amount of heat evolved during the active burning period and the total heat content of the combustible materials in the room as listed in table 4. The quantity of heat given off by the room fire during its vigorous burning stage versus the total available energy of the combustible loads, for all tests with the exception of those involving the door closed or very short test durations, is shown in figure 17. The method of least squares was used to fit a straight line to the set of data points. The ratio of the amount of heat released during the active burning period to the total available energy from the combustible contents and interior finish for these tests ranged from 0.34 to 0.69 with an average of 0.54.

5.3 Effect of Lining Materials

Figure 18 shows the influence of the room linings on the average gas temperature developed in the fire room. For the tests with the combustible walls there is a depression in the gas temperature, presumably due to dilution by the pyrolysis products in a ventilation limited fire, and an extension of the duration of the fire because of the greater total fire load. The burning of the combustible pyrolysis products beyond the doorway caused a large extension of the flames which resulted in intense radiation levels outside of the room as seen in table 7.

The variation with time of the rates of heat produced by the fires in the larger rooms lined with various interior finish materials on the walls and ceiling are given in figure 19. The heat release rate generally increased rapidly up to its peak with increasing rate of fuel volatilization from the burning materials until the fire became ventilation limited, and then remained relatively constant during the stage of full fire development. The heat release rate then dropped sharply with the decline in fuel consumption and the return to the fuel bed controlled burning regime. These fires had similar heat release rates since the rates of combustion of the volatile products and oxidation of the carbonaceous residues were limited by the rate of air entering through the ventilation opening or the size of the doorway which was the same for all of the tests. The rates of heat release by these fires under ventilation limited burning appeared to be independent of the types of wall and ceiling materials used. However, the tests with the plywood walls exhibited vigorous burning of the excess pyrolyzate outside of the room.

5.4 Effect of Room Size

The variation with time of the average room gas temperature measured in two sizes of the rooms having the same movable fire load density and ventilation conditions is given in figure 20. Both rooms had comparable maximum temperature values, but the fire in the larger room had a slightly longer duration. This was attributed to more combustibles present in the large room to support combustion.

Figure 21 displays the measured total heat flux incident at the center of the floor as a function of time for two room sizes. As illustrated in the figure and also shown in table 7, the larger room flux values are generally higher than the corresponding values for the smaller room during the peak steady burning period. The radiation path length through the flame gas or the mean beam length for the room filled with an absorbing grey gas became larger with an increase in the room size, and thus the radiation flux density to the floor from the hot gases increased with the increased gas emissivity.

5.5 Effect of Ignition Source

The average gas temperature versus time curve for the test with an upholstered chair as the ignition source is compared in figure 22 with that for a test involving a sofa normally used as the first ignited item. It can be seen from the figure that both room fires generally had similar peak gas temperature levels and fire duration, except that it took a slightly longer time for the chair fire to involve the plywood panels on the back wall and then to reach full fire development. The burning rate of the sofa was sufficient to bring the room to flashover without any involvement of the plywood panels.

6. DISCUSSION

6.1 The Experimentally Derived Temperature-Time Curve

The range of average gas temperature-time curves for this series of tests in which ordinary domestic furniture and interior finish materials were used as the fuel and burned under a variety of test conditions is shown in figure 23. These temperatures were obtained by averaging the readings of three metallic-sheathed mineral-insulated fast response thermocouples placed within the fire room. The gas temperature rose rapidly as flashover was reached, fell slightly and then increased up to peak levels ranging from approximately 950 to 1100°C followed by a gradual decrease. There were wide variations in

the times to arrive at the peak temperature levels and in the duration of the active burning phase, depending on the quantity and the nature of the combustible materials and the dimensions and ventilation conditions of the room involved. However, the maximum gas temperatures attained in the fire room are similar for most of the tests. Test 9 represents the standard test conditions (i.e., a 3.3 x 3.3 m recreation room finished with plywood paneling walls and a gypsum board ceiling and furnished with a typical loading of 23 kg/m^2 of household furniture). The standard ASTM E 119 curve in which the measurements of gas temperatures are made with the ASTM thermocouples, is also plotted in the figure for comparison purposes. An approximate correction made to take into account the slow response of the ASTM thermocouple at the early stage of fire buildup was estimated to be less than 150 degrees C. It can be seen that these basement recreation room fires had a more rapid temperature rise during their initial stages and a shorter period of time at high temperatures than those represented by the standard ASTM curve. Consequently, the rate of development and the intensity of real fires involving typical furniture and interior linings are significantly different from those represented by the ASTM E 119 fire endurance test.

The temporal variation of the mean upper room gas temperature derived from averaging the readings of three specified fast response thermocouples for test 9 is compared in figure 24 with that obtained from three ASTM E 119 furnace thermocouples placed at the same locations. As expected, the heavy cast-iron covered ASTM thermocouples gave lower readings than the fast response thermocouples during the pre-flashover period due to the heavier mass of its thermocouple assembly. However, both types of thermocouples showed roughly the same temperature levels in the time of post-flashover burning.

The set of data on the average room gas temperature for test 9 as given in figure 23 was fitted with a polynomial equation using a trial and error method based on seven selected experimental points. The fitted curve along with the experimental curve is shown in figure 25 and can be expressed by the equation:

$$T_g = \frac{a_o + a_1 t + a_2 t^2 + a_3 t^3}{1 + b_1 t + b_2 t^2 + b_3 t^3} \qquad (3)$$

where T_g is the average upper room gas temperature, in decrees C, t is the time variable, in seconds; and

for $0 \leq t < 90$ sec :

$a_o = 0.250000 \times 10^2$
$a_1 = -0.786992 \times 10^0$
$a_2 = 0.822586 \times 10^{-2}$
$a_3 = -0.283153 \times 10^{-4}$
$b_1 = -0.344181 \times 10^{-1}$
$b_2 = 0.396824 \times 10^{-3}$
$b_3 = -0.153081 \times 10^{-5}$

for $90 \leq t \leq 3600$ sec :

$a_o = 0.1076 \times 10^4$
$a_1 = -0.1360 \times 10^2$
$a_2 = 0.5987 \times 10^{-2}$
$a_3 = -0.2996 \times 10^{-5}$
$b_1 = -0.1753 \times 10^{-1}$
$b_2 = 0.1786 \times 10^{-4}$
$b_3 = -0.1112 \times 10^{-7}$

This experimentally derived gas temperature versus time curve, which corresponded to an approximate average over the range of test conditions studied in the test series, was considered to be a more realistic representation of room fire severity in residential buildings. It is recommended that this newly-developed fire exposure be employed for evaluating the fire performance of floor-ceiling assemblies used in residential basement (or other similarly furnished) rooms.

6.2 Comparisons of Different Types and Measuring Locations of Thermocouples

In order to provide some information on the influence of different types of thermocouples on the measured gas temperature during a room burnout test, five thermocouples of different construction were similarly exposed during one of the tests. The thermocouples consisted of (a) regular 0.51 mm wire diameter single cable, (b) 0.51 mm wire double cables (i.e., the junction was made from wires from 2 different cables), (c) silica fiber insulated, (d) standard ASTM E 119, and (e) fast response mineral insulated sheathed thermocouples. These were placed 0.58 m below the ceiling at three locations inside the test rooms. The silica fiber insulated thermocouples were constructed from 24 B. and S. gage (0.51 mm or 0.020 in diameter) chromel-alumel wire insulated by a 0.38 mm thick, non-impregnated vitreous silica fiber covering. Figure 26 is a graph of the average gas temperature as measured by the various types of thermocouples employed in test 15. The regular 24 B. and S. gage single and double cables and silica fiber insulated thermocouples led the sheathed fast response and ASTM thermocouples in response to the rapid rise in room gas temperature during the early portion of the fire test. As the test progressed, the temperature lags became less due to the slower rate of gas temperature change. Apparently, these bare beaded thermocouples had relatively small time constants compared with the furnace thermocouples due to the smaller mass of the measuring junction directly exposed to the fire environment.

However, all of these thermocouples, except the regular single cable type, had nearly the same temperature-time curves after 5 minutes. It can be noted that the regular single cable thermocouples began to indicate lower values after the gas temperature exceeded approximately 900°C resulting from the charring of insulation materials impregnated with silicone modified resin. The temperature above 800°C cannot be measured reliably with these thermocouples.

The average gas temperature derived from averaging the readings of three regular double cable 0.51 mm thermocouples in the fire room is compared to that obtained based on 27 thermocouples in figure 27. These three thermocouples were positioned along the centerline of the room at 0.58 m below the ceiling where the fast response and ASTM E 119 furnace thermocouples were also located. The 27 thermocouples used for the mean gas temperature were distributed evenly in nine equally-spaced stations and placed 0.025, 0.58 and 1.17 m beneath the ceiling. The average gas temperature based on three measuring points was slightly higher, but generally within 50 degrees C of that with 27 locations in the early stage of the room fire, since an inhomogeneity of the local gas temperature existed in the hot upper layer resulting from the mass addition of fuel volatiles from the decomposing ceiling materials. However, there was no appreciable difference in the temperature levels as the test progressed and a uniform temperature developed within the room volume. In general, the average gas temperature obtained based on the thermocouples placed at three locations was consistent with that derived from the 27 evenly-spaced stations.

The average upper room gas temperature and the heat release rate at the time of room flashover is shown in table 9. Flashover corresponds to the time at which the newsprint indicator placed at the center of the floor ignited spontaneously. The average upper room gas temperature varied from test to test and ranged from approximately 625 to 820°C. There were some differences in the temperature levels registered by the different types of thermocouples due to thermal inertia as noted before. The average upper room gas temperature at flashover was found to be 706 $\pm$ 56°C with a 68.3% confidence level and 706 $\pm$ 92°C with a 90% confidence level based on the regular double cable 0.51 mm thermocouples. The fast response and the ASTM thermocouples had reached 326 $\pm$ 123°C and 78 $\pm$ 56°C respectively at the time of flashover. Also, the rate of heat release by the fire at flashover appeared to be independent of the room size, over the range studied, and varied from 1030 to 2420 kW probably depending upon the insulation properties of the room walls involved. The heat release rate at the time of flashover was found to be approximately 1480 kW for the rooms lined with plywood walls and wood fiber tile ceiling, 1780 kW for gypsum board walls and ceiling, 1510 kW for plywood

walls/gypsum board ceiling and 2060 kW for concrete block walls/gypsum board or exposed floor joist ceiling, respectively. It can be noted that the heat release rates required to produce flashover also depend on how long they are maintained and on the ventilation conditions of the room involved.

6.3 Doorway Flow Due to Ventilation Controlled Fires

Information relative to the induced flow rates of air entering and combustion gases leaving through an opening in the fire room is essential in the development of the mathematical models for predicting fire behavior. The hydraulics orifice flow analogy has been used reasonably successfully for the prediction of the fire induced flow through the opening of an enclosure [9-11]. For a fully-developed room fire, the hot gas layer often descends to the floor level immediately after the occurrence of room flashover and thus the height of thermal discontinuity may be neglected compared to the neutral plane height during the active burning period. At this vigorous combustion stage, the mass flow rates of cold air in and hot gas out of the fire room under "choked" conditions [10] can be expressed in terms of the average gas temperature and the neutral plane height [9] as

$$\dot{m}_i = \frac{2}{3} C_D \rho_o A_o \sqrt{2gH_o \left(1-\frac{T_o}{T}\right)\left(\frac{Z_n}{H_o}\right)^{\frac{3}{2}}} \qquad (4)$$

$$\dot{m}_o = \frac{2}{3} C_D \rho_o A_o \sqrt{2gH_o \left(\frac{T_o}{T}\right)\left(1-\frac{T_o}{T}\right)\left(1-\frac{Z_n}{H_o}\right)^{\frac{3}{2}}} \qquad (5)$$

where $\dot{m}_i$ and $\dot{m}_o$ are the mass flow rates of the gases entering and leaving the room, respectively, C_D is the orifice coefficient, ρ_o is the density of the ambient air, A_o and H_o are the area and the height of the opening, respectively, Z_n is the neutral plane height, and T_o and T are the absolute temperatures of the ambient air and the room gas, respectively.

Summary data on the average room gas temperature, the rate of heat produced within the room, the neutral plane height, and the measured mass flow rates of the hot and cold gases at the doorway during the active burning period for the tests performed are tabulated in table 10. The height of neutral plane above the floor was determined from the measured velocity reversal in the doorway opening. The table also lists the air inflow rates estimated from the average heat release rates along with a K value of 17010 kJ/m^3 of oxygen consumed. As shown, the calculated rates of air flowing into the room are normally higher than those obtained from direct measurement. Gas velocity measurements were made along the vertical centerline of the

doorway opening. An experimentally determined coefficient, which is defined as $C_v = \dot{m}/\dot{m}_L$, in which $\dot{m}$ and $\dot{m}_L$ are the mass flow rates based on average and local velocities, respectively, is introduced to account for the variation between the average and the centerline velocity. The ratios of the orifice coefficient to the correction factor for velocity distribution across the doorway width, C_D/C_V for gas inflows and outflows are determined with the use of equations 4 and 5 together with the measured or estimated flow rates, the average room gas temperature and the neutral plane height, and are tabulated in table 10. These doorway coefficients ranged from approximately 0.4 to 0.7 with a mean value of 0.54 for inflow and 1.0 to 1.6 with an average of 1.29 for outflow streams, respectively.

In the ventilation controlled burning regime, the amount of oxygen contained in the cold air entering into the fire room was consumed completely by combustion since the measured oxygen concentrations at the top part of the doorway opening generally dropped to zero. From the heat release rate data along with a calorific value of 18.6 MJ/kg for the room combustibles, the rate of burning for the rooms with an open doorway can be related to air supply or the size of the opening and expressed by the approximate relation: $\dot{m} = (0.112 \pm 0.006)\ A_o\ H_o^{1/2}$, where m in kg/s, and A_o and H_o are the area, in m^2 and the height, in m, of the opening, respectively. It can be seen that for these test conditions, the ratio for $\dot{m}/A_oH_o^{1/2}$ has a constant coefficient of 0.112 $kg/m^{5/2}s$, which is approximately 24 percent greater than the conventional value of 0.09 $kg/m^{5/2}s$ derived from the burning of wood-like materials [12,13].

6.4 Gas Temperatures Influenced by Types of Ceiling Materials

Typical vertical temperature profiles of the gas near the center of the fire room for a test involving concrete block walls and wood joists/plywood subfloor ceiling (test 15) and one test with gypsum board walls and ceiling (test 13) for various times after full-involvement of the room are given in figure 28. These profiles illustrate the nonuniformity of the temperature distribution in the vicinity of the combustible ceiling attributed to the cooling effect of the mass injection of gaseous volatiles from the decomposing cellulosic materials. As shown for the gypsum board ceiling, the room gas is well-mixed and exhibits no variation in gas temperature during the vigorous burning stage of the fire.

6.5 Incident Heat Fluxes Calculated from Surface Temperatures

A method was sought for estimating the heat fluxes to the bounding walls during the room fire and for assessing the accuracy and reliability of the direct measurements by heat flux gauges. The total heat flux incident at the enclosure walls can be calculated using the surface temperature histories and the assumption that the ceiling or walls are semi-infinite solids. The equations and procedures used for the computation are presented in appendix B. Figures 29(a) and (b) show a comparison of the calculated and measured surface heat fluxes incident at the center of the gypsum board ceiling and at the mid-point of the upper half of the west gypsum board wall as a function of time for test 6. As shown, the calculated peak heat fluxes are generally in reasonably good agreement with the measured values. However, the measured heat fluxes are to a water-cooled heat flux gauge and should be higher than the calculated ones. Some of the differences between these curves are due to the fact that the calcining of the gypsum board is not taken into account in the calculation.

7. CONCLUSIONS

Based on the experimental results of 16 full-scale fire tests involving furnished basement recreation rooms with prescribed variations in room size, fire load densities, interior finish materials and ventilation conditions, the following conclusions may be drawn:

1. The rate of development and the intensity of real fires involving the burning of typical furniture and interior linings in a room during the first 20 minutes may be significantly greater than those defined by the ASTM E 119 standard time-temperature curve. A more realistic time temperature curve for residential occupancies is presented in this report. This curve is considered suitable for testing exposed floor constructions, floor-ceiling assemblies, wall assemblies, columns or doors.

2. Room flashover did not occur for a closed room of the size tested, even with normal forced air ventilation. However, for fires involving a single open doorway, the rate of heat release within the room increased with the addition of a forced air supply.

3. The addition of combustible interior finish materials on the wall and ceiling did not increase the maximum temperature of a ventilation limited fire over that produced by the combustible

contents but did prolong its duration. Similarly, the fire duration time increased with the fire load density. While the intensity of the fire within the room was controlled by the available air supply, the rate of burning outside of the room was markedly increased due to the additional fuel produced by the combustible finish and thus could be a major factor in fire spread beyond the room of origin.

4. The effect of the room size on the fire intensity was small, although the duration of the fire increased with an increase in room dimensions for the same movable fire load density.

8. ACKNOWLEDGMENTS

The room burnout test program was accomplished through the team efforts of many members of the Fire Safety Engineering Division, especially Messrs. Thomas Maher, Oscar Owens, Charles Veirtz, Ben Ramey, William Bailey, Sam Steel, Daniel Debold, Roy Lindauer, Billy Lee and Douglas Walton, whose valuable assistances are gratefully acknowledged.

The authors wish to thank Mr. Jack Bumgarner of National Archives and Records Service, GSA, through Mr. Harold Nelson of the Center for Fire Research, for providing disposable old record files used in the fire experiments.

This project is being sponsored by the U.S. Department of Housing and Urban Development, under the program management of Mr. James C. McCollom of the Division of Energy, Building Technology and Standards, a component of the Department's Office of Policy Development and Research.

9. REFERENCES

[1] Thomas, P.H. and Heselden, A.J.M., Fully-Developed Fire in Single Compartments, A Cooperative Research Programme of the Conseil International du Batiment, Fire Research Note No. 923, Fire Research Station, August 1972.

[2] Issen, L.A., Single Family Residential Fire and Live Loads Survey, Nat. Bur. Stand. (U.S.), NBSIR, in process.

[3] McCaffrey, B.J. and Heskestad, G., A Robust Bidirectional Low-Velocity Probe for Flame and Fire Application, Combustion and Flame, 26, 125 (1976).

[4] Thornton, W.M., The Relation of Oxygen to the Heat of Combustion of Organic Compounds, Philosophical Magazine, 33, 196 (1917).

[5] Parker, W.J., An Investigation of the Fire Environment in the ASTM E 84 Tunnel Test, Nat. Bur. Stand. (U.S.), Tech Note 945 (August 1977).

[6] Christian, W.J. and Waterman, T.E., Characteristics of Full-Scale Fires in Various Occupancies, Fire Technology, 7(3), 205 (1971).

[7] Huggett, C., Oxygen Consumption Calorimetry, a paper presented at the 1978 Technical Meeting of the Eastern Section, The Combustion Institute, Nov. 29-Dec. 1, 1978.

[8] Harmathy, T.Z., A New Look at Compartment Fires, Part I, Fire Technology, 8(3), 196 (1972).

[9] Rockett, J.A., Fire Induced Gas Flow in an Enclosure, Combustion Science and Technology, 12, 165 (1976).

[10] Prahl, J. and Emmons, H.W., Fire Induced Flow Through an Opening, Combustion and Flame, 25, 369 (1975).

[11] Quintiere, J.G., The Growth of Fire in Building Compartments, ASTM-NBS Symposium on Fire Standards and Safety, National Bureau of Standards, Gaithersburg, Md. April 5-6, 1976.

[12] Heselden, A.J.M., Thomas, P.H. and Law, M., Burning Rate of Ventilation Controlled Fires in Compartments, Fire Technology, 6(2), 123 (1970).

[13] Bullen, M.L., A Combined Overall and Surface Energy Balance for Fully-Developed Ventilation Controlled Liquid Fuel Fires in Compartments, Fire Research, 1, 171 (1977/78).

[14] Carslaw, H.S. and Jaeger, J.C., Conduction of Heat in Solids, Second Edition (Oxford University Press, Oxford, 1959).

[15] Myers, G.E., Analytical Methods in Conduction Heat Transfer (McGraw-Hill Book Co., New York, 1971).

Table 1. Types of interior finish materials found in basement rooms

Room Type	Number of Rooms and Percentage	Ceiling			Walls			
		Exposed Wood Joists	Finished		Masonry Walls	Finished		Total
			Plywood, Fiberboard, Wood	Gypsum Wallboard, Plaster		Plywood, Wood	Gypsum Wallboard, Plaster	
Recreation	Number	2	10	27	18	19	2	39
	%	5	26	69	46	49	5	100
Utility	Number	18	6	12	11	8	17	36
	%	50	17	33	31	22	47	100
Other	Number	25	4	7	7	4	25	36
	%	69	11	20	20	11	69	100

Table 2. List of combustible contents

Item	Material	Size	Initial Weight (Kg)
Sofa	Grade 1 100% olefin upholstery fabric, cotton batting side arms, foamed polyurethane seat, back and side cushions, wood frame	2.15 m wide 0.85 m deep 0.81 m high	frame-24 cover-6.4 foam-6.8 springs-7.3 cotton batting/ cardboard-8.5 Total 53
Upholstered Chair	Grade 1 100% olefin cover fabric, urethane foam seat cushion, cotton batting, wood frame	(1) 0.78 m W 0.90 m D 0.91 m H	(1) 24
		(2) 0.79 m W 0.91 m D 0.93 m H	frame-11.3 cover-1.8 foam-2.3 springs-1.4 cotton batting/ cardboard-6.2 Total 23
Ottoman	Grade 1 100% olefin cover fabric, urethane foam, wood frame	0.61 m M 0.46 m D 0.43 m H	frame-4.5 cover-0.9 foam-0.9 cotton batting/ cardboard-1.4 Total 7.7
Loveseat	Grade 1 100% olefin cover fabric, cotton batting side arms, urethane foam seat, back and side cushions, wood frame	1.52 m W 0.85 m D 0.81 m H	40
Coffee Table	Laminated veneer top and sides, finished hardwood	(1) 1.52 m W 0.56 m D 0.43 m H	(1) 20
		(2) 1.52 m W 0.51 m D 0.41 m H	(2) 22
End Table	Laminated veneer top and sides, finished hardwood	(1) 0.58 m W 0.69 m D 0.51 m H	(1) 10.9
		(2) 0.66 m W 0.36 m D 0.56 m H	(2) 7.3
Bookcase	Wood particle board with melamine finished surface	0.76 m W 0.36 m D 1.83 m H	42
Carpet	Level-loop olefin pile with foam rubber backing	3.2 x 3.2m x 9.5 mm thick	20

Table 3. Experimental conditions of basement room fire tests

Test No.	Room Size (m^2)	Lining Materials		Fire Load Density (kg/m^2)				Ventilation Condition	
		Walls	Ceiling	Combustible Contents	Interior Finishes	Carpet	Total Fire Load	Door	Forced Air (m^3/s)
1	10.2	Plywood	Gypsum Board	22.9	10.0	1.9	34.8	Open	0
2	10.2	Concrete Block	Gypsum Board	22.9	0	2.0	24.9	Open	0
3	10.2	Plywood	Gypsum Board	22.9	12.1	2.2	37.2	Open	0.047
4	10.2	Plywood	Gypsum Board	15.1	12.1	2.0	29.2	Open	0
5	10.2	Plywood	Gypsum Board	37.1	11.5	2.1	50.7	Open	0
6	10.2	Gypsum Board	Gypsum Board	22.9	6.0	2.1	31.0	Open	0
7	10.2	Plywood	Gypsum Board	22.9	11.6	2.1	36.6	Closed	0
8	10.2	Plywood	Suspended Tile	22.9	16.6	2.2	41.7	Open	0
9	10.2	Plywood	Gypsum Board	22.9	11.6	2.2	36.7	Open	0
10	10.2	Plywood	Gypsum Board	22.9	11.5	2.4	36.8	Open	0.047
11	10.2	Plywood	Gypsum Board	22.9	12.0	2.2	37.1	Closed	0.047
11A	10.2	Plywood	Gypsum Board	22.9	12.0	2.2	37.1	Open	0
12	15.6	Plywood	Gypsum Board	22.9	8.9	2.2	34.0	Open	0
13	15.6	Gypsum Board	Gypsum Board	22.9	5.0	2.3	30.2	Open	0
14	15.6	Plywood	Suspended Tile	22.9	12.5	2.0	37.4	Open	0
15	15.6	Concrete Block	Wood Joists	22.9	19.6	2.1	44.6	Open	0
16	15.6	Concrete Block	Steel Joists	22.9	9.8	2.2	34.9	Open	0

Table 4. Initial weights and total available heat of combustible loads used for fire tests

Test No.	Sofa (kg)	Chair (kg)	Ottoman (kg)	Coffee Table (kg)	Loveseat (kg)	End Table		Bookcase		Paper (kg)	Carpet (kg)	Interior Finishes		Total Available Heat (MJ)
						Quant.	Weight (kg)	Quant.	Weight (kg)			Walls (kg)	Ceiling (kg)	
1	54.9	24.9	7.7	20.4	-	1	10.9	1	41.7	73.9	19.1	101.6	0	7300
2	54.9	23.6	7.3	19.1	-	1	10.4	1	41.7	77.6	20.0	0	0	5440
3	55.3	24.0	7.3	19.5	-	1	10.4	1	41.7	76.2	23.1	123.4	0	7890
4	52.2	24.9	-	-	-	1	10.9	1	41.3	25.4	20.9	123.4	0	6360
5	53.5	23.1	7.7	19.5	-	1	10.4	2	83.0	181.9	21.3	117.5	0	10190
6	55.3	24.5	7.7	20.4	-	1	10.0	1	40.8	75.8	21.3	60.8	0	6650
7	53.5	24.5	7.3	20.9	-	1	10.4	1	42.2	75.8	21.3	118.4	0	7700
8	57.2	23.1	7.7	20.9	-	1	10.9	1	42.6	72.1	23.1	117.3	52.2	8770
9	55.8	23.1	7.3	20.0	-	1	11.3	1	41.3	75.8	23.1	118.4	0	7800
10	50.0	24.9	8.2	20.0	-	1	11.3	1	41.7	79.4	24.5	117.5	0	7820
11	47.6	23.6	7.3	20.0	-	1	10.9	1	41.7	83.5	22.7	122.0	0	7800
11A	46.9	23.6	7.3	20.0	-	1	10.9	1	41.7	84.2	22.7	122.0	0	7800
12	55.3	23.6	8.6	22.7	39.0	2	22.2	2	84.8	102.1	33.6	138.8	0	11070
13	50.3	23.6	7.7	21.8	37.6	2	21.8	2	84.4	111.6	35.4	78.0	0	9990
14	53.5	22.7	7.3	22.2	41.7	2	14.5	2	84.4	112.0	30.8	132.0	64.0	11990
15	49.4	23.6	7.3	21.3	41.7	2	14.5	2	83.0	117.5	33.1	0	305.7*	14110
16	53.5	22.7	7.3	22.7	40.8	2	14.5	2	84.4	112.5	34.5	0	152.4**	11340

*Includes wood joists and plywood subfloor

**Includes plywood subfloor

Table 5. Test log during test 14

Time (min:s)	Events
0	Ignition
0:04	Light smoke rising from the back of newspaper
0:15	Smoke over entire newspaper
0:19	Smoke almost to ceiling height
0:22	More smoke on the R.H.S. of paper than the L.H.S.
0:25	Smoke increasing more on the R.H.S. than the L.H.S.
0:35	Smoke hitting ceiling and spreading radially
0:38	Flame visible on left side of newspaper
0:50	Dark smoke halfway across ceiling
0:58	Back-rest cushion of sofa involved in burning
1:05	Flame height of about 0.91 m (3 ft) above sofa
1:11	Entire newspaper involved in burning
1:22	Hot smoke gas flowing out of the doorway opening
1:25	Central portion (1/3) of sofa involved in burning
1:33	Flames almost reaching to ceiling
1:40	Center half of sofa involved in fire
1:45	Smoke layer depth descending to 1/2 of room height
1:48	Fabric of arm cushions on sofa melting and splitting
1:55	Flames engulfing 2/3 to 3/4 of sofa
2:02	The flames halfway across left seat cushion, and still localized
2:05	Arm cushions burning and coffee table pyrolyzing
2:12	Wall paneling next to sofa involved in fire
2:19	Light smoke flames emerging from the top of doorway
2:20	Top of coffee table is burning
2:23	Newspaper indicator on floor ignites and is burning
2:26	Filter paper flashover indicator on floor catches fire
2:25	Heavy flames coming out from the doorway
2:30	Olefin carpet covering floor ignites

Table 5. Test log during test 14 (continued)

Time (min:s)	Events
2:35	Ottoman in front of bookcase is burning
2:38	Hot flaming zone extends down to 0.61 m (2 ft.) above floor
2:45	The whole front of the fire room appears to be in active burning
3:39	Intense radiation emitted from the room through the doorway
3:49	Crackling sound occurs within the fire room
3:55	Mostly flames coming out of room down to 1.5 m below ceiling in plane of doorway
4:20	A photoflood light exploding to produce a loud sound
5:35	Trace of smoke leaking out of room through cracks on the back concrete block wall
5:55	Carpet is virtually consumed
6:25	Curls from wall paneling fall onto floor
7:00	A piece of ceiling tile drops down on the left load cell platform containing chair
8:05	Ceiling tiles almost burned away
10:05	The interface between the outgoing hot gas and the inflowing cold air at the doorway is still at 1.5 m (third velocity probe above floor) below ceiling
14:05	The upholstered chair starts collapsing
15:30	Smoky hot gas in the room begins lightening up
16:10	The bottom boundary of flames coming outside of room through doorway still at level of third velocity probe
16:15	Chair collapsed
16:45	Crackling within the room is decreasing
17:10	Bright orange flames covering floor and dark orange flames coming out of doorway
19:10	Flames in room become brighter
20:10	Bright orange flames filling the entire room volume
20:55	Most wall paneling are consumed; some furring strips still burning
21:05	Flames out of room down to 1.14 m (at fourth velocity probe above floor) below ceiling in plane of doorway
22:45	Crackling in the room is almost gone

Table 5. Test log during test 14 (continued)

Time (min:s)	Events
25:10	Piles of paper from bookcases still burning on floor
25:30	Very light intermittent flames coming out of doorway; no black smoke visible in room
29:25	Little flaming is still going on some furring strips near room corners; piles of glowing embers from bookcases remain on floor
30:00	Stoppage of tape recording

Table 6. Summary of critical times, heat release rates and gas temperatures

Test No.	Duration of Test (min)	Initial Room Temp. (°C)	Time to Flame Appearance (min)	Time from Flame Appearance to (min)					Maximum Heat Release Rate in Room (kW)	Max. Average Upper Gas Temp. (°C)
				Room Flashover			Flames Emerging from Doorway	Ignition of Carpet		
				Ignition of		20 W/cm^2 on floor				
				Newsprint	Filter paper					
1	7.5	24	0.35	1.93	2.0	1.95	2.02	2.23	4170	> 819
2	14	20	0.22	2.55	2.72	2.97	2.23	2.80	3590	> 831
3	31	--	0.2	1.97	2.07	1.90	1.95	2.17	--	--
4	30	20	0.38	1.85	1.95	1.68	2.02	1.98	3530	> 952
5	60	21	0.78	1.97	2.07	1.80	1.80	2.13	4420	> 937
6	60	23	0.62	1.83	2.13	1.67	1.82	2.02	5560	> 958
7	60	26	0.50	∞	∞	∞	∞	∞	--	405
8	60	26	0.62	2.08	2.15	2.05	2.05	2.35	5590	1063
9	60	30	0.45	1.80	1.87	1.77	1.92	2.10	5600	1074
10	60	28	1.30	1.88	2.0	1.73	1.85	2.08	--	1004
11	60	28	0.13	∞	∞	∞	∞	∞	--	193
11A	60	28	0.65	3.85	4.0	3.75	3.77	4.68	6210	1013
12	60	24	1.40	2.10	2.17	1.93	2.22	2.23	6240	950
13	60	23	0.12	2.08	2.13	2.02	2.17	2.27	5790	1077
14	60	23	0.63	1.75	1.80	2.17	1.68	1.87	6160	1077
15	60	22	0.40	2.08	2.12	1.87	1.93	3.15	6050	1044
16	60	25	0.50	2.52	2.57	2.87	4.32	3.50	5300	987

Table 7. Summary of incident heat fluxes

	Maximum Heat Flux to									
	Ceiling			Walls			Floor		Outside of Room	
Test No.	Time (min)	Total (kw/m^2) Max.	Total (kw/m^2) Avg.	Time (min)	Total (kW/m^2) Max.	Total (kW/m^2) Avg.	Time (min)	Total (kW/m^2) Max.	Time (min)	Total (kW/m^2) Max.
1	2.3	106.0	99.9	2.1	116.0	90.7	3.1	133.0	--	--
2	8.9	115.0	67.9	12.0	137.0	119.0	3.5	23.2	--	--
3	12.9	107.0	75.5	11.5	192.0	150.0	11.3	120.0	--	--
4	2.1	98.5	79.1	13.6	145.0	124.0	2.8	143.0	--	--
5	12.6	124.0	73.8	15.1	180.0	146.0	12.9	138.0	--	--
6	11.6	167.0	85.2	12.1	220.0	194.0	3.2	132.0	--	--
7	1.9	32.7	26.0	1.6	36.7	19.5	2.0	2.7	--	--
8	14.1	167.0	138.0	12.3	181.0	133.0	13.7	130.0	--	--
9	13.3	87.0	47.4	15.3	178.0	154.0	13.6	124.0	--	--
10	12.3	153.0	82.1	13.7	176.0	157.0	13.6	112.0	4.3	33.1
11	2.0	38.8	25.6	2.0	20.7	14.8	2.0	2.7	--	--
11A	13.6	121.0	82.1	15.3	162.0	132.0	5.1	119.0	5.6	33.2
12	19.1	130.0	72.2	24.4	136.0	112.0	4.0	134.0	6.3	27.4
13	16.4	138.0	101.0	18.3	229.0	175.0	13.6	162.0	--	--
14	22.6	176.0	126.0	23.7	186.0	144.0	2.7	117.0	3.7	36.9
15	26.1	171.0	147.0	32.9	166.0	132.0	25.9	142.0	13.3	39.6
16	24.8	138.0	94.8	31.6	148.0	113.0	22.0	120.0	13.2	29.2

Table 8. Summary of air flows, static pressures, smoke densities and gas concentrations

Test No.	Max. Flow Rate Through Doorway (kg/s)		Max. Room Static Pressure (Pa)	Min Neutral Plane Height (m)	Max. Smoke Density (O.D./m)		Max. Concentration (Vol. %)			
							CO		CO_2	
	In	Out			Doorway (Avg.)	Hood	Doorway	Stack	Doorway	Stack
1	--	--	--	0.76	1.75	3.21	9.4	0.4	17.1	9.2
2	0.98	2.46	13.7	0.64	5.15	2.78	5.5	0.7	18.3	4.4
3	--	--	--	--	2.64	2.63	9.8	0.4	17.8	8.8
4	1.53	2.15	14.6	0.62	3.29	2.83	10.2	0.4	19.1	5.1
5	1.36	2.17	13.8	0.67	3.28	2.36	9.6	0.3	19.7	4.4
6	1.08	2.83	14.9	0.59	--	3.22	5.6	0.3	19.8	2.9
7	--	--	--	--	--	--	1.3	0.0	11.8	0.1
8	1.11	2.75	13.8	0.59	2.05	--	10.0	0.1	23.7	2.7
9	1.25	2.98	--	0.68	4.57	4.96	9.2	0.3	19.4	3.8
10	1.22	3.38	14.1	0.57	2.84	3.15	9.0	0.2	20.1	--
11	--	--	31.3	--	--	--	0.7	--	10.4	--
11A	1.20	2.88	14.2	0.66	3.05	2.78	8.6	--	18.2	--
12	1.38	2.85	13.5	0.59	3.72	2.63	7.8	--	20.1	--
13	1.77	2.69	14.0	0.71	4.49	3.48	7.0	--	22.4	--
14	1.56	2.55	13.9	0.58	4.20	2.44	11.2	--	20.4	--
15	1.04	2.74	14.8	0.66	4.08	2.45	12.1	--	19.0	--
16	1.31	2.47	14.8	0.66	3.94	3.28	8.4	--	19.8	--

Table 9. Average upper room gas temperature and heat release rate at time of room flashover

Test No.	Average Upper Room Gas Temperature (°C)			Heat Release Rate (kW)
	Regular	Fast Response	ASTM E 119	
1	624	--	--	1030
2	822	--	--	1620
4	694	--	--	1190
5	710	--	--	1880
6	757	--	--	2420
8	726	264	52	1560
9	705	214	49	1610
10	763	325	54	1850
11A	755	398	86	1470
12	699	254	50	1560
13	632	256	45	1130
14	685	231	36	1390
15	666	394	118	2360
16	640	602	212	2210

Table 10. Average room gas temperature, heat release rate, flow rates and calculated orifice coefficients for inflowing and outflowing gases during active burning period

Test No.	Active Burning Period (min)		Avg. Room Gas Temp. (C)	Avg. Neutral Plane Height (m)	Avg. Heat Release Rate (kW)	Mass Flow Rate (kg/s)			Doorway Coefficient (C_D/C_V)		
						Air Inflow		Gas Outflow (Measured)	Inflow		Outflow (Measured)
	From	To				Measured	Estimated from H.R.R.		Measured	Estimated from H.R.R.	
2	2.6	12.8	757	0.73	3010	0.82	1.00	1.80	0.57	0.70	0.99
4	1.9	15.2	806	0.75	3070	0.99	1.02	1.67	0.66	0.68	0.96
5	2.0	18.7	803	0.74	3973	0.78	1.32	1.82	0.53	0.91	1.00
6	1.9	12.1	813	0.64	4920	0.81	1.64	2.36	0.70	1.41	1.21
8	2.5	20.7	892	0.69	4370	0.86	1.46	2.25	0.66	1.12	1.25
9	2.0	17.0	850	0.71	4960	0.68	1.65	2.45	0.51	1.24	1.40
10	2.0	17.4	881	0.65	5640	0.51	1.82	2.84	0.43	1.54	1.52
11A	4.0	17.4	899	0.73	5440	0.59	1.81	2.59	0.42	1.29	1.52
12	2.2	23.8	834	0.69	5560	0.70	1.85	2.48	0.53	1.40	1.36
13	2.2	20.7	907	0.88	5120	1.18	1.71	2.26	0.62	0.89	1.58
14	1.9	25.4	867	0.72	5180	0.58	1.73	2.29	0.41	1.22	1.31
15	2.1	34.4	809	0.74	4990	0.75	1.66	2.42	0.51	1.13	1.39
16	2.7	30.4	817	0.73	4410	0.60	1.47	2.19	0.43	1.04	1.25

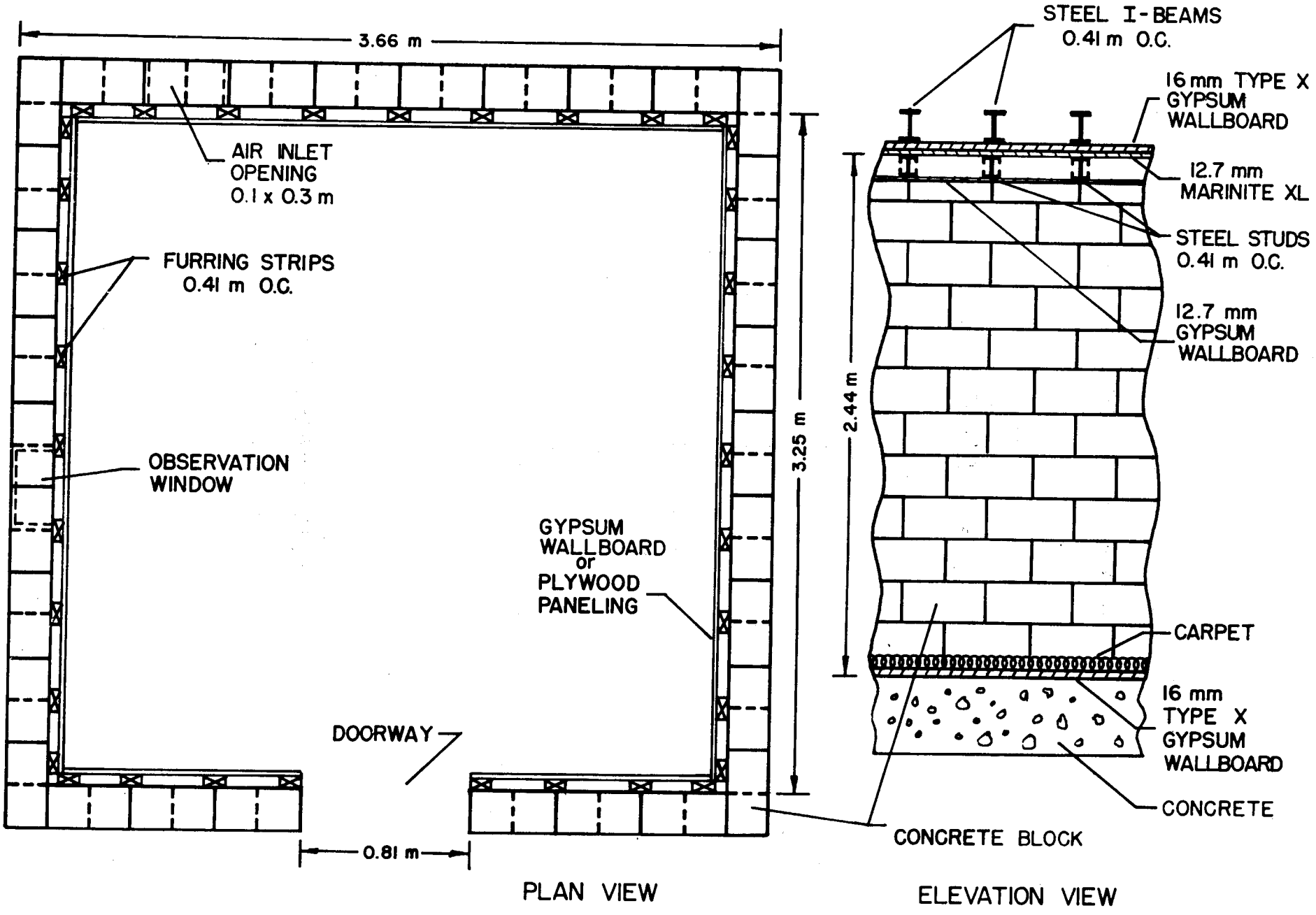

Figure 1. Construction details of the test room

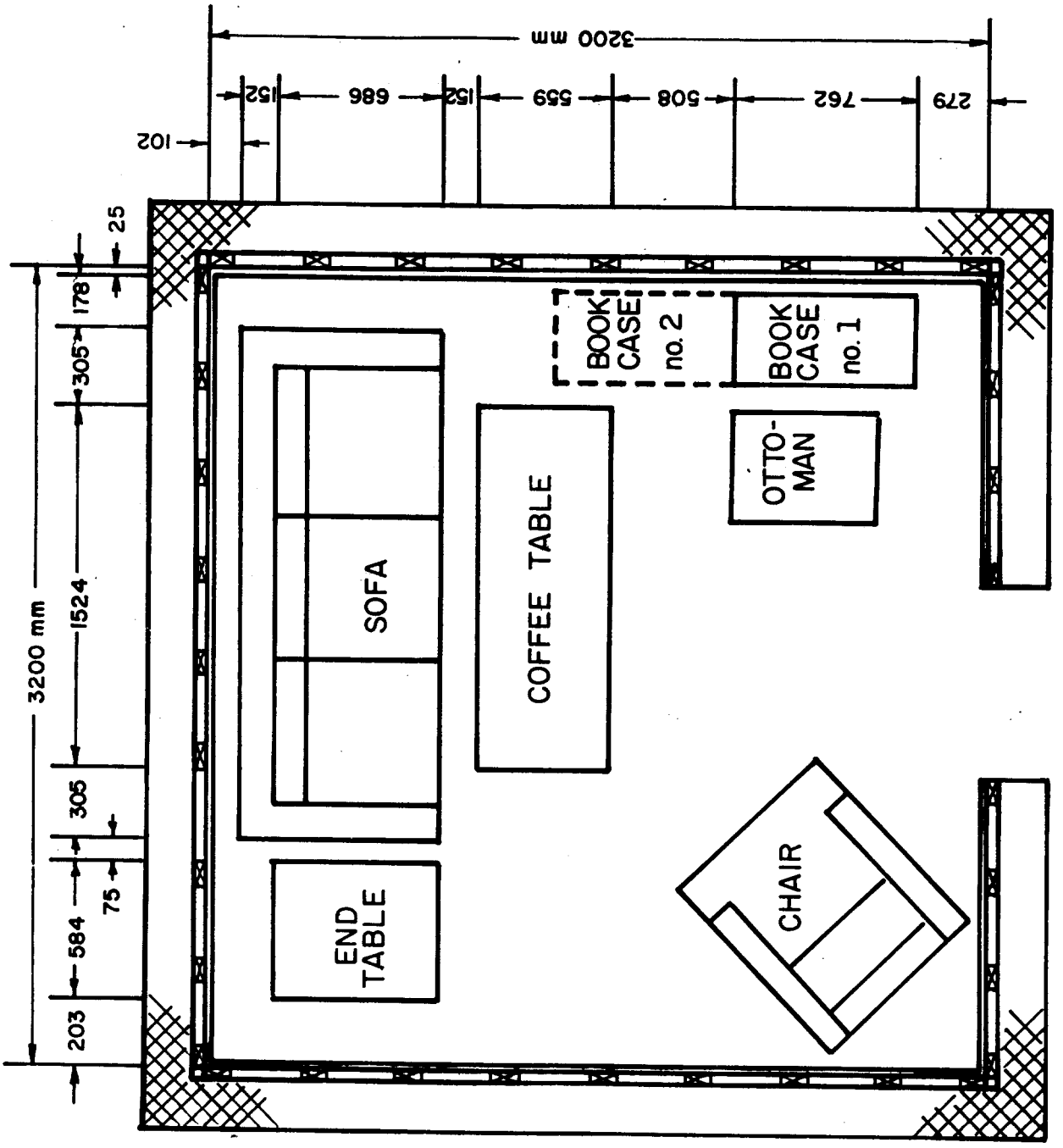

Figure 2. Layout of furniture and wall linings for the 3.3 x 3.3 m test room

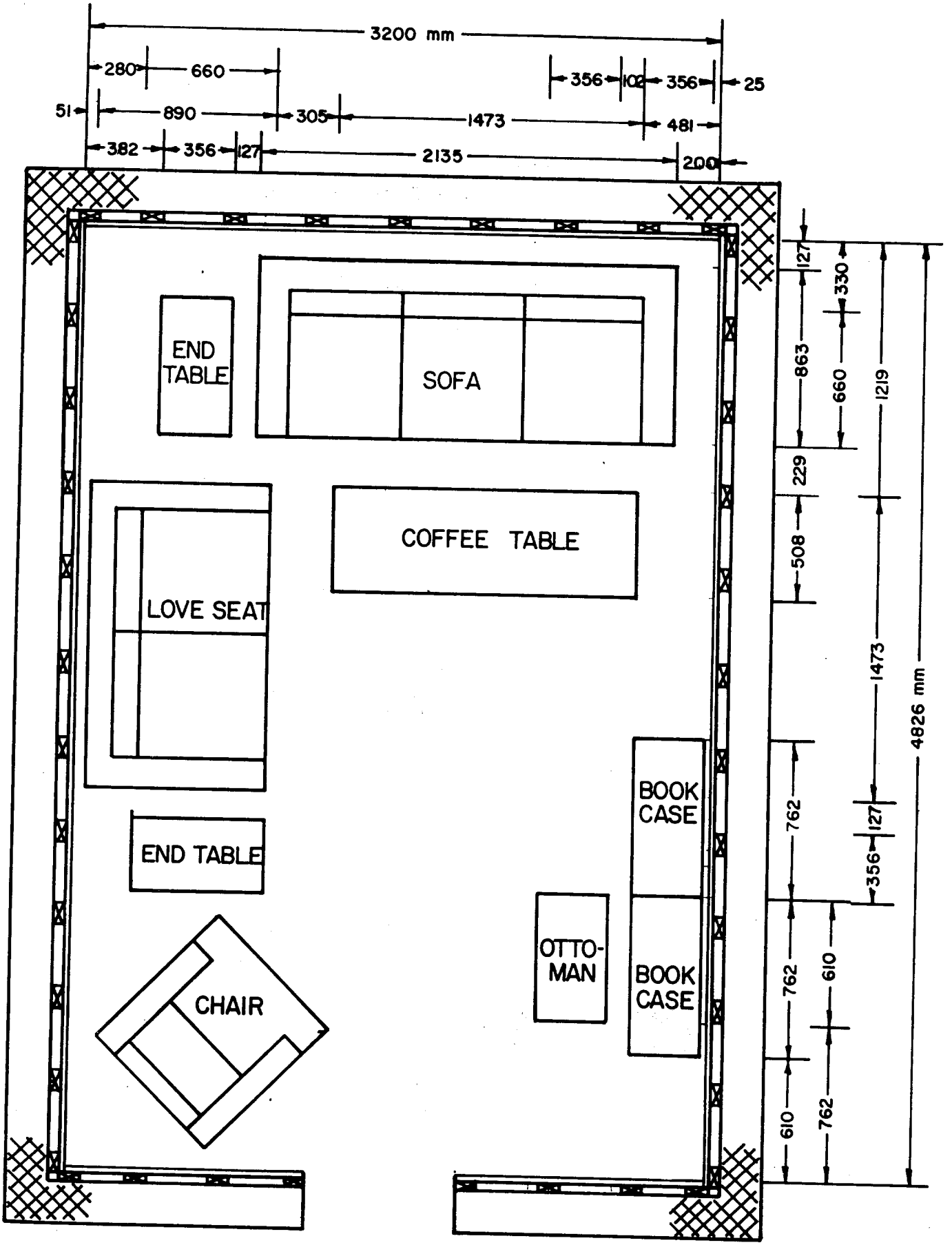

Figure 3. Layout of furniture and wall linings for the 3.3 x 4.9 m test room

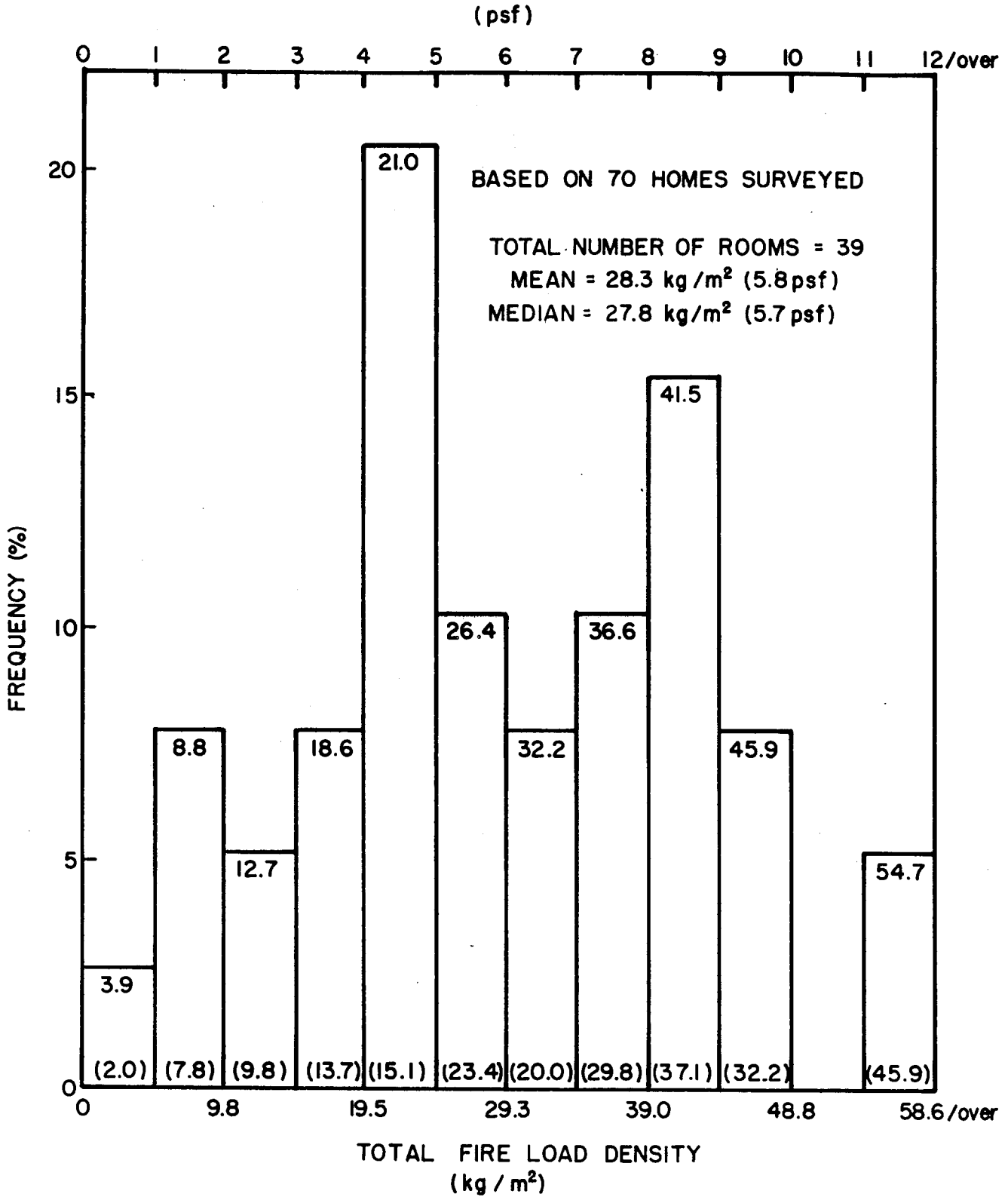

Figure 4. Frequency distribution of fire load data for residential recreation rooms

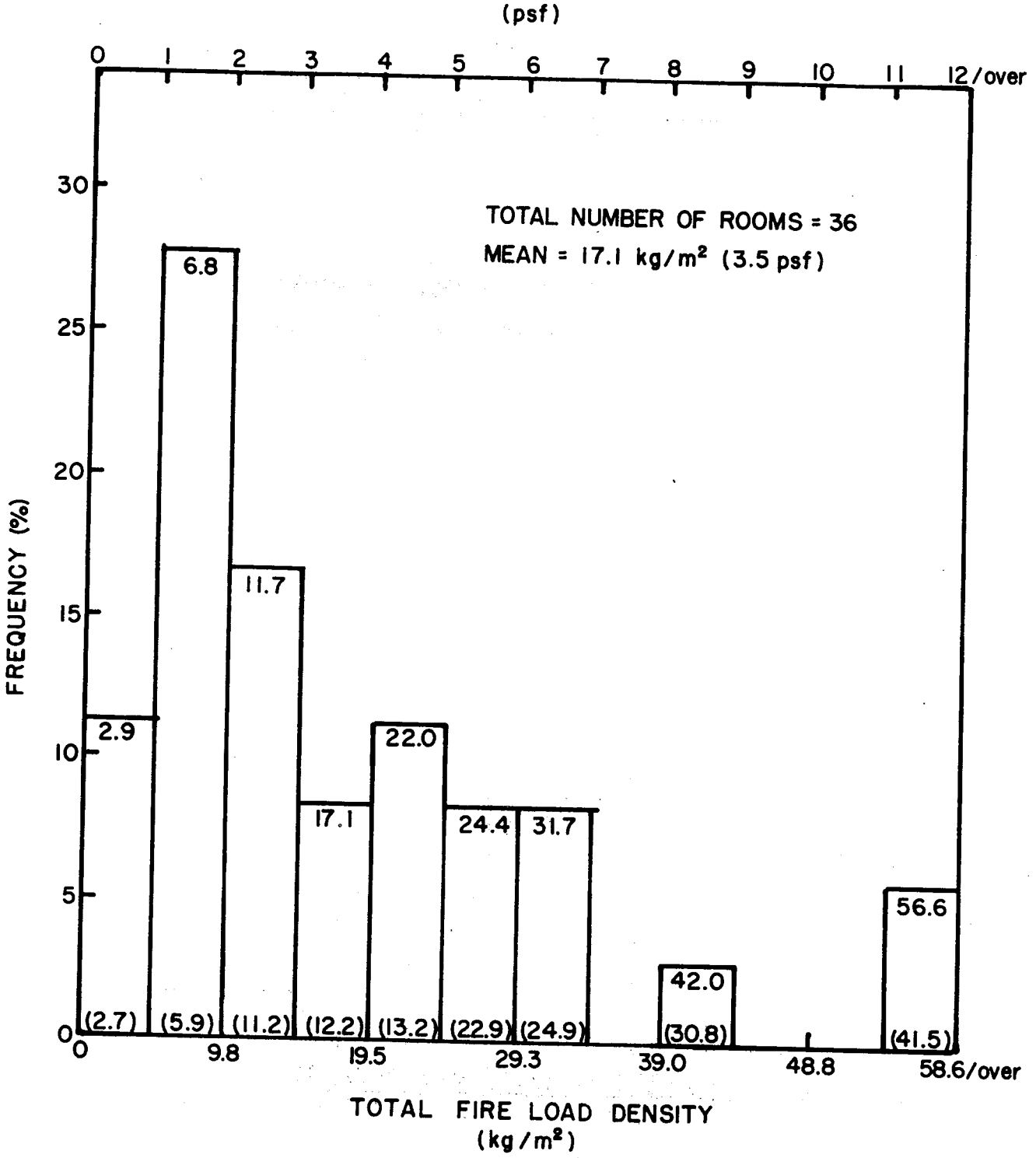

Figure 5. Frequency distribution of fire load data for utility rooms

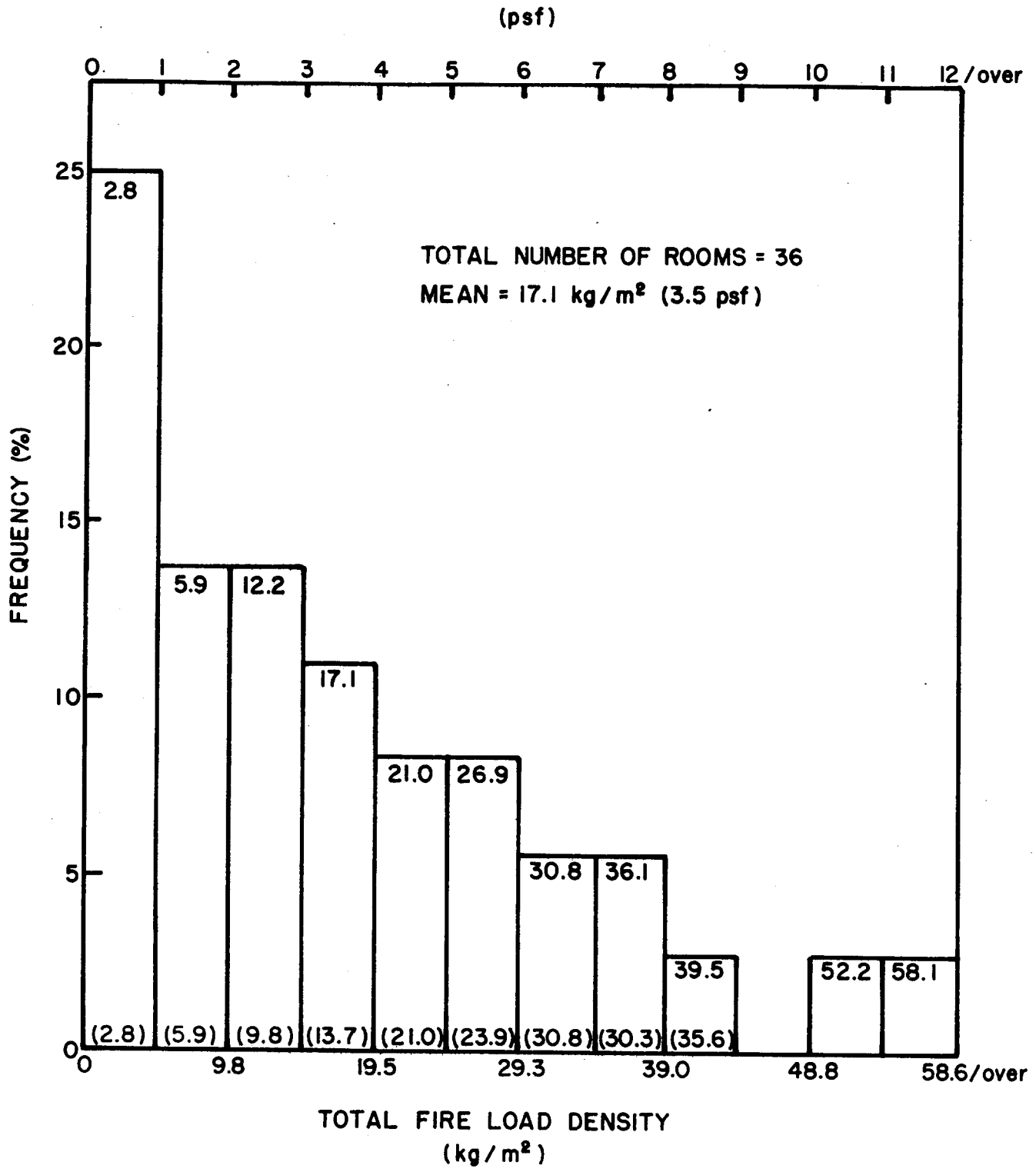

Figure 6. Frequency distribution of fire load data for other basement rooms

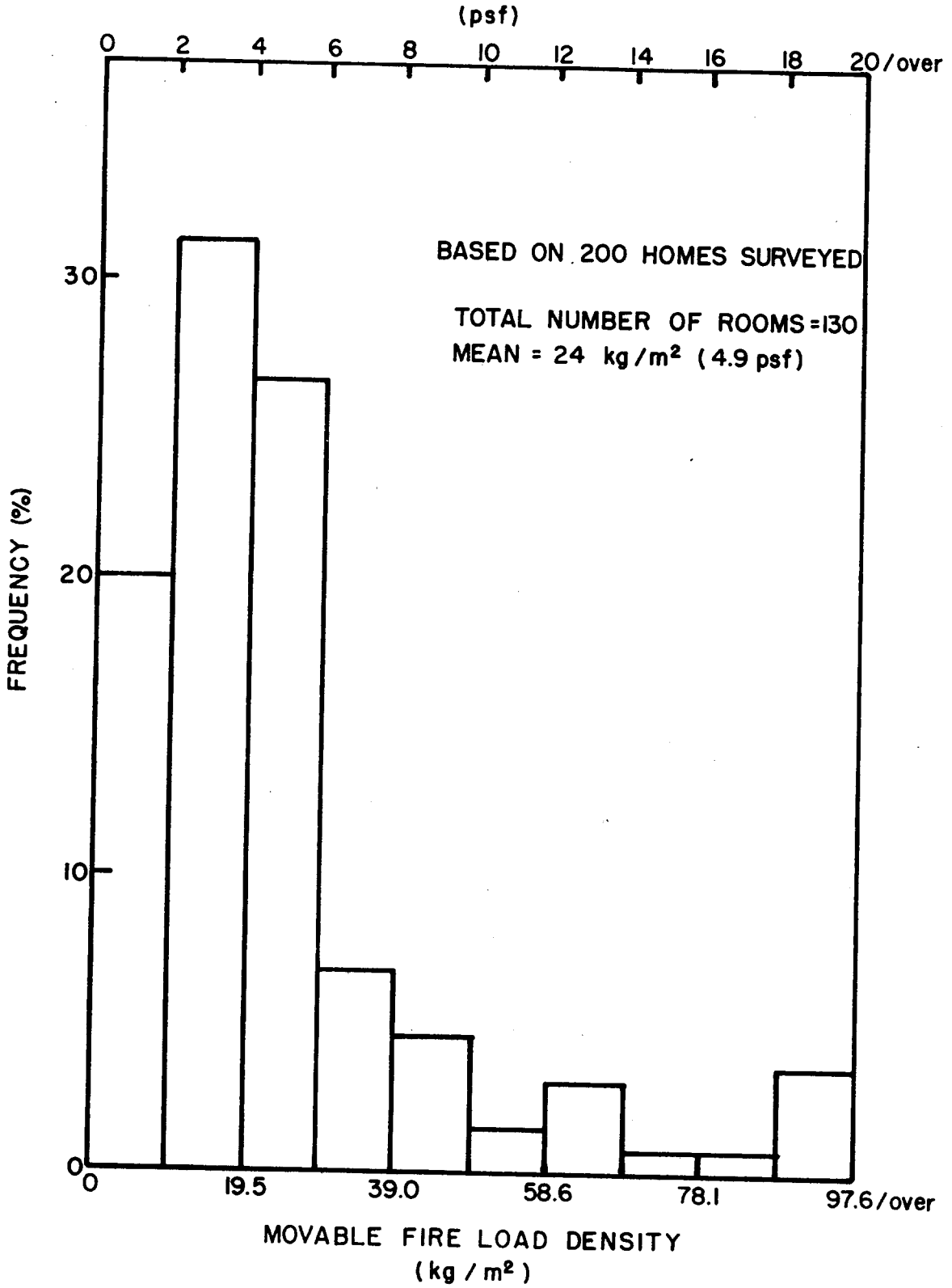

Figure 7. Frequency distribution of the movable fire load density in basement recreation rooms

Key to figures 8a and 8b

Symbol	Type of Transducers	Distance Below the Ceiling (m)
	3 Thermocouples	0.025, 0.58, 1.17
	7 Thermocouples	0, 0.025, 0.15, 0.30, 0.58, 1.17, 1.73
	5 Thermocouples	0, 0.025, 0.30, 0.58, 1.17
	5 Thermocouples	0, 0.025, 0.58, 1.17, 1.73
	11 Thermocouples	0, 0.025, 0.15, 0.30, 0.58, 0.89, 1.17, 1.45, 1.73, 1.93, 2.31
	1 ASTM E 119 and 1 Fast Response Furnace Thermocouple	0.58
	1 Total Heat Flux Meter	0
	1 Total Heat Flux Meter	-0.09 (above the ceiling)
	1 Total Heat Flux Meter	2.34
	1 Radiometer	0
	5 Static Pressure Probes	0.10, 0.30, 0.76, 1.32, 2.13
	1 Static Pressure Probe	0.10
	3 Gas Sample Ports	0.38, 0.69, 1.07
	1 Load Cell	
	Sprinkler	

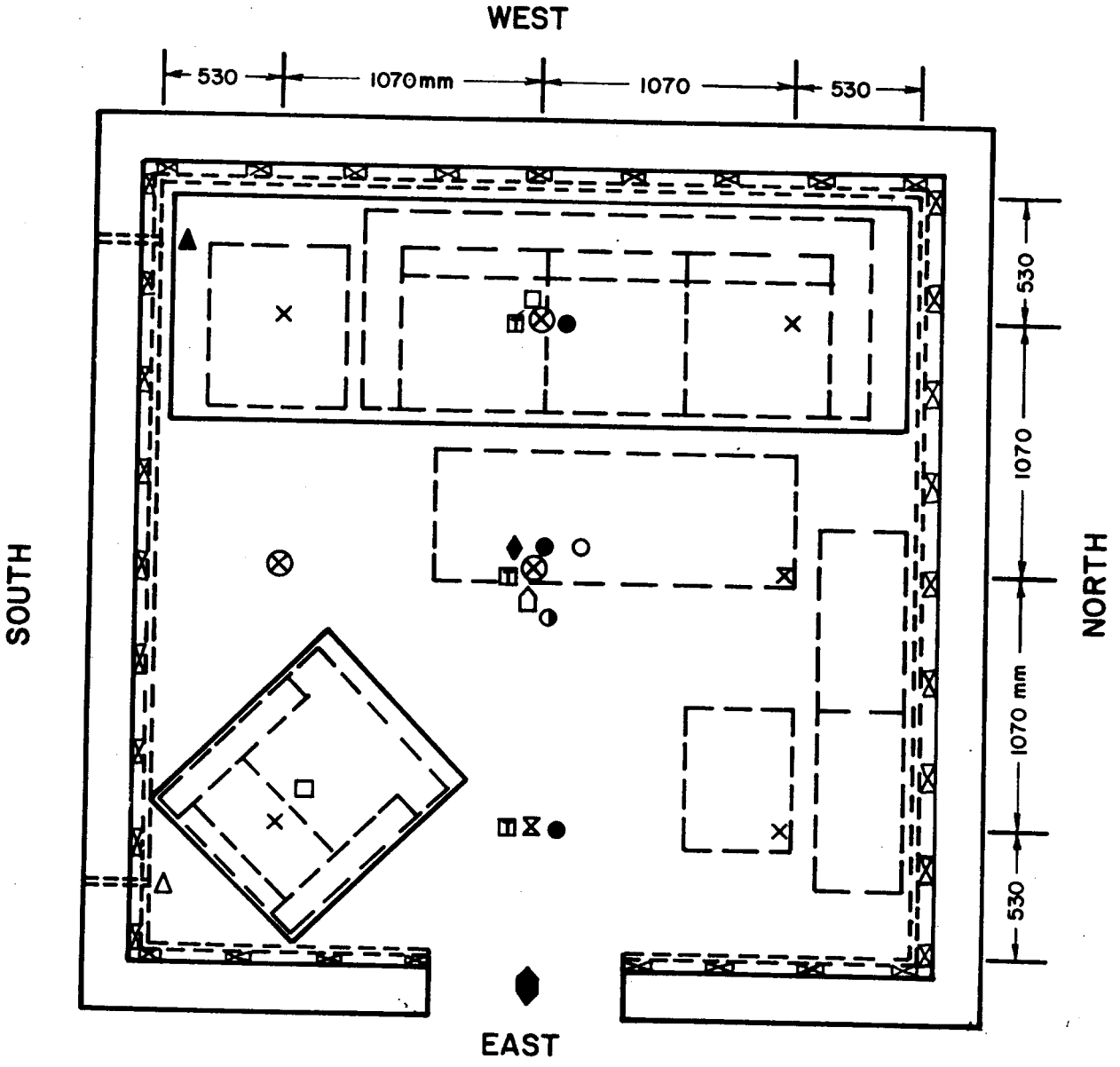

Figure 8a. Plan view of the 3.3 x 3.3 m test room showing instrumentation layout

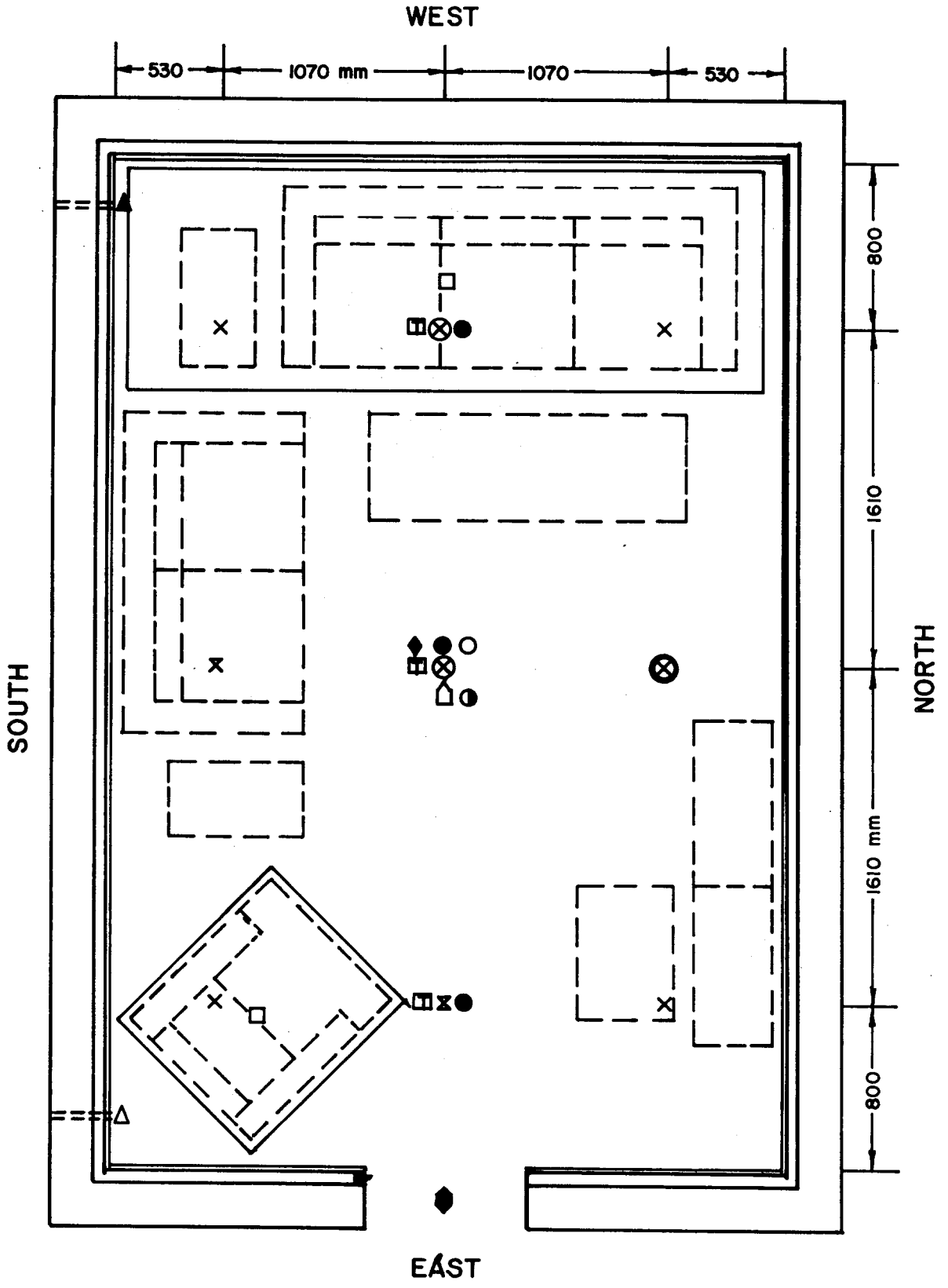

Figure 8b. Plan view of the 3.3 x 4.9 m test room showing instrumentation layout

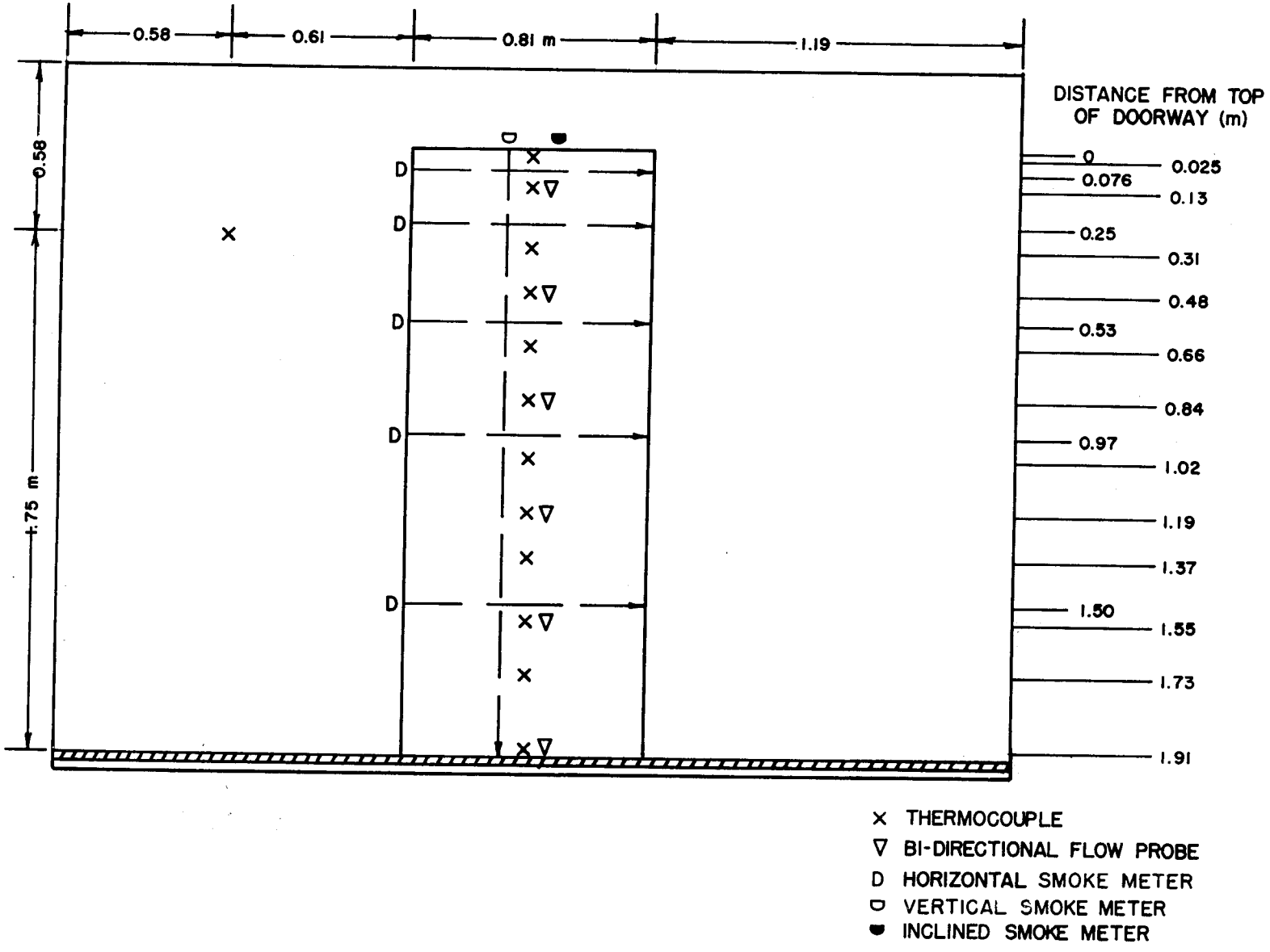

Figure 9. Instrumentation layout - view of doorway and east (front) wall showing gas thermocouples, velocity probes, and smoke meters

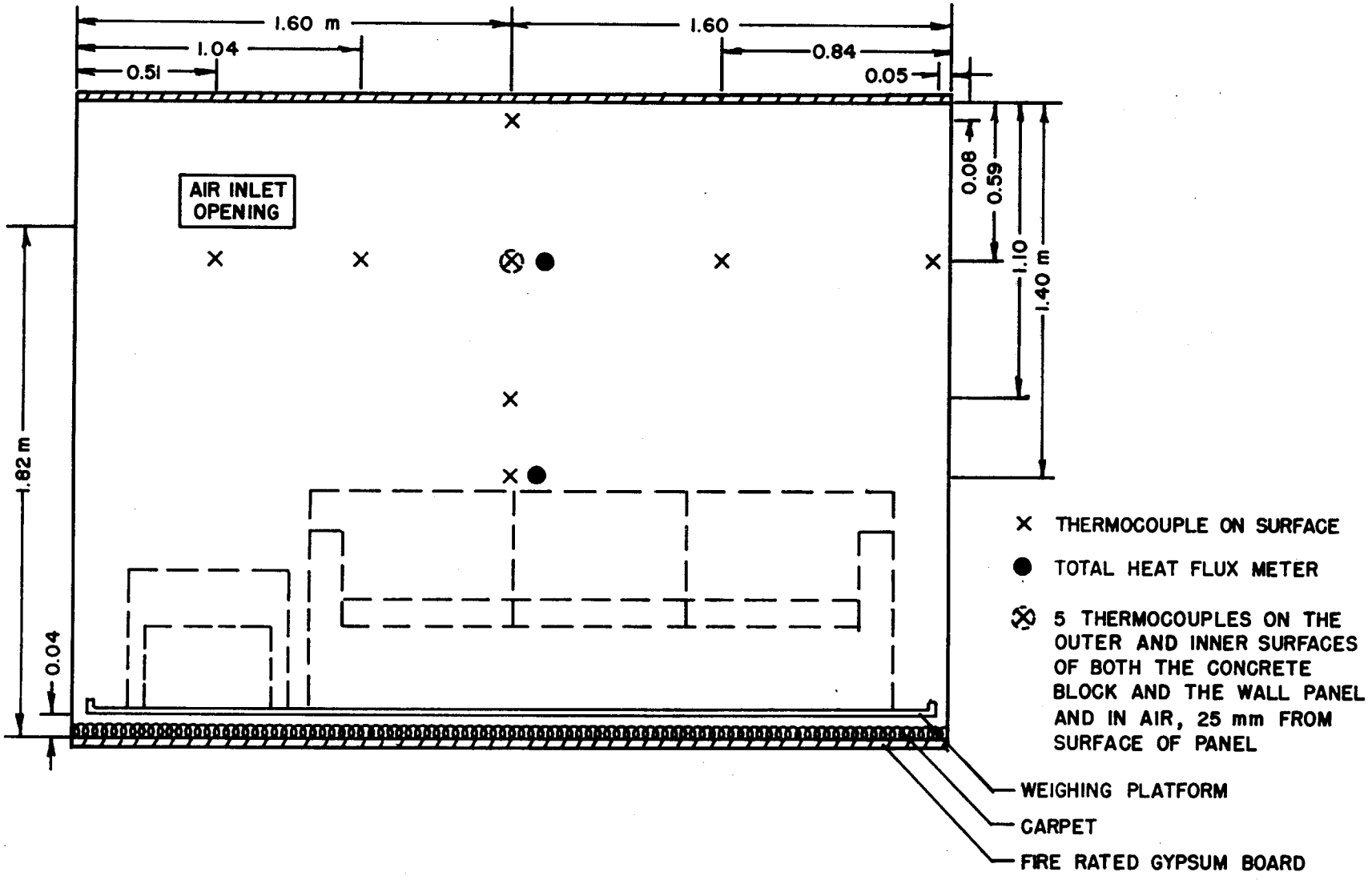

Figure 10. Instrumentation layout - view of west (back) wall showing wall thermocouples and heat flux meters

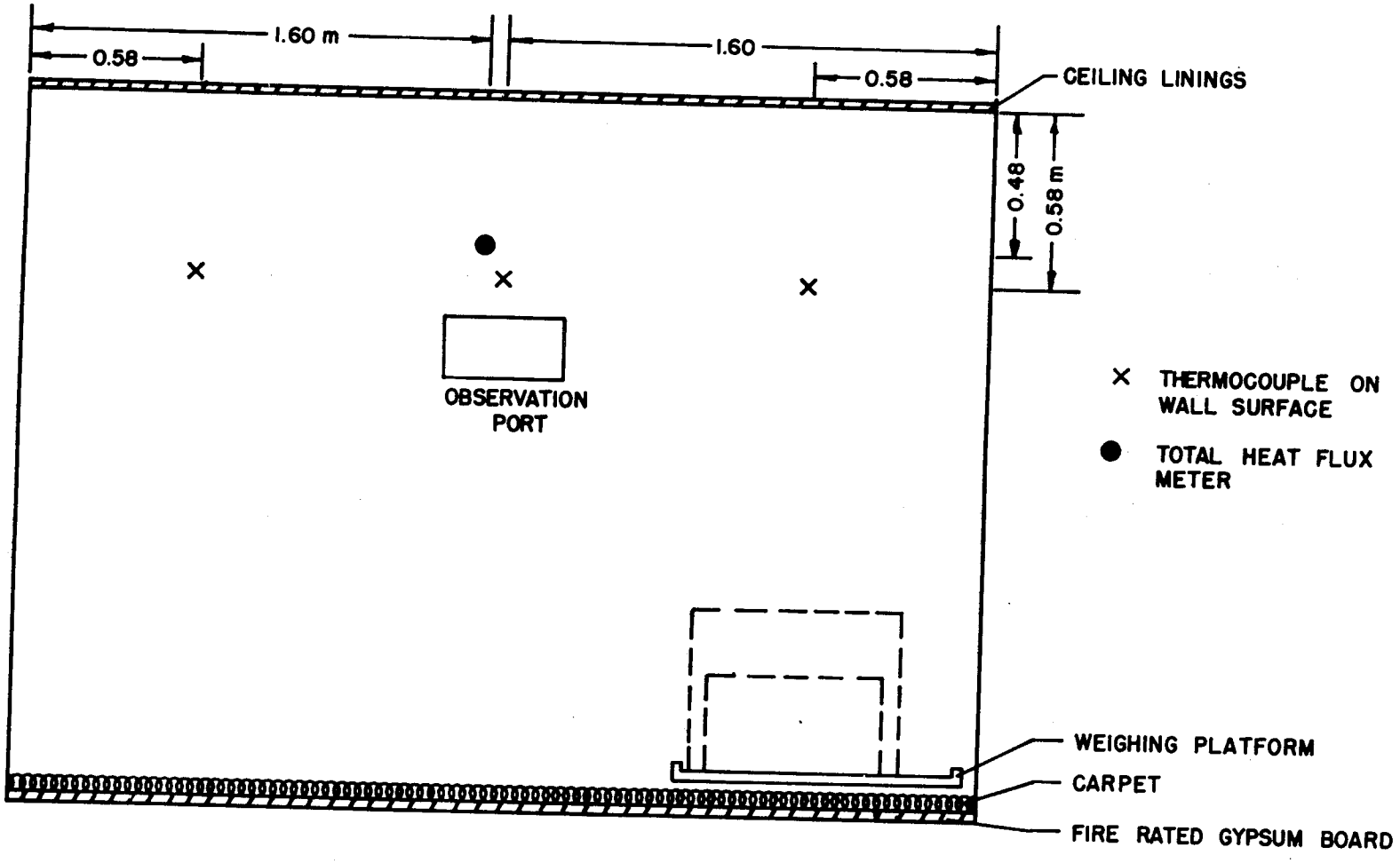

Figure 11a. Instrumentation layout - view of south wall of the 3.3 x 3.3 m test room showing wall thermocouples, heat flux meter, and observation port

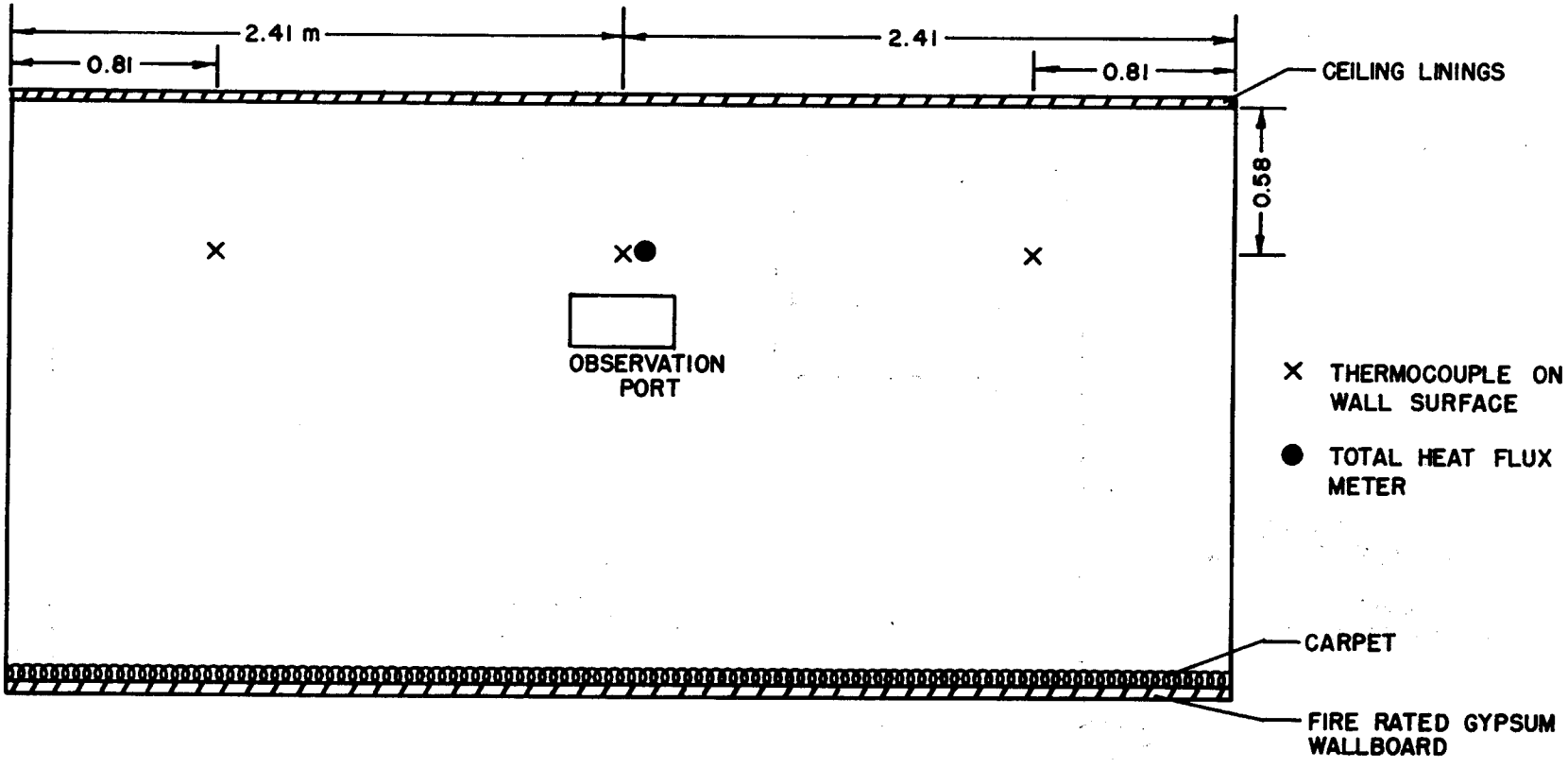

Figure 11b. Instrumentation layout - view of south wall of the 3.3 x 4.9 m test room

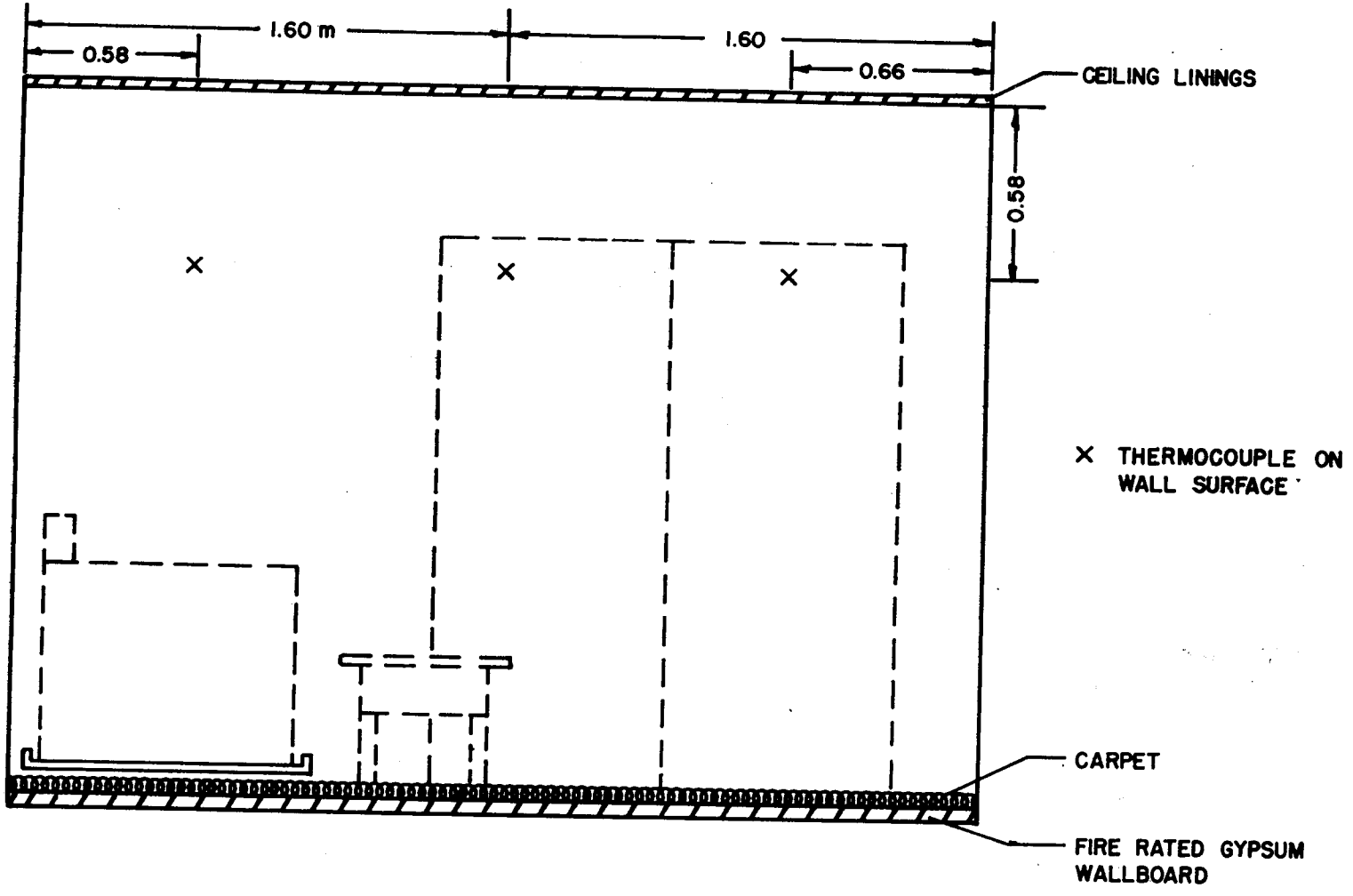

Figure 12a. Instrumentation layout - view of north wall of the 3.3 x 3.3 m test room showing wall thermocouples

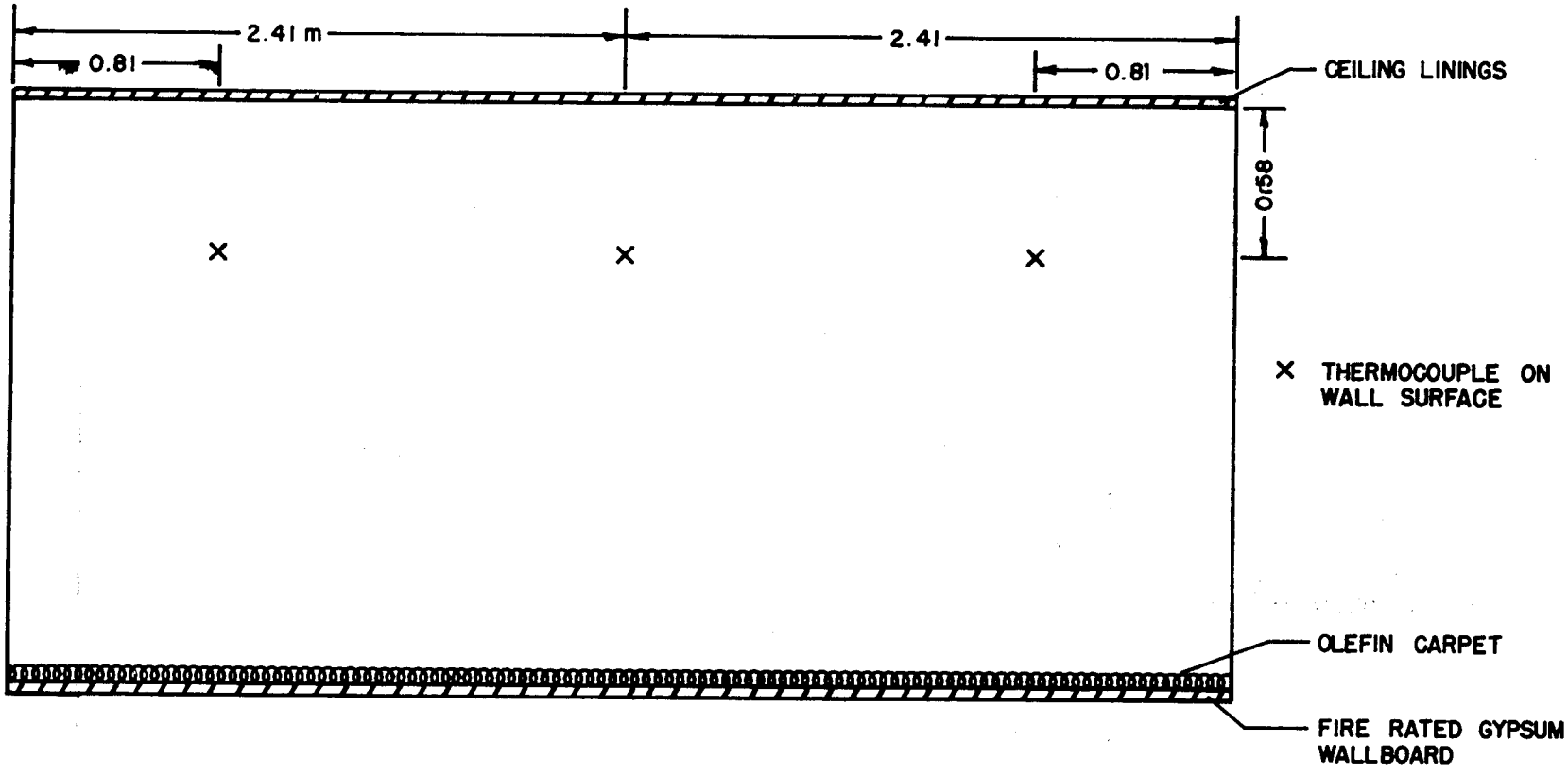

Figure 12b. Instrumentation layout - view of north wall of the 3.3 x 4.9 m test room

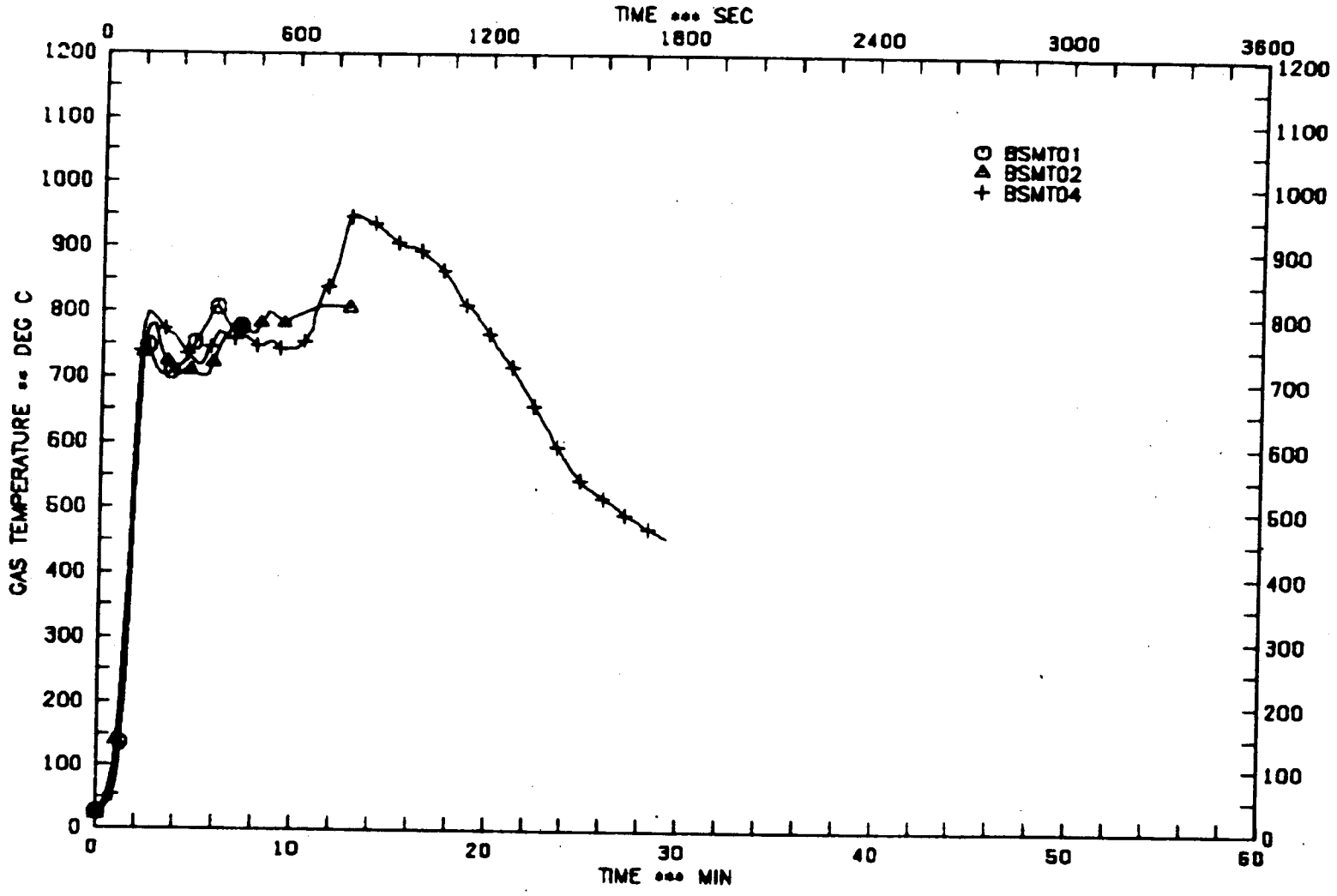

Figure 13a. Average gas temperatures as a function of time for tests 1, 2, and 4 (temperatures above 800°C are not reliable)

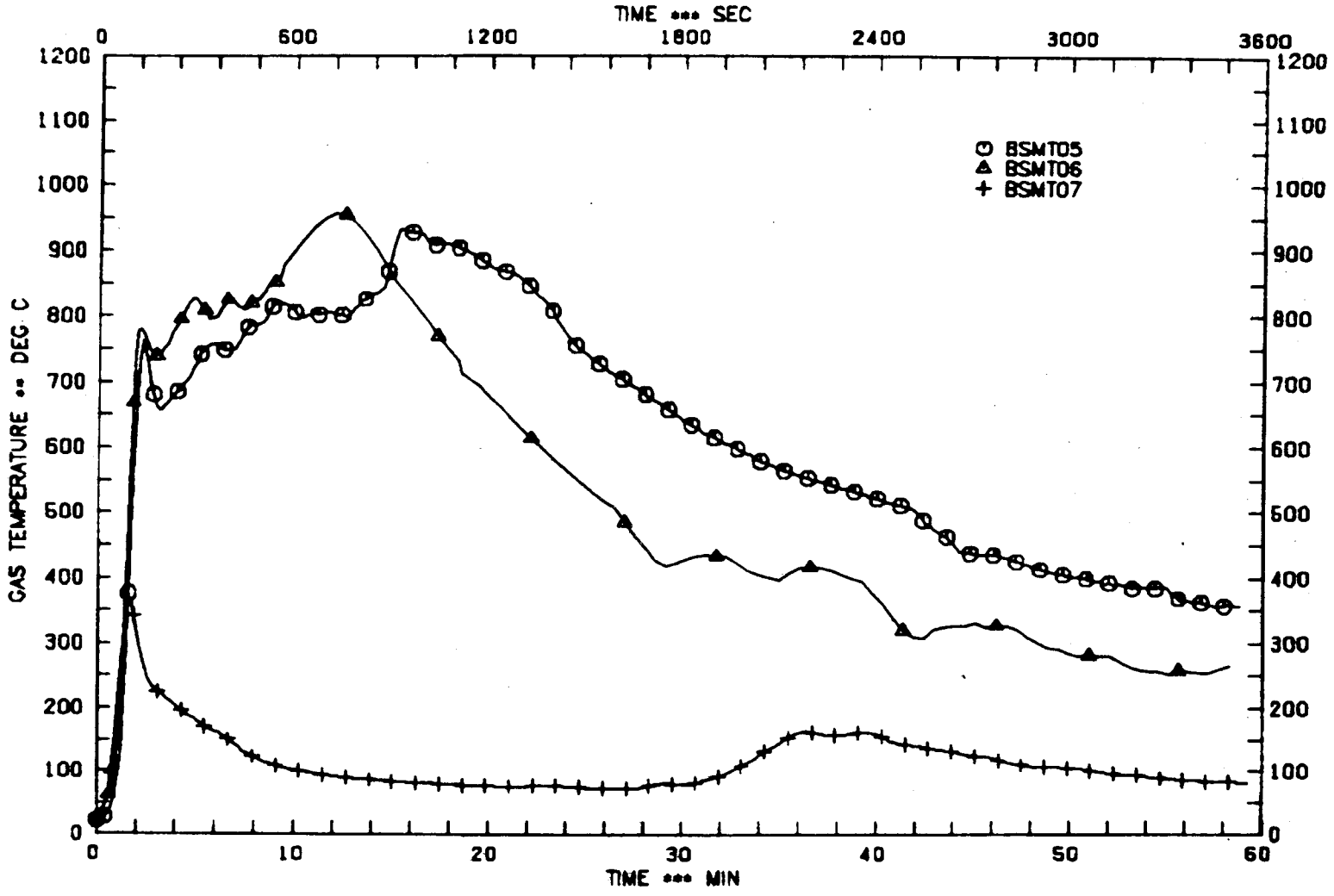

Figure 13b. Average gas temperatures as a function of time for tests 5, 6, and 7 (temperatures above 800°C are not reliable)

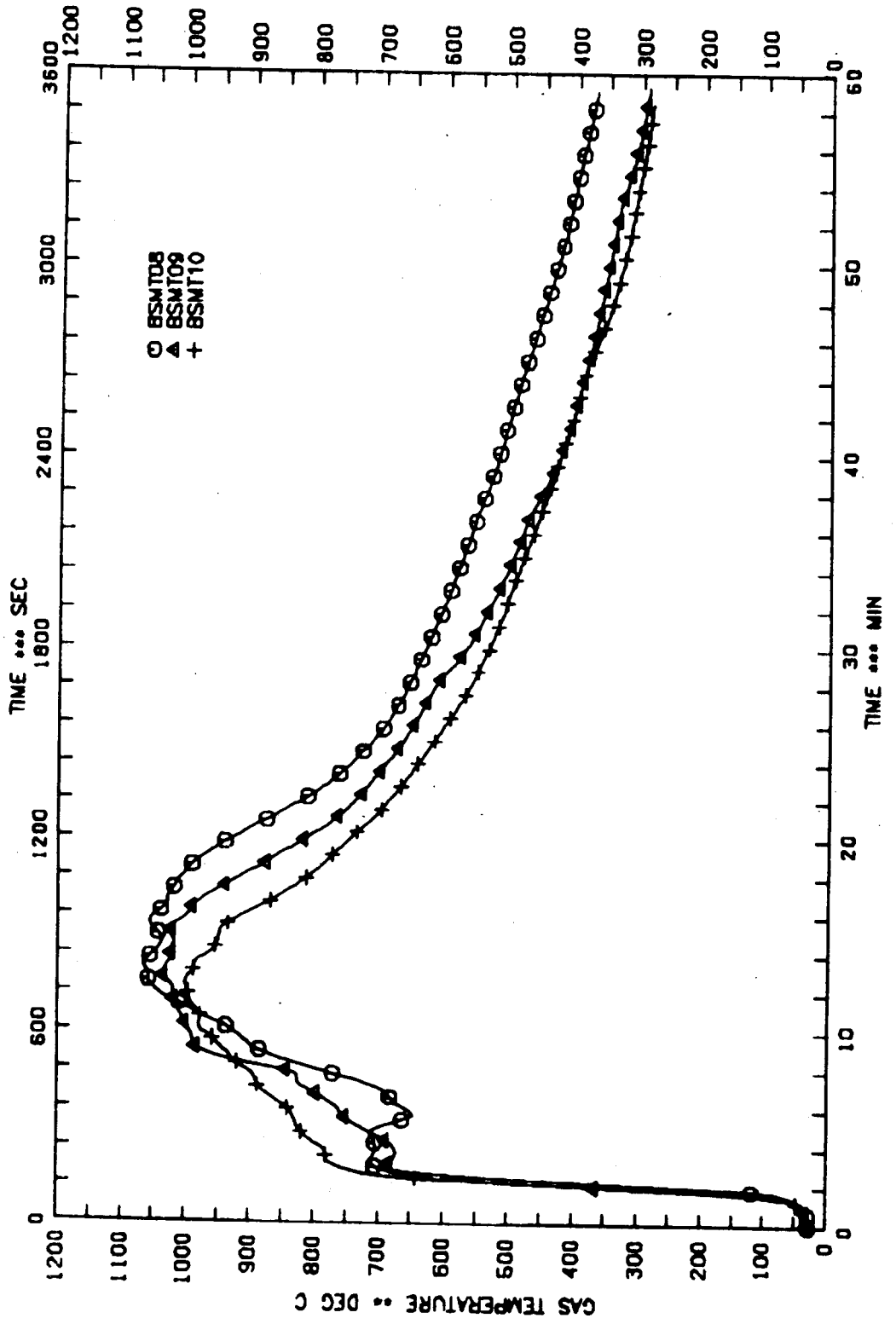

Figure 13c. Average gas temperatures as a function of time for tests 8, 9, and 10

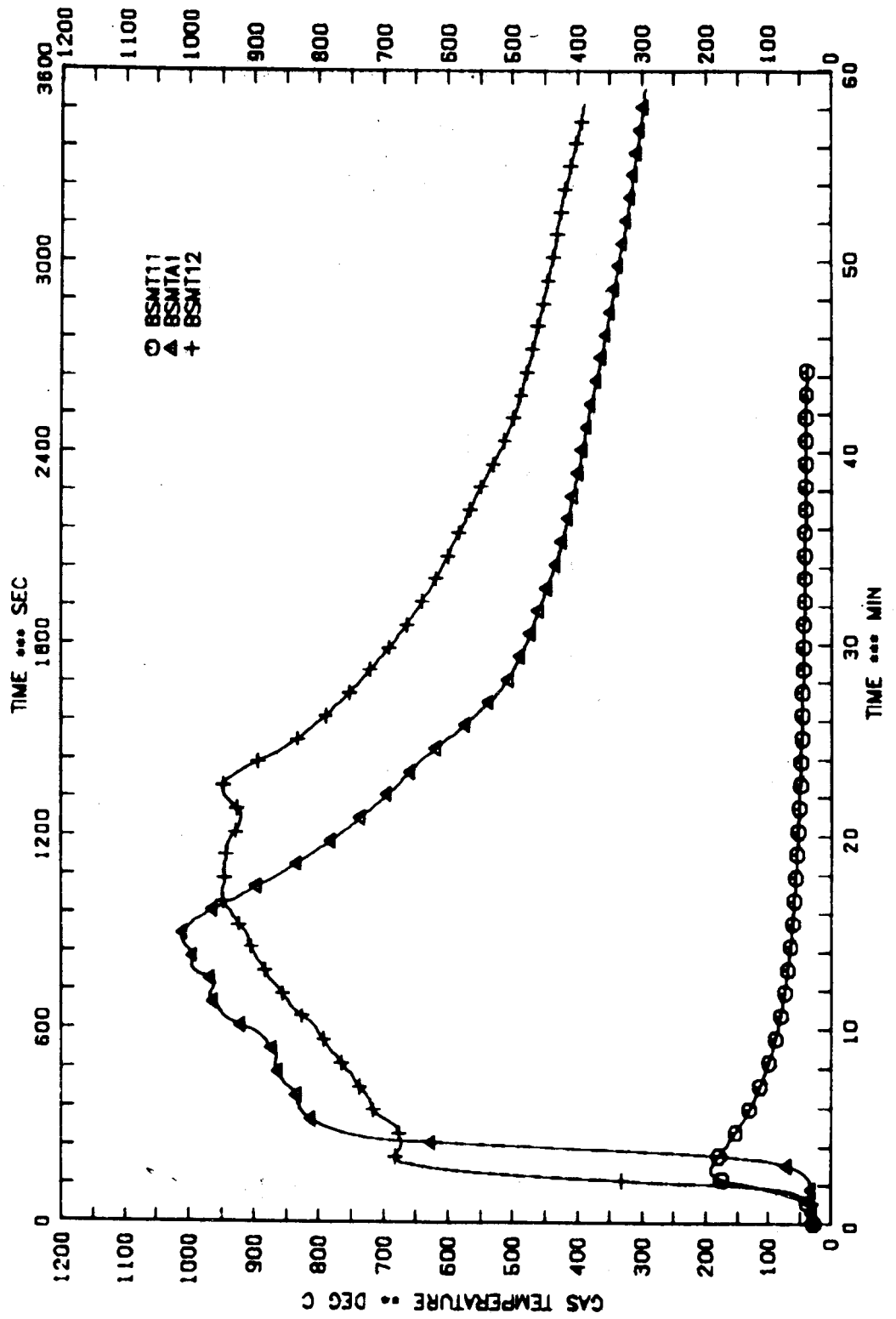

Figure 13d. Average gas temperatures as a function of time for tests 11, 11A, and 12

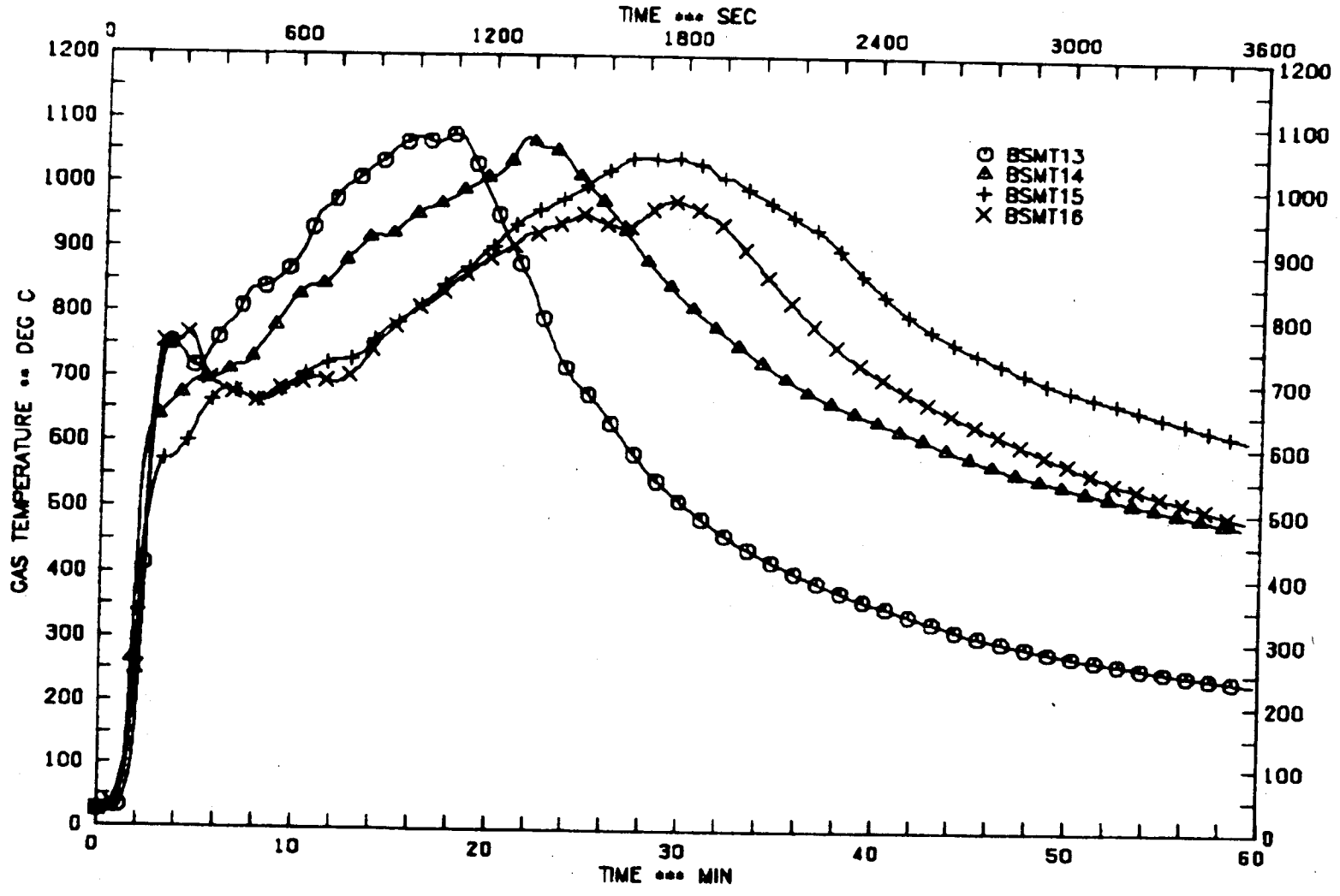

Figure 13e. Average gas temperatures as a function of time for tests 13, 14, 15, and 16

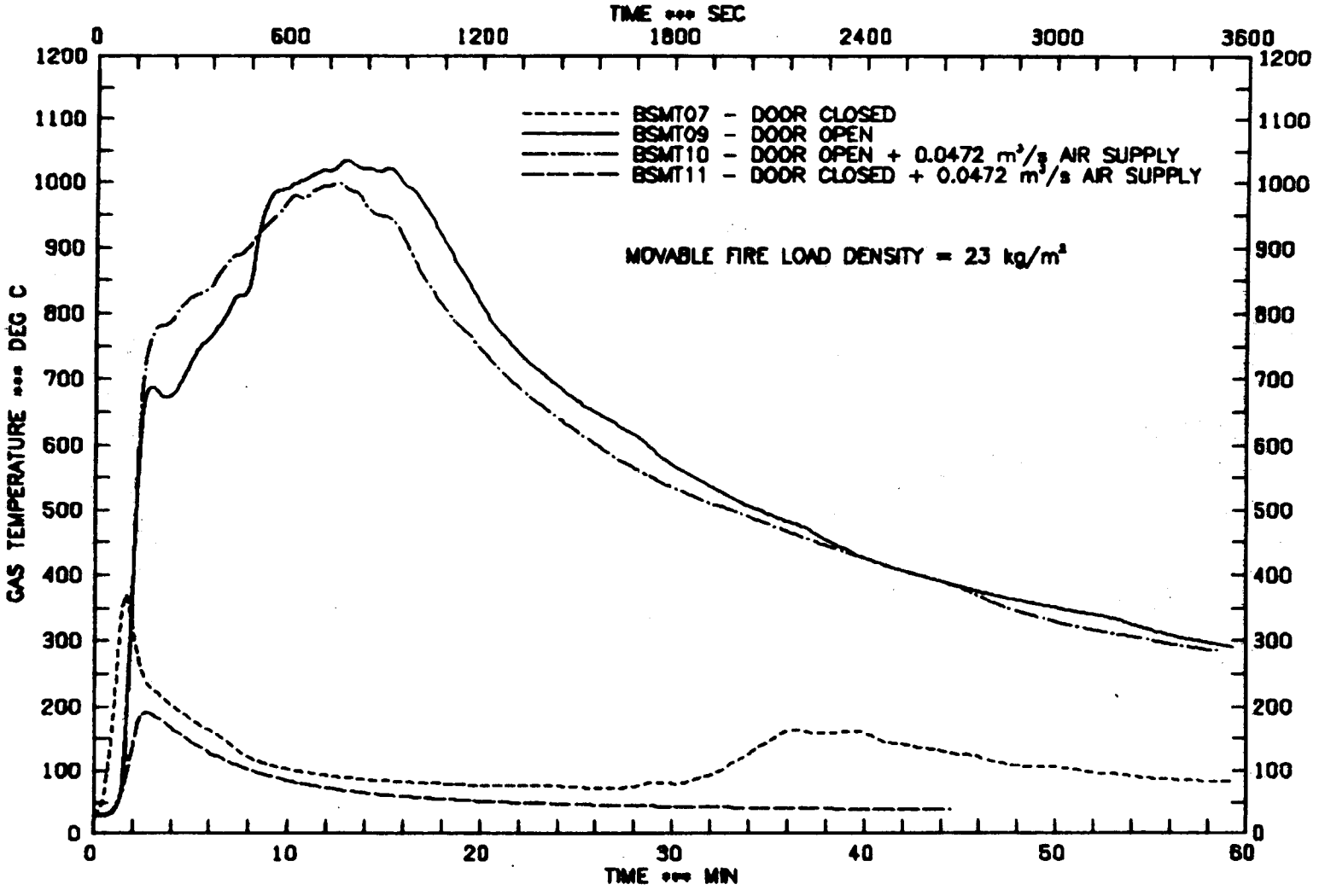

Figure 14. Time variation of average gas temperatures as a function of room ventilation

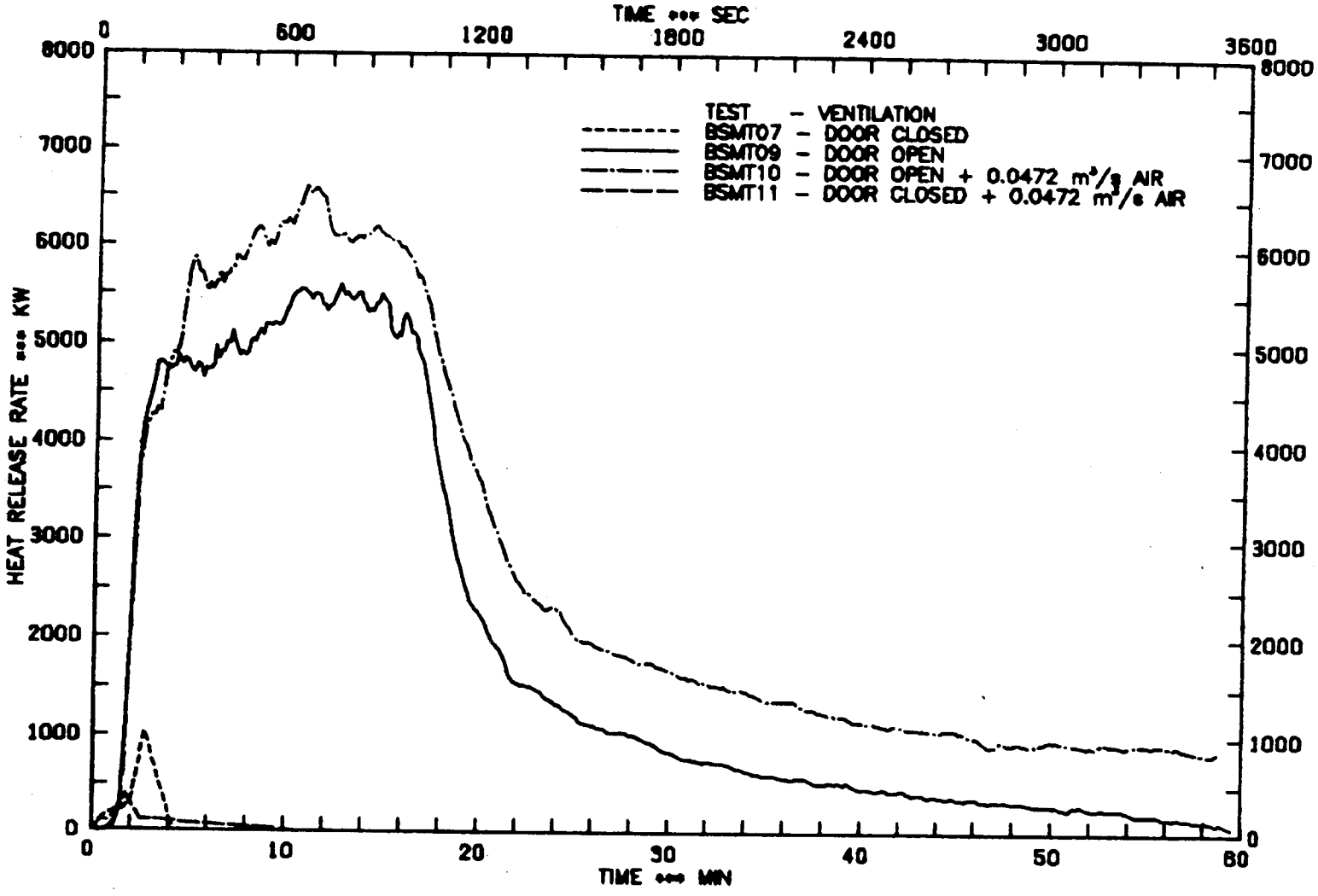

Figure 15. Time variation of total heat release rate as a function of room ventilation

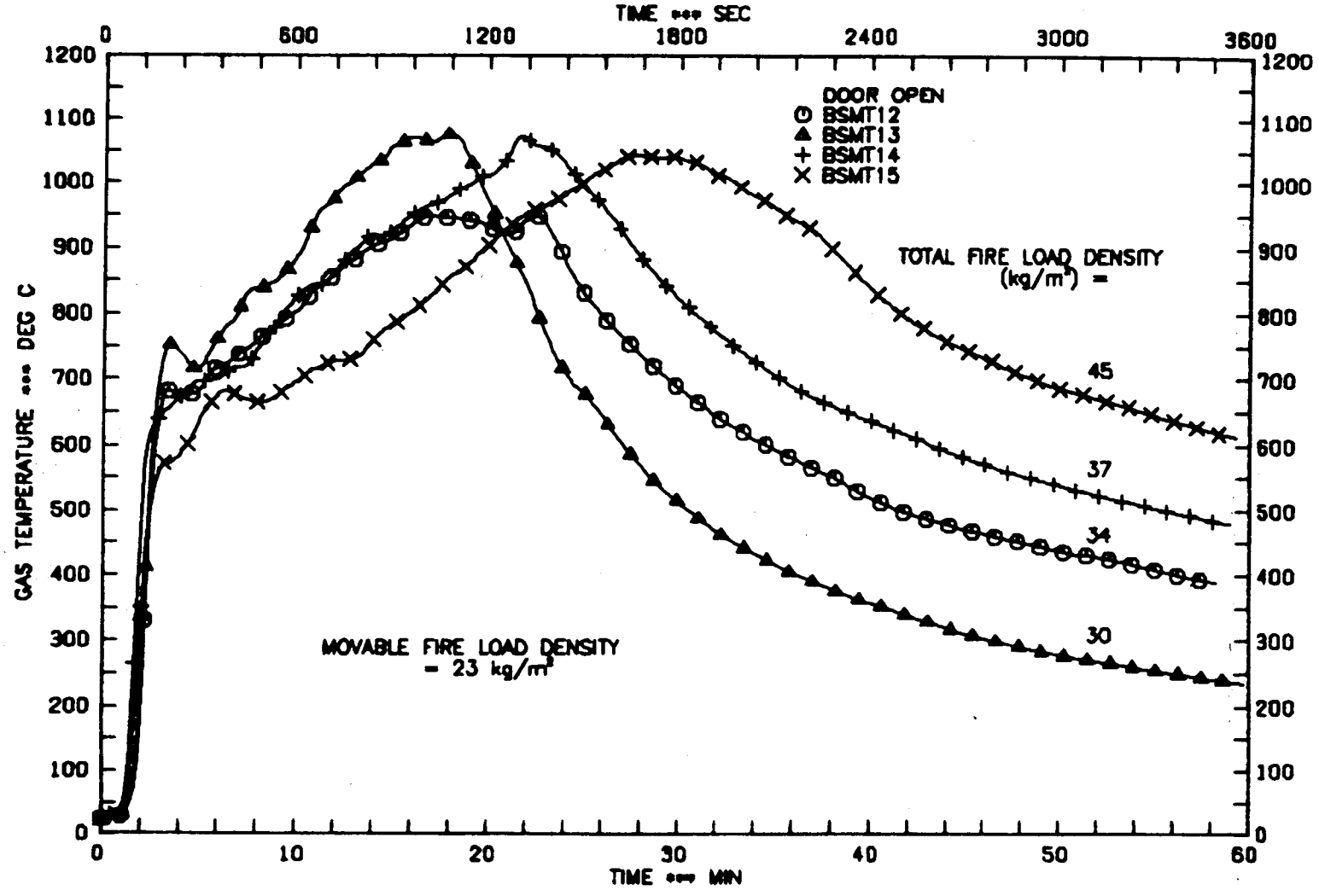

Figure 16. Time variation of average gas temperatures as a function of fire load density

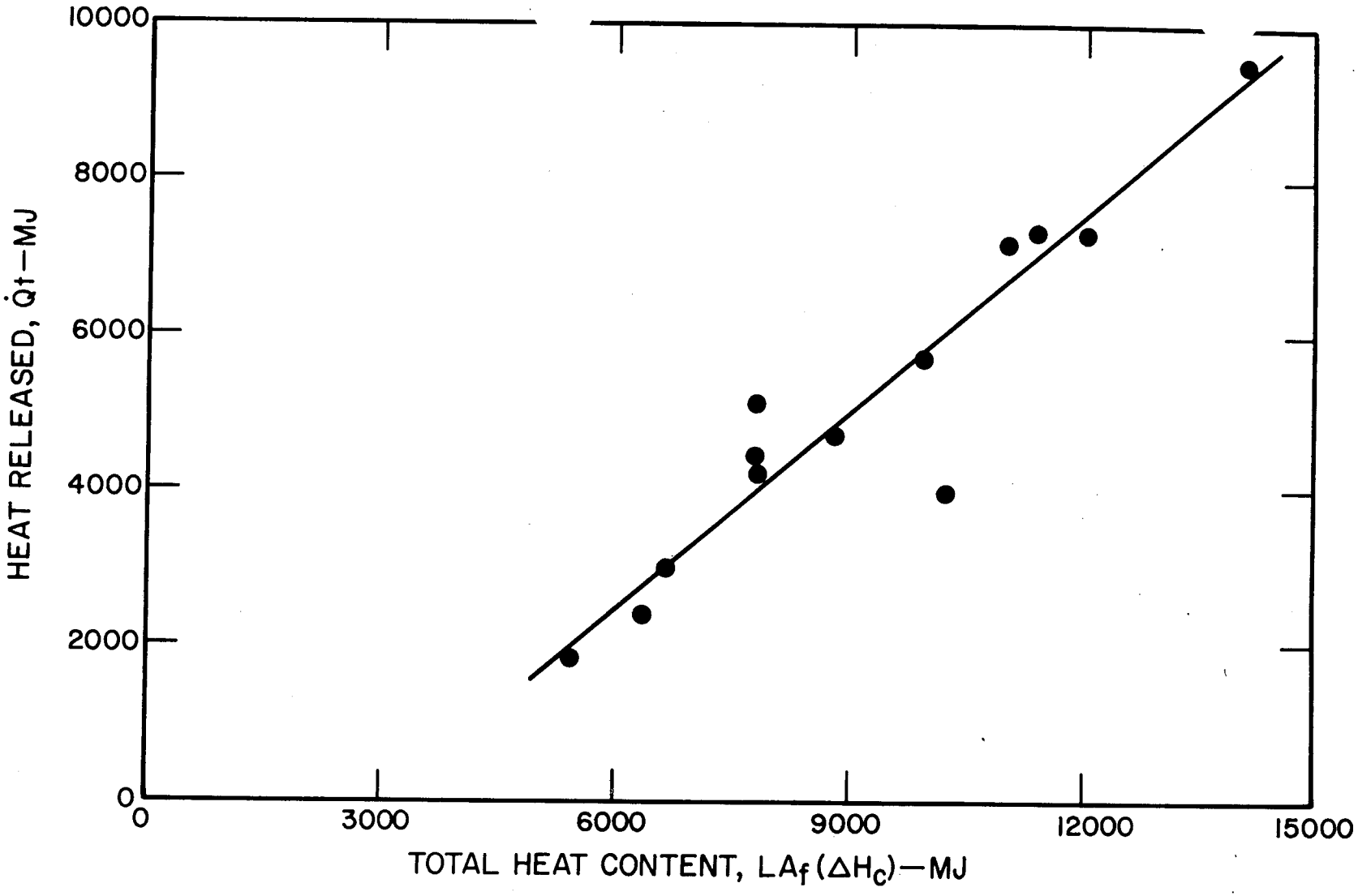

Figure 17. Relationship between heat released within fire room during active burning period and total heat content of combustible materials

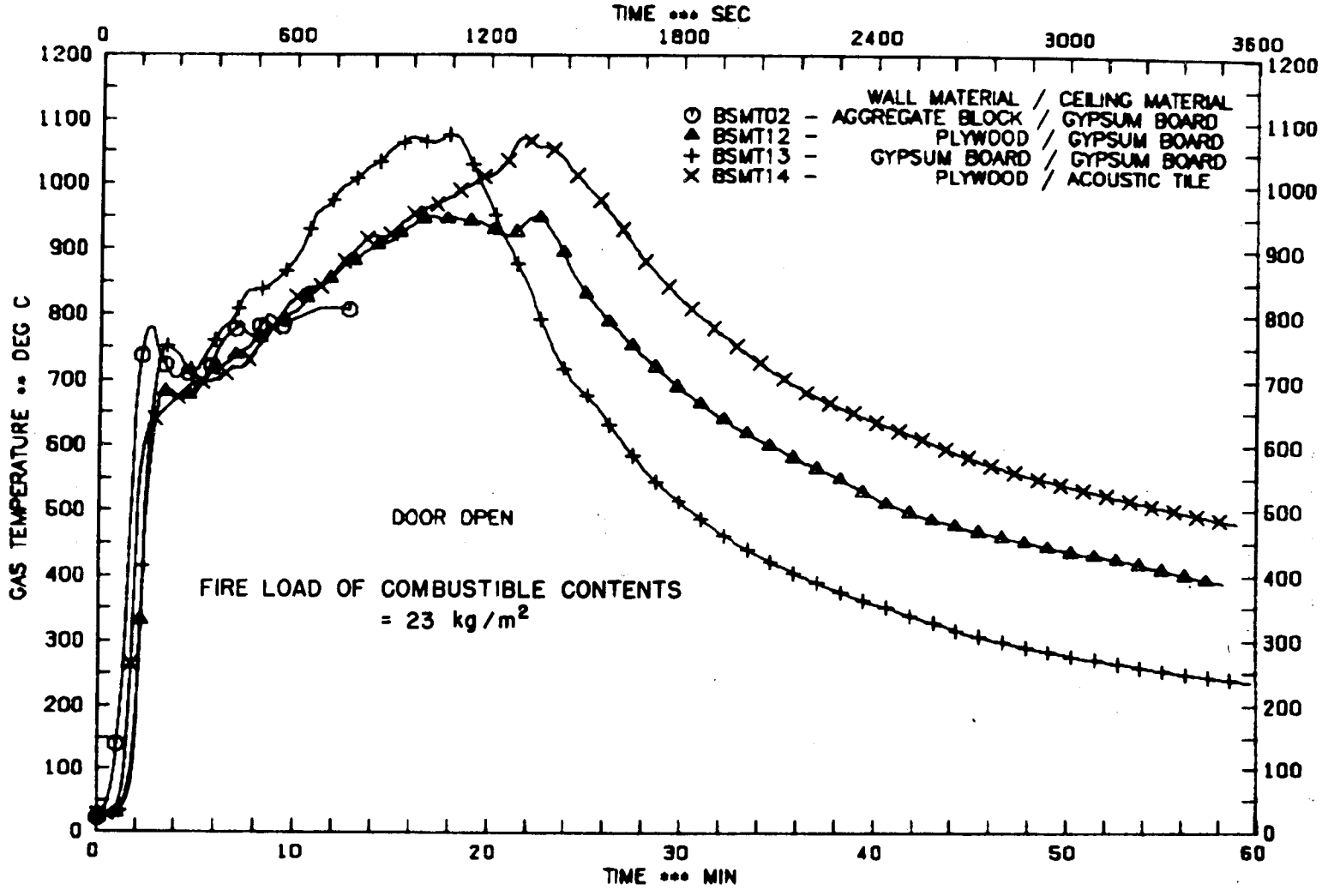

Figure 18. Time variation of average gas temperatures as a function of room lining materials

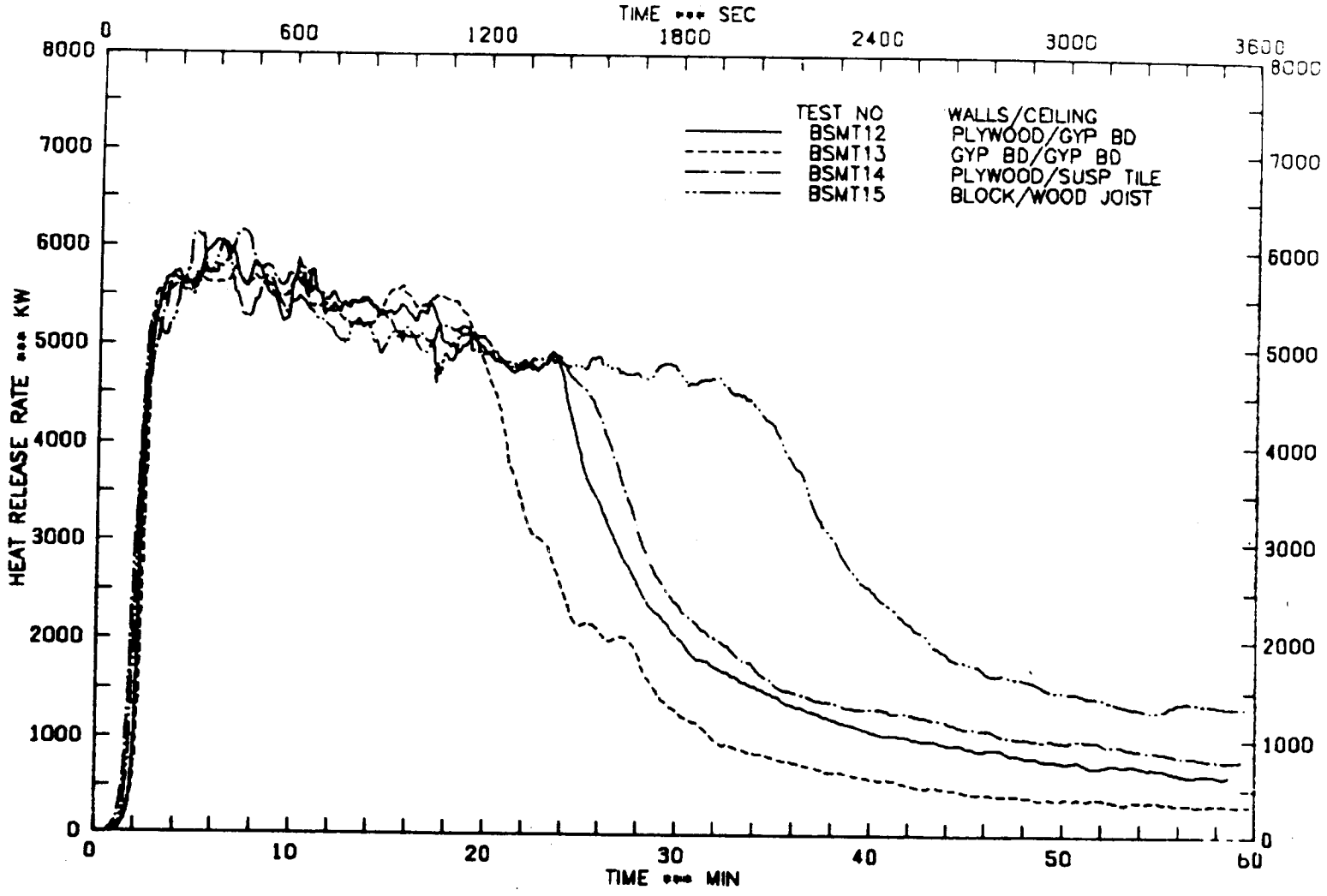

Figure 19. A comparison of heat release rates with various interior finish materials

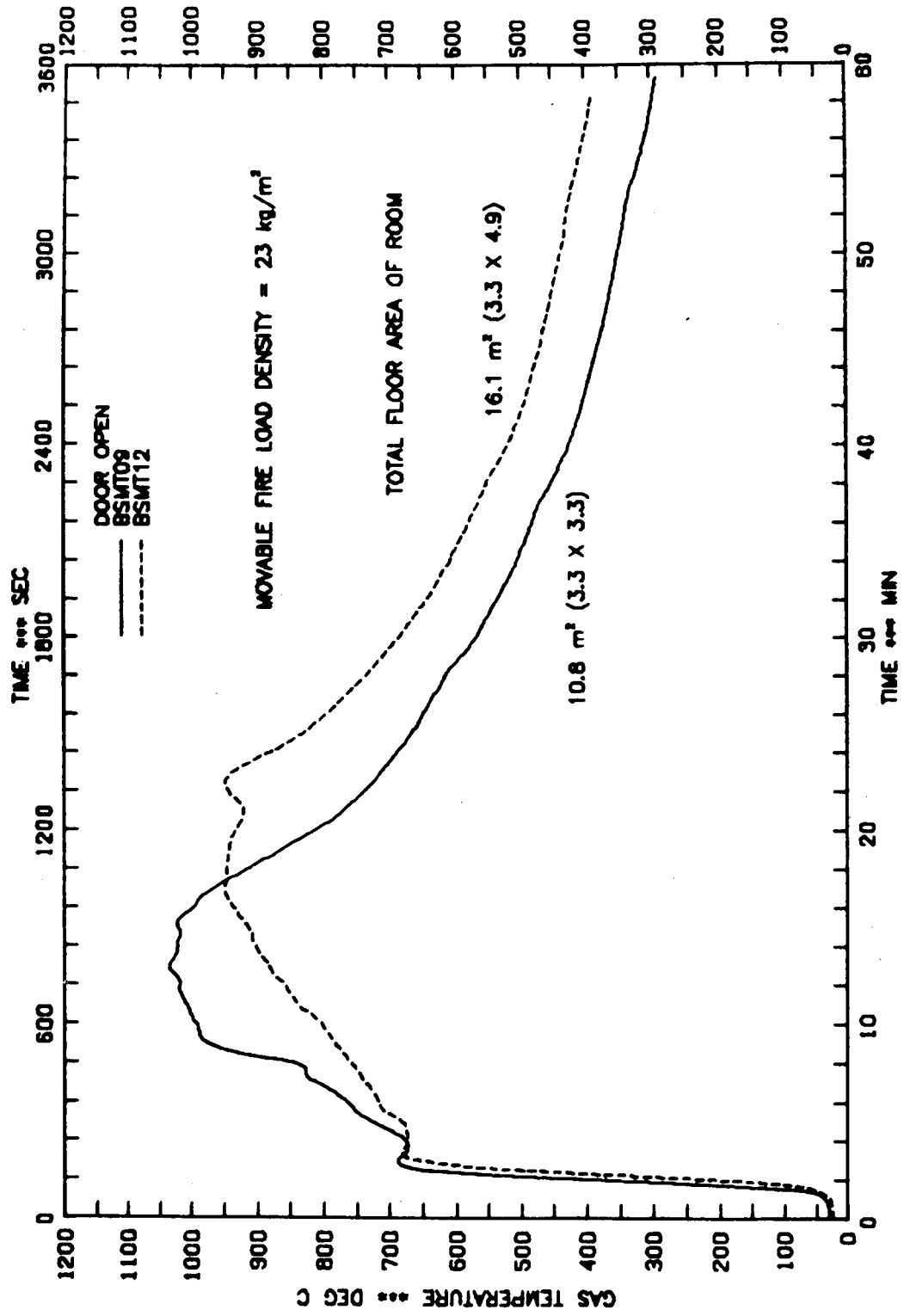

Figure 20. Time variation of average gas temperatures as a function of room size

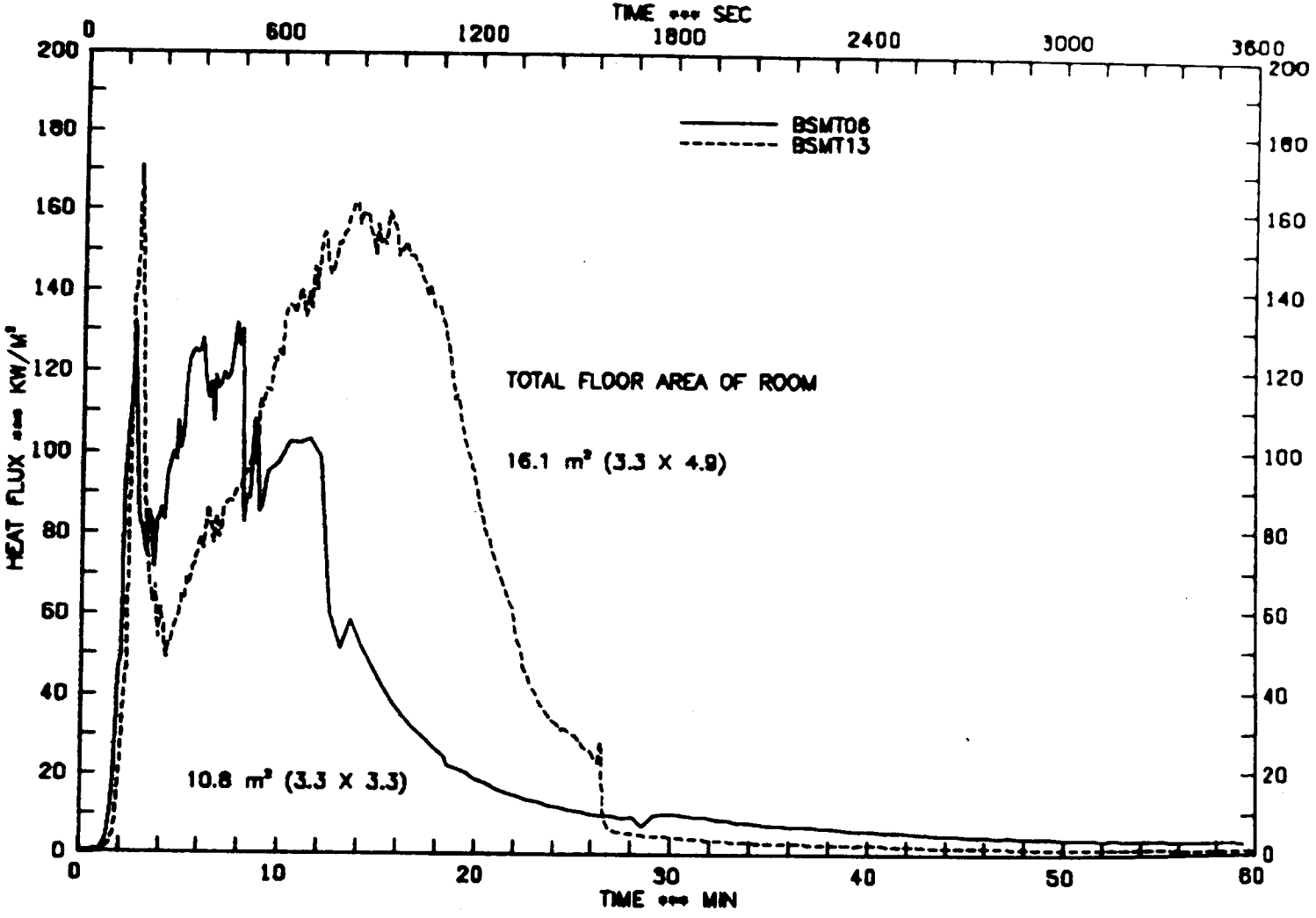

Figure 21. Time variation of heat flux incident at the center of the floor as a function of room size

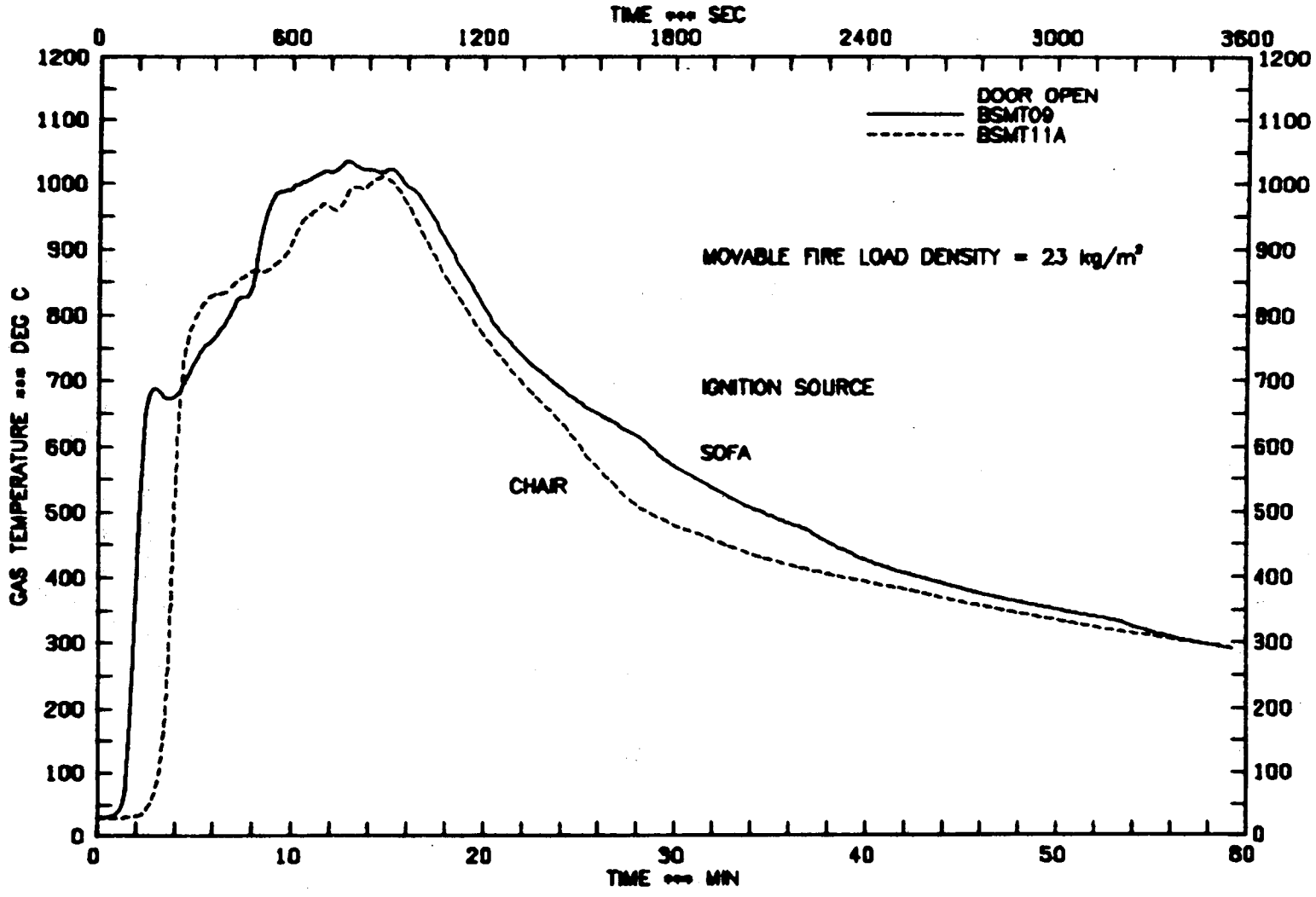

Figure 22. Time variation of average gas temperatures as a function of ignition source

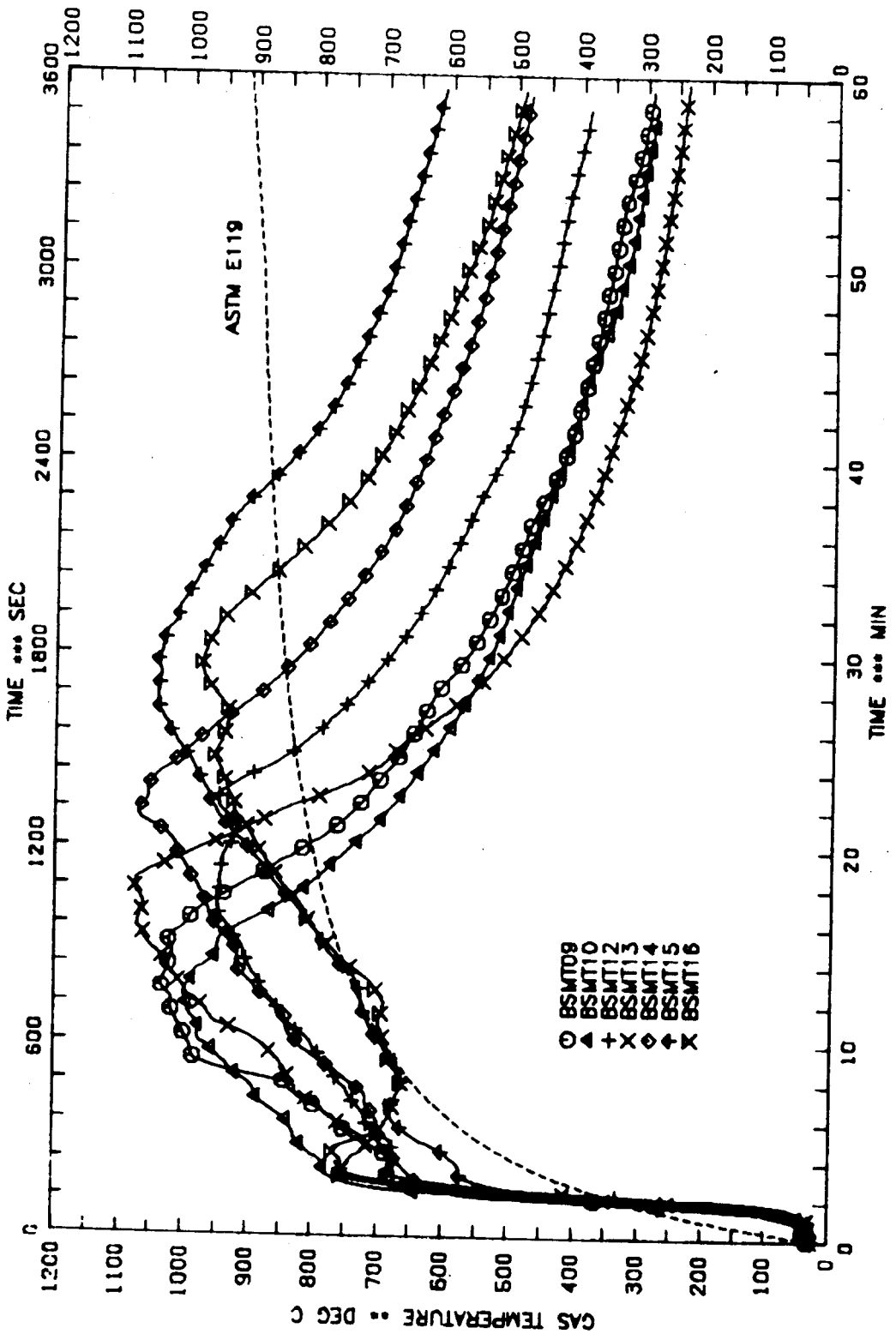

Figure 23. The range of variation in average gas temperatures for residential room fires

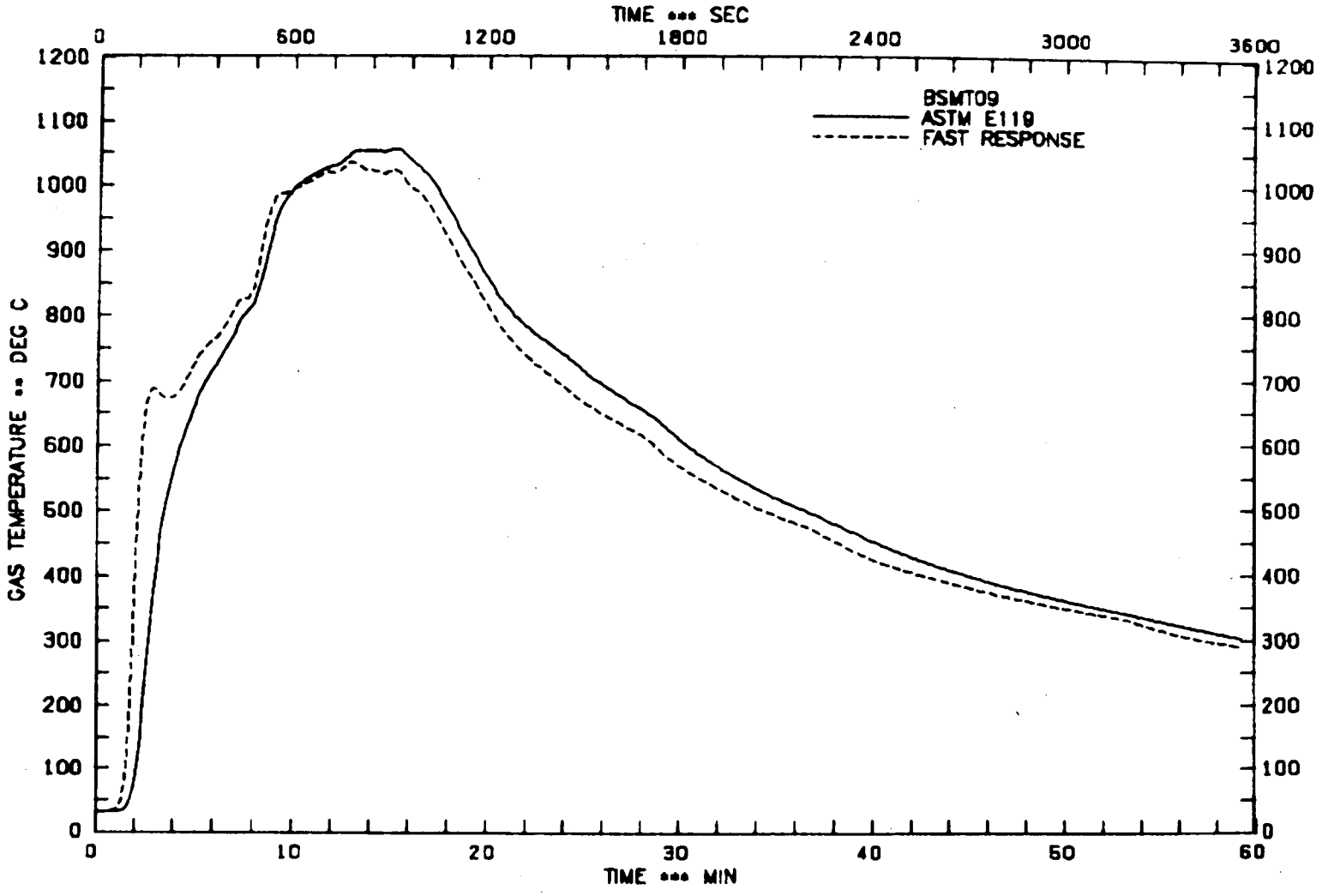

Figure 24. A comparison of results obtained from ASTM E 119 and fast response thermocouples for average gas temperatures

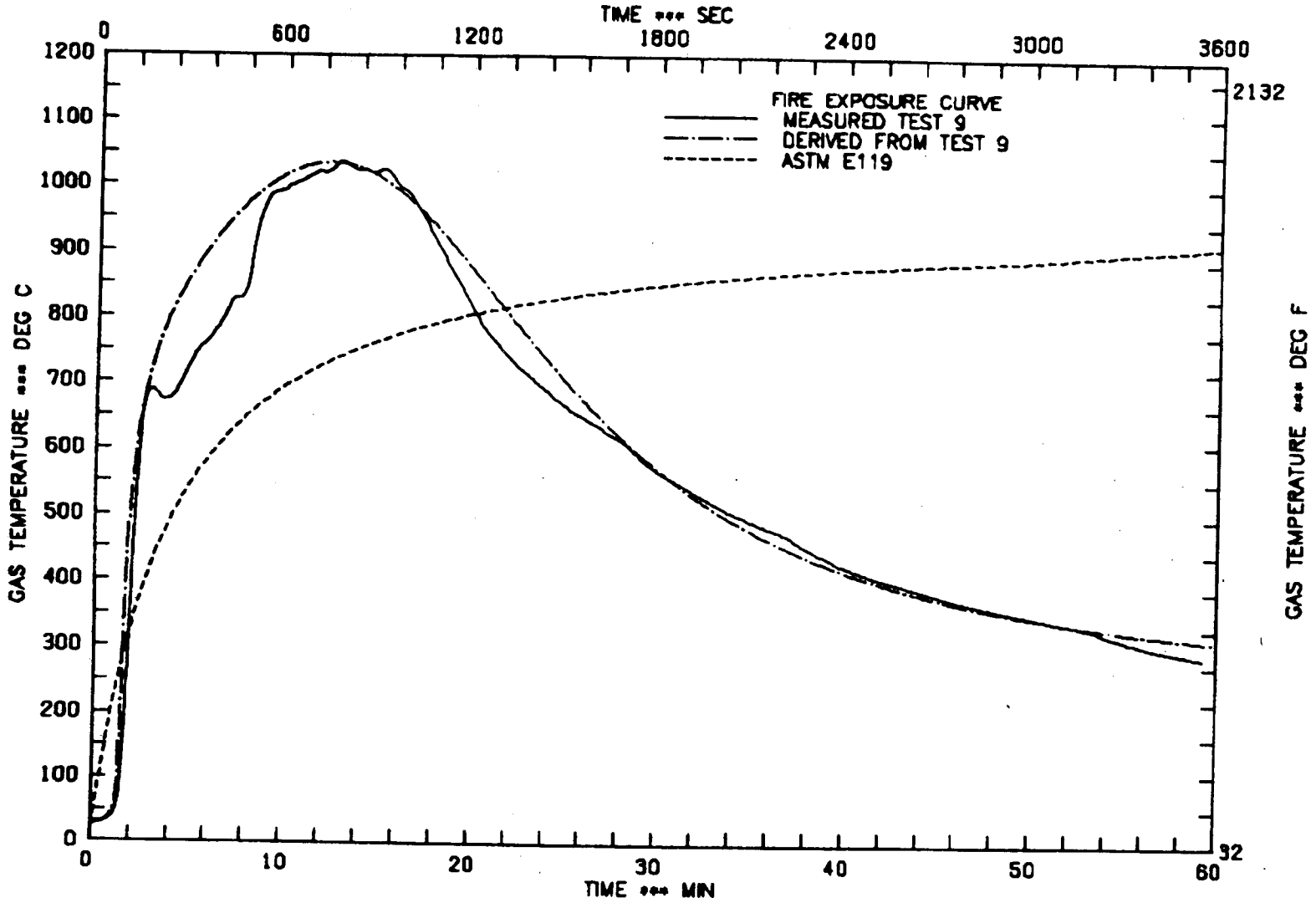

Figure 25. Comparison of fire exposure curve derived from room fire test 9 and ASTM E 119 standard curve

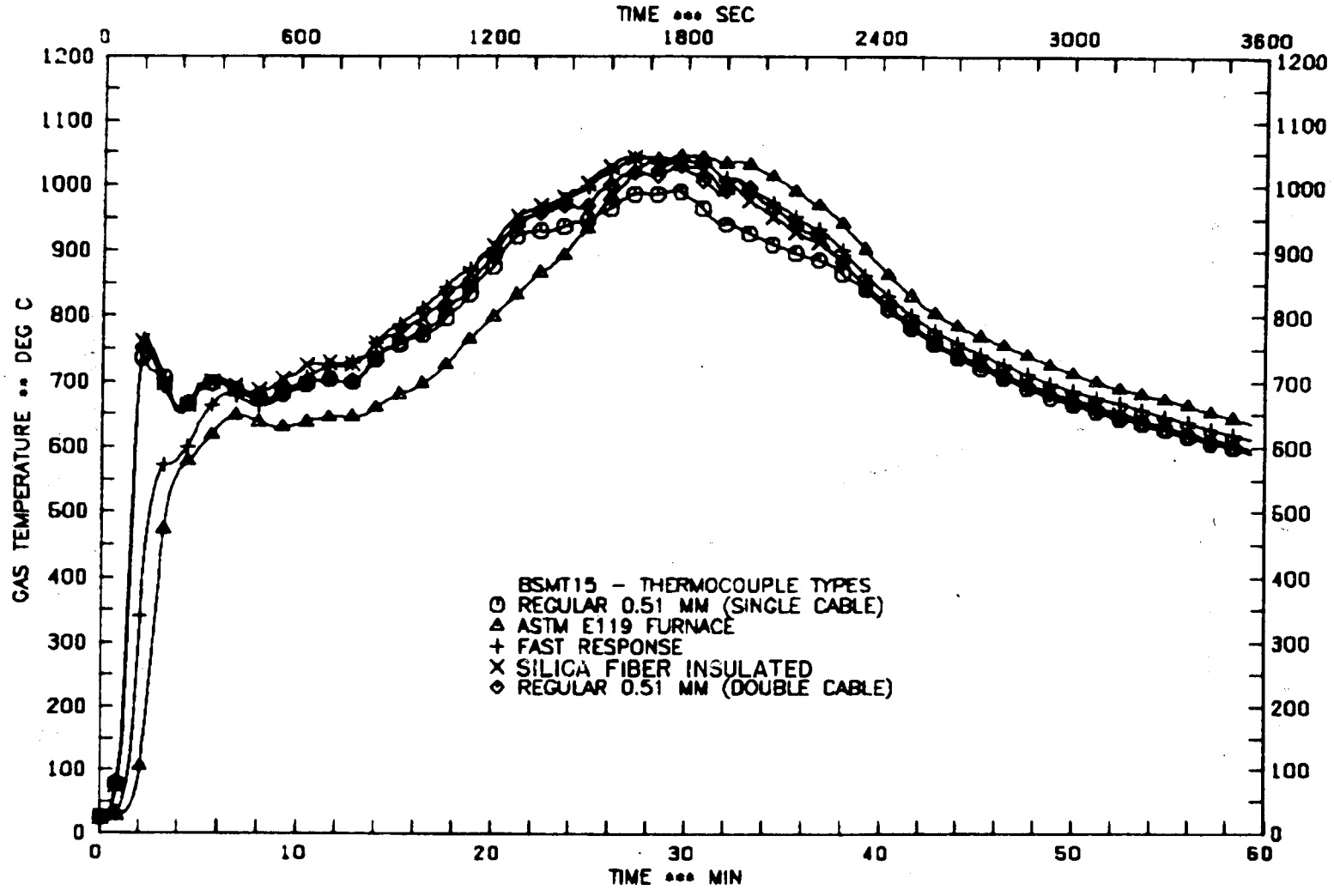

Figure 26. Comparison of average gas temperatures as measured by different types of thermocouples

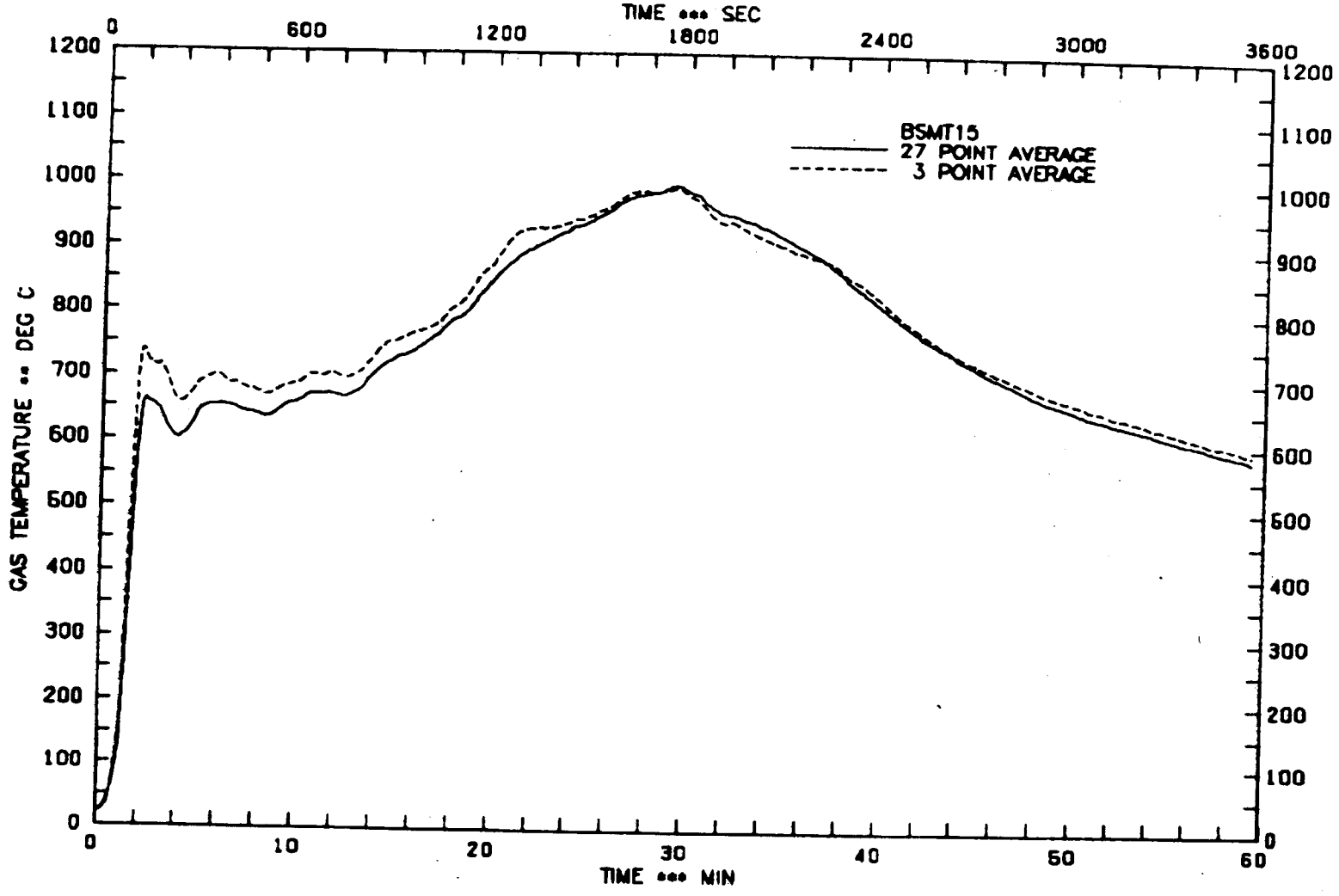

Figure 27. A comparison of gas temperature averages calculated using 27 and 3 locations

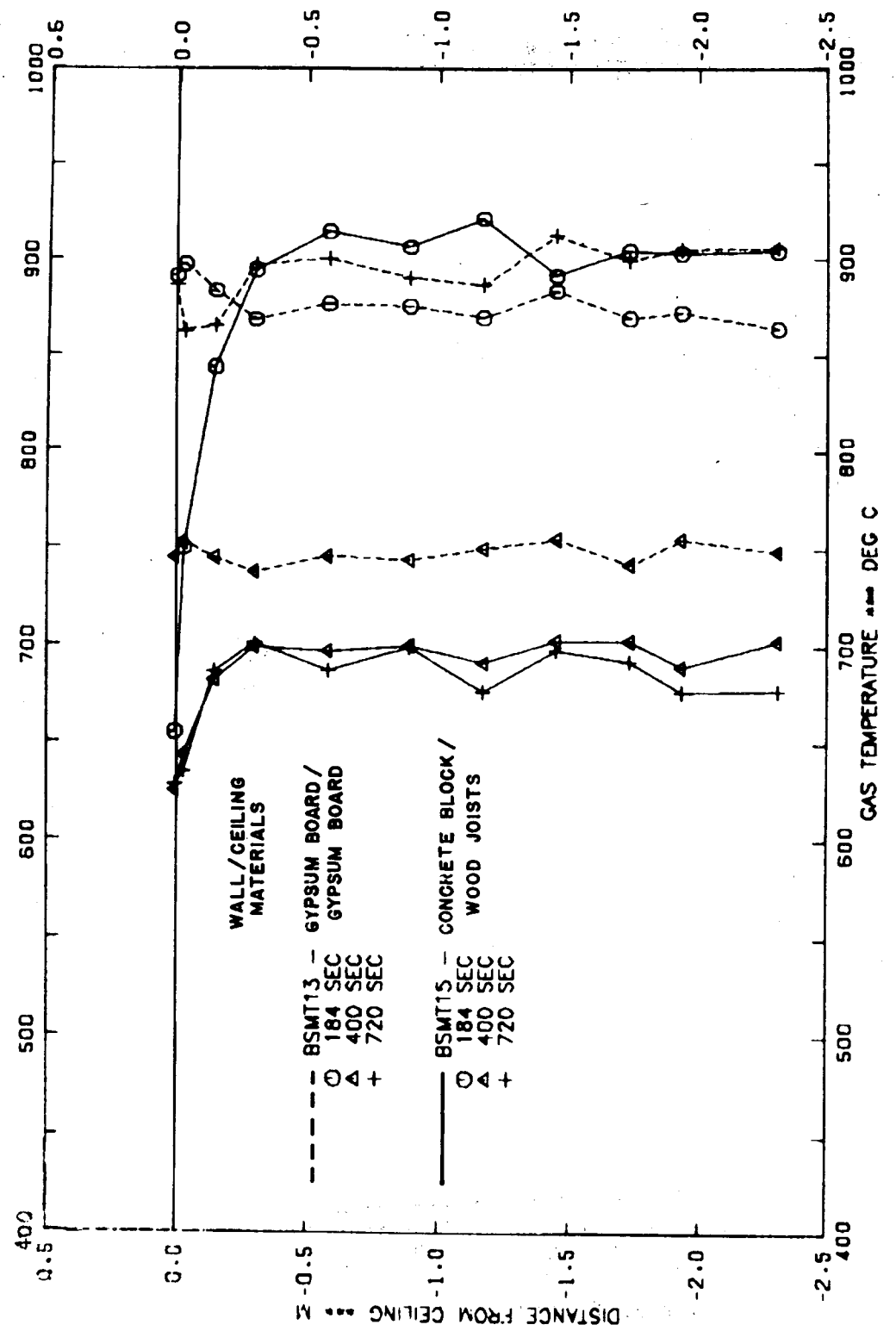

Figure 28. The influence of the combustibility of the ceiling materials on the vertical gas temperature profiles

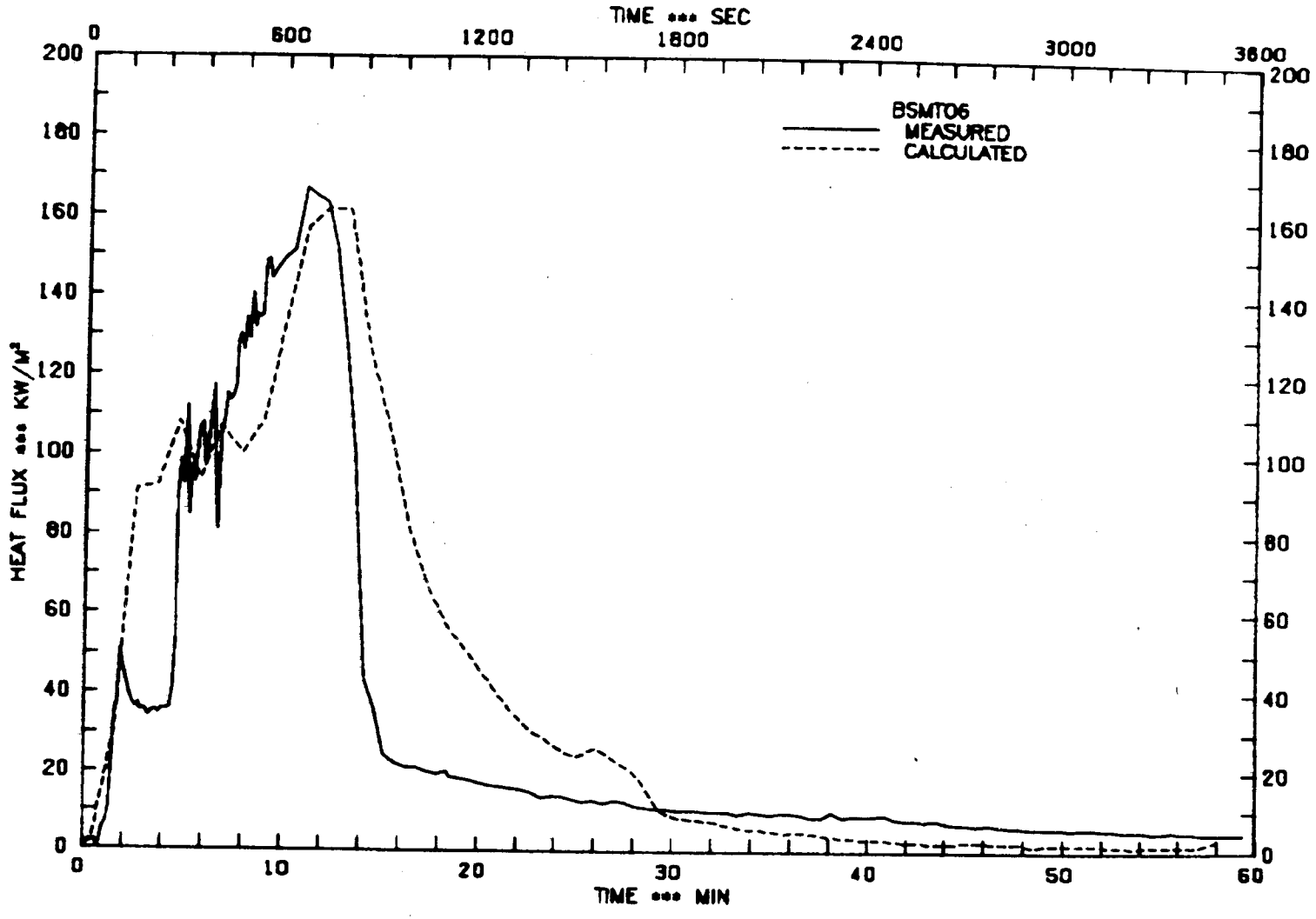

Figure 29a. Comparison of the calculated and measured total heat flux incident on the gypsum board ceiling

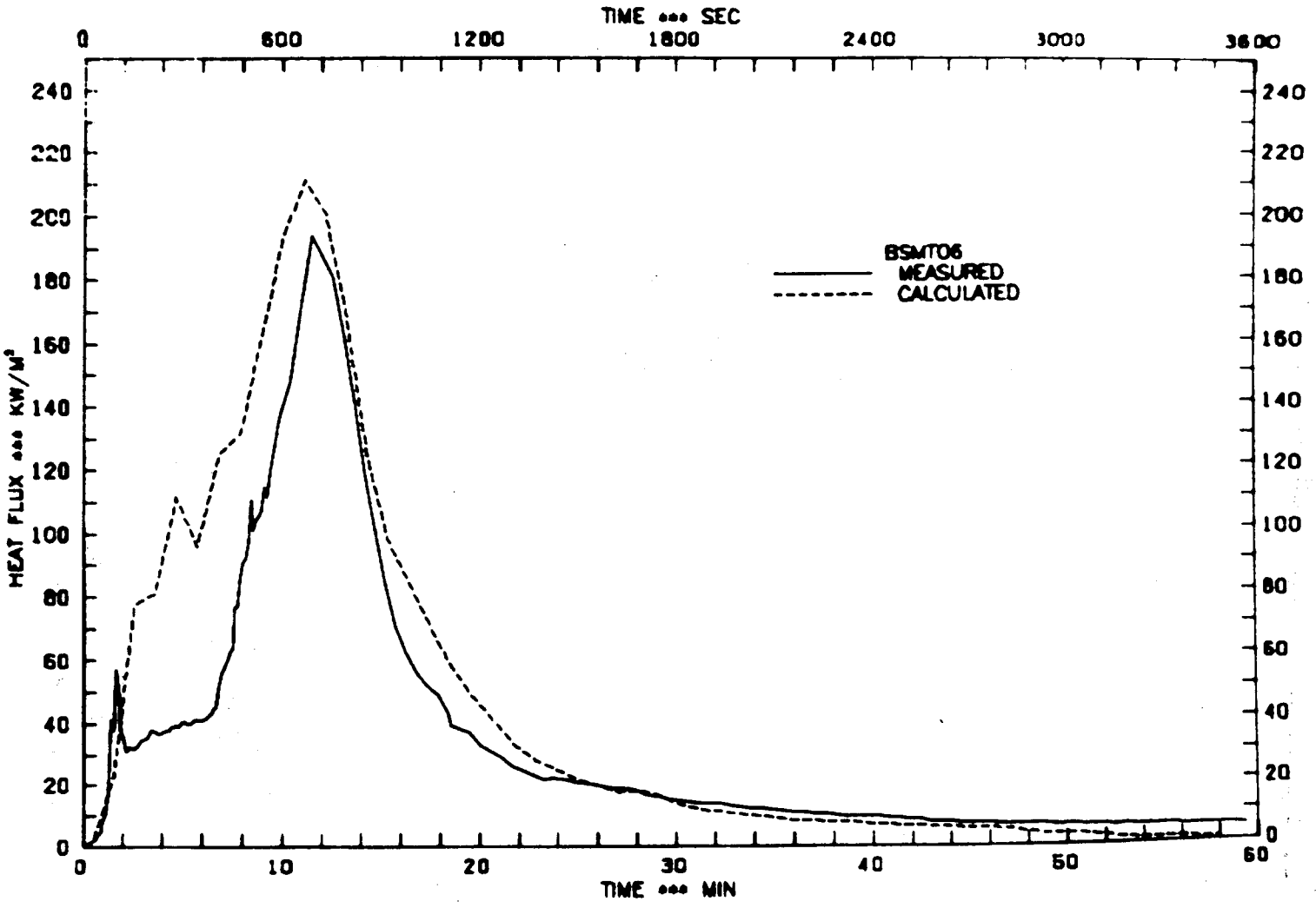

Figure 29b. Comparison of the calculated and measured total heat flux incident on the gypsum board walls

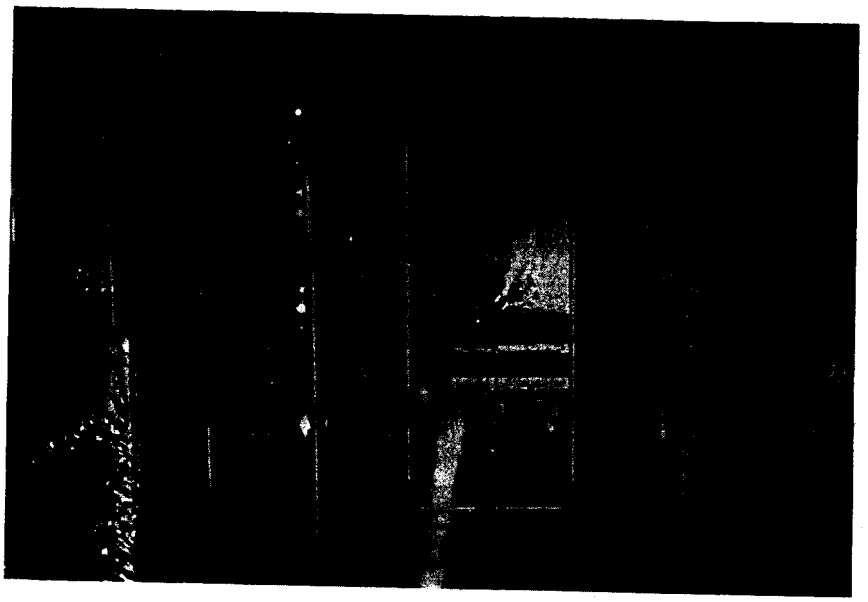

Photo 1. Spread of fire over sofa cushions 3 min after ignition in test 12

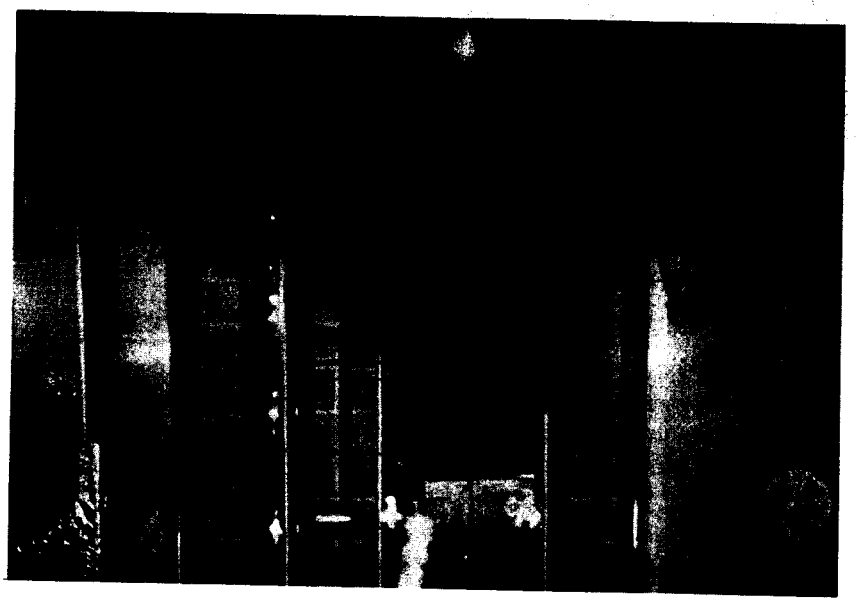

Photo 2. Full involvement of room contents 4 min after ignition in test 12

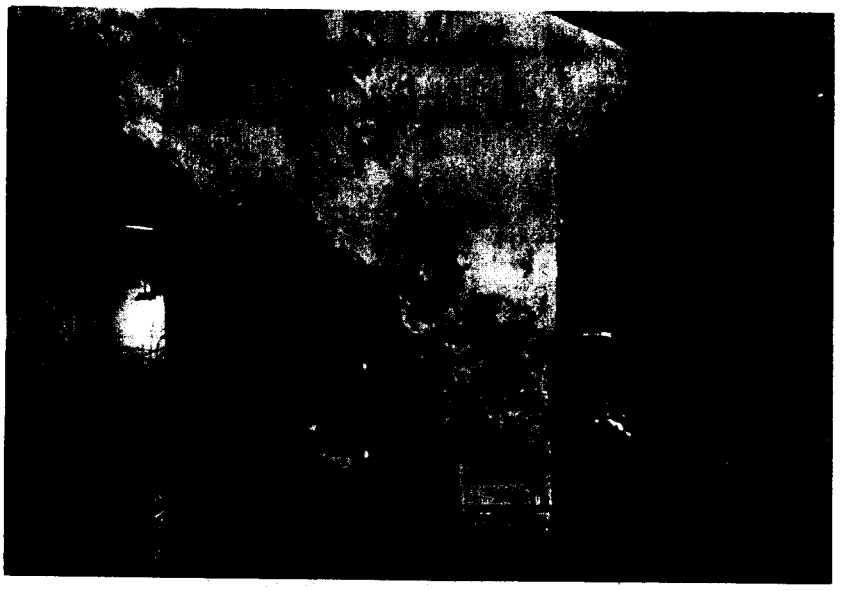

Photo 3. Active burning stage
8 min after ignition in test 12

APPENDIX A - DERIVATION OF THE EQUATIONS USED FOR THE HEAT RELEASE RATE CALCULATIONS

Consider a burning compartment where the combustible materials being heated by the fire, the hot gas layer and the compartment walls degrade into volatile decomposition products and carbonaceous residue or char. The volatile components and the char react with the air surrounding the materials, and the mixture of combustion products and depleted air subsequently moves upward to fill the upper space. The heat is liberated during the combustion of the volatiles in the gas-phase and char oxidation on the solid surfaces. The fire induces an inflow of cold air through the lower part and an outflow of combustion gases via the upper part of the ventilation opening.

In order to derive the relevant equations for calculating the rate of heat release in the compartment, the following simplifying assumptions were made:

1. The fire compartment can be divided into two separate regions with a layer of hot gas above and a cold air layer below. In each region the gases are perfectly mixed with no variations in their composition and temperature.

2. Following the pyrolysis of the combustible materials, the fuel volatiles and the char react instantaneously with the surrounding air.

The continuity equations describing the conservation of the total mass and the gas species around the upper region of the compartment can be written as

$$\frac{d\left(V\rho_g\right)}{dt} = F_a W_a + F_f W_f - F_g W_g \qquad \text{(A-1)}$$

$$\frac{d\left(V\rho_g X_{jg}/W_g\right)}{dt} = F_a X_{ja} - F_g X_{jg} - \nu_j^* r_f V \qquad \text{(A-2)}$$

where V is the volume occupied by the combustion gases or the hot gases in the upper part of the compartment; ρ_g is the density of combustion gases; t is time; F_i and W_i are the molar flow rate and the average molecular weight of the gas in stream i, respectively; the subscripts a, f and g denote the air, fuel and combustion gas streams, respectively; X_{ji} is the concentration of the gas species j in the stream i expressed in mole fraction; the gas species include oxygen, fuel, nitrogen, CO_2, CO and H_2O; r_f is the

reaction rate or the rate of disappearance of the fuel in moles per unit volume of the combustion gas, and ν_j^* is the ratio of the stoichiometric coefficient of the gas species j to that of the fuel.

These mass balance equations contain terms to account for the change in the mass of the gases in the compartment, the flow in of the cold air and the fuel, the flow out of the effluent gas, and the consumption of the fuel by combustion. In general, the rate of change of the total mass of the gases in the compartment is negligible compared with the inlet and outlet mass flow rates.

An expression for the rate of oxygen consumption in the compartment can be obtained from equation (A-2) by neglecting the rate of mass accumulation term. Thus,

$$\nu_{O_2}^* r_f V = \left(F_a X_{O_2 a} / F_g - X_{O_2 g} \right) F_g \qquad \text{(A-3)}$$

Using this equation, the rate of heat release in the fire compartment is expressed by

$$\begin{aligned} \dot{Q} &= r_f V \left(\Delta H_c \right) \\ &= \left(\Delta H_c / \nu_{O_2}^* \right) \left(F_a X_{O_2 a} / F_g - X_{O_2 g} \right) F_g \\ &= K \left(F_a X_{O_2 a} / F_g - X_{O_2 g} \right) \left(298.15 / T_g \right) \dot{V}_g \end{aligned} \qquad \text{(A-4)}$$

where ΔH_c is the heat of combustion of the fuel, in kJ/g-mole; $K = \Delta H_c / (\nu_{O_2}^* v)$, the heat of combustion of the fuel per unit volume of oxygen consumed at the standard state of 25°C and 1 atm; v is the molar volume of oxygen at 25°C and 1 atm, e.g., v is equal to 22.414×10^{-3} x (298.15/273.15) or 0.02446 m^3/g-mole for an ideal gas; T_g and $\dot{V}_g$ are the absolute temperature and the volumetric flow rate of the combustion gases leaving the compartment, respectively.

With the assumption that both the combustion gas and the air behave as perfect gases, equation (A-4) can be rewritten as

$$\dot{Q} = K \left[X_{O_2 a} \dot{V}_a T_g / \left(\dot{V}_g T_a \right) - X_{O_2 g} \right] \left(298.15 / T_g \right) \dot{V}_g \qquad \text{(A-5)}$$

where $\dot{V}_a$ and T_a are the volumetric flow rate and the absolute temperature, respectively, of the air flowing into the compartment.

The fuel is assumed to react irreversibly with the air to form carbon dioxide, carbon monoxide and water according to the reaction,

$$\nu_f[\text{Fuel}] + \nu_{O_2}[O_2 + dN_2] = \nu_{CO_2}CO_2 + \nu_{CO}CO + \nu_{H_2O}H_2O + d\nu_{O_2}N_2 \qquad \text{(A-6)}$$

where ν_f, ν_{CO_2}, ν_{CO}, and ν_{H_2O} are the stoichiometric coefficients of the fuel, CO_2, CO and H_2O, respectively, and d is the nitrogen/oxygen mole ratio of air.

The stoichiometric combustion equation for a fuel of composition $C_aH_bO_c$ with air can be expressed in the following form:

$$C_aH_bO_c + \left(a + \frac{b-2c-2x}{4}\right)\left[O_2 + 3.76\ N_2\right]$$
$$= (a-x)CO_2 + \frac{b}{2}H_2O + xCO + 3.76\left(a + \frac{b-2c-2x}{4}\right)N_2 \qquad \text{(A-7)}$$

For the overall reaction, the molar rate of consumption or production of a gas species can be related to its stoichiometric coefficients. Thus

$$\frac{r_f}{-\nu_f} = \frac{r_{O_2}}{-\nu_{O_2}} = \frac{r_{CO_2}}{\nu_{CO_2}} = \frac{r_{CO}}{\nu_{CO}} = \frac{r_{H_2O}}{\nu_{H_2O}} \qquad \text{(A-8)}$$

Using equation (A-2) an overall mole balance of all of the component gases in the upper hot gas layer can be written as

$$F_g\left(X_{Fg} + X_{O_2g} + X_{CO_2g} + X_{COg} + X_{H_2Og} + X_{N_2g}\right)$$
$$= F_f + F_a + r_fV\ (\Delta\nu^*) \qquad \text{(A-9)}$$

where $\Delta\nu^* = \Delta\nu/\nu_f$, the change in the mole numbers per mole of the fuel reacted, and $\Delta\nu = \nu_{H_2O} + \nu_{CO_2} + \nu_{CO} - \nu_{O_2} - \nu_f$.

During the fire growth period, the rate of burning is generally controlled by the fuel supply rate, and all of the fuel volatiles and char produced convert completely into the combustion products. For fires in the fuel limited burning regime the molar flow rate of combustion gas venting through the opening can be obtained by simplifying equation (A-9) based on the mole fraction constraint for the effluent stream and $r_fV = F_f$. Thus,

$$F_g = F_a + (\Delta\nu^* + 1)F_f \qquad \text{(A-10)}$$

For post-flashover fires, the burning rate is limited by the compartment ventilation or the rate of air inflow. Since there is no oxygen present in the combustion gas, its molar flow rate can be derived in a similar manner with the exception that $r_f V = \alpha F_f$, where α is the fraction of the fuel reacted.

$$F_g = F_a + (\alpha \Delta\nu^* + 1)F_f \tag{A-11}$$

Combining equations (A-3) and (A-10) to solve for F_a/F_g and substituting the resulting expression into equation (A-4) gives

$$\dot{Q} = K\left(X_{O_2 a} - X_{O_2 g}\right) \Big/ \left[1 + (\Delta\nu^* + 1)X_{O_2 a} \Big/ \nu^*_{O_2}\right] \left(298.15/T_g\right) \dot{V}_g \tag{A-12}$$

For the fires under ventilation controlled burning, another expression for the heat release rate can be obtained from equations (A-3), (A-4) and (A-11) as

$$\dot{Q} = K\left(X_{O_2 a} - X_{O_2 g}\right) \Big/ \left[1 + (\alpha \Delta\nu^* + 1)X_{O_2 a} \Big/ \nu^*_{O_2}\right] \left(298.15/T_g\right) \dot{V}_g \tag{A-13}$$

The analysis of the combustion gas leaving the compartment is usually made on a dry basis where the water vapor in the sampling line is condensed and removed prior to the determination of the gas composition. The moisture-free combustion gas produced from the fires under fuel limited burning consists of CO_2, CO, O_2 and N_2. The concentrations of these gases as measured with the gas analyzers can be expressed by

$$\begin{aligned} X^A_{CO_2} &= F_g X_{CO_2 g}/P \\ X^A_{CO} &= F_g X_{COg}/P \\ X^A_{O_2} &= F_g X_{O_2 g}/P \end{aligned} \tag{A-14}$$

where $P = F_g\left(X_{CO_2 g} + X_{COg} + X_{O_2 g}\right) + F_a X_{N_2 a}$

These simultaneous equations are solved for the concentrations of CO_2, CO and O_2 in the combustion gas stream. Thus,

$$\begin{aligned} X_{CO_2 g} &= \left(F_a X_{N_2 a}/F_g\right)\left(X^A_{CO_2}/X^A_{N_2}\right) \\ X_{COg} &= \left(F_a X_{N_2 a}/F_g\right)\left(X^A_{CO}/X^A_{N_2}\right) \\ X_{O_2 g} &= \left(F_a X_{N_2 a}/F_g\right)\left(X^A_{O_2}/X^A_{N_2}\right) \end{aligned} \tag{A-15}$$

where $X^A_{N_2} = 1 - X^A_{O_2} - X^A_{CO_2} - X^A_{CO}$

The concentration of water vapor contained in the combustion gases can be estimated based on the ratio of the moles of H_2O produced to the moles of CO_2 and CO formed from the burning of the fuel as given in the general combustion equation. Thus,

$$X_{H_2Og} = \left[\nu_{H_2O} \Big/ \left(\nu_{CO_2} + \nu_{CO}\right)\right] \left(X_{CO_2g} + X_{COg}\right)$$

$$= \left[\nu_{H_2O} \Big/ \left(\nu_{CO_2} + \nu_{CO}\right)\right] \left(X^A_{CO_2} + X^A_{CO}\right) \left[F_a X_{N_2a} \Big/ \left(F_a X^A_{N_2}\right)\right] \qquad \text{(A-16)}$$

The mole fraction of the nitrogen, which lumps all of the components of air except oxygen and is considered as an inert species throughout the fire process, can be expressed by

$$X_{N_2g} = F_a X_{N_2a} \Big/ F_g \qquad \text{(A-17)}$$

Since the summation of all of the mole fractions of O_2, CO_2, CO, H_2O and N_2 gases in the combustion gas stream must be equal to unity, this results in

$$F_a X_{N_2a} \Big/ \left(F_g X^A_{N_2}\right) = 1/(1 + Y) \qquad \text{(A-18)}$$

where $Y = \nu_{H_2O} \left(X^A_{CO_2} + X^A_{CO}\right) \Big/ \left(\nu_{CO_2} + \nu_{CO}\right)$

Substituting this relation into equations (A-15) to (A-17) yields

$$X_{CO_2g} = X^A_{CO_2} \Big/ (1 + Y)$$

$$X_{COg} = X^A_{CO} \Big/ (1 + Y)$$

$$X_{O_2g} = X^A_{O_2} \Big/ (1 + Y)$$

$$X_{N_2g} = X^A_{N_2} \Big/ (1 + Y)$$

$$X_{H_2Og} = Y/(1 + Y) \qquad \text{(A-19)}$$

The average molecular weight of the combustion gases can be determined from the equation,

$$W_g = 32X_{O_2g} + 44X_{CO_2g} + 28X_{COg} + 18X_{H_2Og} + 28X_{N_2g} \qquad \text{(A-20)}$$

For the fires under ventilation controlled burning, the combustion gas consists of CO_2, CO, H_2O, N_2 and the unburned fuel. The molar concentrations of these gases can be derived in a similar manner to those for fuel controlled fires. Thus,

$$X_{CO_2g} = X^B_{CO_2} \Big/ (1 + Y')$$

$$X_{COg} = X^B_{CO} \Big/ (1 + Y')$$

$$X_{fg} = X^B_f \Big/ (1 + Y')$$

$$X_{N_2g} = X^B_{N_2} \Big/ (1 + Y')$$

$$X_{H_2Og} = Y'/(1 + Y') \qquad \text{(A-21)}$$

where X^B_j is the concentration of the moisture-free gas j in the combustion gas stream during the ventilation limited burning regime;

$$Y' = \nu_{H_2O} \left(X^B_{CO_2} + X^B_{CO}\right) \Big/ \left(\nu_{CO_2} + \nu_{CO}\right) \quad \text{and} \quad X^B_{N_2} = 1 - X^B_{CO_2} - X^B_{CO} - X^B_f$$

The average molecular weight of the combustion gas can be estimated from the following equation:

$$W_g = 44X_{CO_2g} + 28X_{COg} + 18X_{H_2Og} + W_fX_{fg} + 28X_{N_2g} \qquad \text{(A-22)}$$

The combination of equation (A-1), in which the mass accumulation term is neglected, and equation (A-11) gives the ratios of the molar flow rates of the air inflow or fuel supply to that of the exhausting combustion gas. Thus

$$F_a/F_g = \left[W_g(\alpha\, \Delta\nu^* + 1) - W_f\right] \Big/ \left[W_a(\alpha\, \Delta\nu^* + 1) - W_f\right] \qquad \text{(A-23)}$$

$$F_f/F_g = \left(W_a - W_g\right) \Big/ \left[W_a(\alpha\, \Delta\nu^* + 1) - W_f\right] \qquad \text{(A-24)}$$

An expression for the fraction of the fuel converted can be obtained by the rearrangement of equation (A-23). Thus,

$$\alpha = \left[W_f - W_g + F_a\left(W_a - W_f\right)\Big/F_g\right] \Big/ \left[\Delta\nu^*\left(W_g - F_aW_a\Big/F_g\right)\right] \qquad \text{(A-25)}$$

where $F_a/F_g = \dot{V}_aT_g/(\dot{V}_gT_a)$ and $\dot{V}_a$ is the volumetric flow rate of inflowing air.

The total rate of heat release within the fire compartment can be calculated by substituting these derived and measured quantities into either equation (A-5) or equations (A-12) and (A-13).

APPENDIX B - ESTIMATION OF THE INCIDENT HEAT FLUX

The temperature distribution in a semi-infinite slab initially at a uniform temperature and subjected to a constant heat flux on the exposed surface is given by [14]

$$T(\chi,t) = \frac{2\,\dot{q}''_a}{k}\left\{\sqrt{\frac{\alpha t}{\pi}}\,\exp\left(-\frac{\chi^2}{4\alpha t}\right) - \frac{\chi}{2}\,\mathrm{erfc}\left(\frac{\chi}{2\sqrt{\alpha t}}\right)\right\} + T_i \qquad \text{(B-1)}$$

where $\dot{q}''_a$ is the net heat flux entering the slab at its exposed surface; k and α are the thermal conductivity and thermal diffusivity, respectively, of the slab; t is the time; χ is the distance into the slab from the exposed surface and T_i is its initial temperature.

From Duhamel's theorem [15], the unsteady temperature at the surface of a slab exposed to a time varying heat flux, $\dot{q}''_a(t)$, is given by

$$T_s(o,t) = \frac{1}{k}\sqrt{\frac{\alpha}{\pi}}\int_0^t \frac{\dot{q}''_a(\tau)}{\sqrt{t-\tau}}\,d\tau + T_i \qquad \text{(B-2)}$$

The integral in the above equation can be evaluated numerically. Thus, the surface temperature at any time can be calculated from the following equation, with a constant duration Θ for each time step,

$$T_s(0,t) = \frac{2}{\sqrt{\pi}}\,\frac{\sqrt{\alpha}}{k}\sum_{n=1}^{N}\dot{q}''_a(n)\left[\sqrt{t-(n-1)\Theta} - \sqrt{t-n\Theta}\right] + T_i \qquad \text{(B-3)}$$

where $N = t/\Theta$.

An expression for the net heat flux into the slab can be obtained by rearranging equation (B-3) to give

$$\dot{q}''_a(N) = \Theta^{-1/2}\left\{C\left[T_s(0,t)-T_i\right] - \sum_{n=1}^{N-1}\dot{q}''_a(n)\left[\sqrt{[N-(n-1)]\Theta} - \sqrt{(N-n)\Theta}\,\right]\right\} \qquad \text{(B-4)}$$

where $C = \frac{k}{2}\sqrt{\frac{\pi}{\alpha}}$

The time variation of the net heat flux absorbed by the walls and ceiling of the recreation room through their exposed surfaces was computed using the measured surface temperature history data. The heat fluxes incident at the room walls and ceiling, which were assumed to be semi-infinite solids with temperature-independent thermal properties, were estimated from the calculated net heat flux and the experimentally determined surface temperatures using the following expressions for the net flux entering into the material, $\dot{q}''_a$,

and the incident heat flux acting on the exposed surface, $\dot{q}''_i$.

$$\dot{q}''_a = \varepsilon_s \, (H - \sigma T_s^4) + h \, (T_g - T_s) \qquad \text{(B-5)}$$

$$\dot{q}''_i = \varepsilon_s H + h \, (T_g - T_s) \qquad \text{(B-6)}$$

where ε_s is total emissivity of the surface of the slab, H is the incident radiative heat flux, h is the convective heat transfer coefficient, σ is the Stefan-Boltzmann constant, and T_g is the bulk temperature of the surrounding hot gas. It is assumed that the total absorptivity of the surface for the incident radiation is equal to its total emissivity at the temperature, T_g, as it would be for a "grey" body.